CHEMICAL REVIEWS

Review

pubs.acs.org/CR

Drug Strategies Targeting CYP51 in Neglected Tropical Diseases

Jun Yong Choi,[†] Larissa M. Podust,*[,‡,§] and William R. Roush*[,†]

[†]Department of Chemistry, Scripps Florida, 130 Scripps Way, Jupiter, Florida 33458, United States

[‡]Center for Discovery and Innovation in Parasitic Diseases, and [§]Department of Pathology, University of California—San Francisco, San Francisco, California 94158, United States

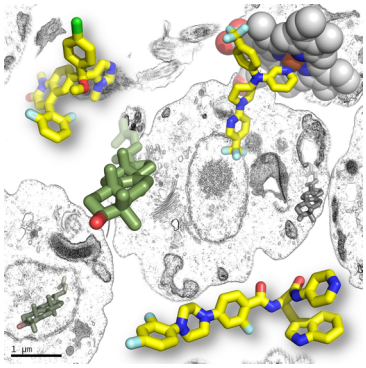

CONTENTS

1. INTRODUCTION

CYP51 is considered one of the most ancient P450 protein families.[1] It is perhaps the only P450 protein family whose members are spread across all biological kingdoms, although it is lost in certain lineages including insects and worms which do not perform *de novo* sterol biosynthesis.[2−5] CYP51 has a conserved metabolic function in eukaryotes, being part of the sterol biosynthesis pathway downstream from squalene epoxidase, the first oxygen-dependent step in the sterol pathway and the branch point between hopanoid and sterol biosynthesis that distinguishes eukaryote biochemistry from that of prokaryotes.[6] Sterols are absent from archaea and sparsely represented in bacteria.[7] For example, *Methylococcus capsulatus*,[8] *Gemmata obscuriglobus*,[9] and some myxobacteria[10,11] produce a limited array of sterols. P450s sharing common ancestors with eukaryotic CYP51 have been identified in some bacteria, including *Methylococcus capsulatus*,[12] *Mycobacterium tuberculosis*,[13,14] *Mycobacterium avium*,[15] and *Mycobacterium vanbaalenii*,[16] although the *in vivo* function of CYP51 in *Mycobacteria* is unknown. By contrast, CYP51 is essential in higher eukaryotes. For instance, CYP51 knockout in mice is embryonically lethal on day 15.[17] In yeast, CYP51 knockout is fatal.[18] Consequently, this enzyme is an attractive target for antifungal agents in human and veterinary medicine[19] and for fungicides in agriculture,[20] provided that selectivity over the mammalian CYP51 is achieved.

In protozoa, sterol biosynthesis pathway is absent in strict anaerobic organisms, including human pathogens, *Giardia, Entamoeba, Cryptosporidium*, and *Trichomonas*.[5] This is consistent with the oxygen demand: 11 molecules of oxygen are required for the synthesis of one molecule of cholesterol.[6] A variety of free-living and symbiotic protist species, some of

Special Issue: 2014 Drug Discovery and Development for Neglected Diseases

Received: June 13, 2014
Published: October 22, 2014

   dx.doi.org/10.1021/cr5003134 | *Chem. Rev.* 2014, 114, 11242−11271

which are important human parasites, are reported to synthesize sterols *de novo*.[5] Thus, the sterol biosynthesis pathway is present in free-living amoebas, *Acanthamoeba*[21,22] and *Naegleria*.[23] *Acanthamoeba* belonging to several different genotypes cause an insidious and chronic disease, granulomatous amebic encephalitis (GAE), in immunocompromised hosts, and infection of the human cornea, *Acanthamoeba* keratitis.[24] *Naegleria fowleri* is responsible for severe primary amebic meningoencephalitis (PAM) which mostly occurs in healthy children and young adults with recent recreational fresh water exposure.[24] PAM due to *N. fowleri* has a worldwide distribution although it occurs most frequently in tropical areas and during hot summer months.

Sterols are synthesized from squalene in kinetoplastid protozoa, *Trypanosoma cruzi*, *Trypanosoma brucei*, and *Leishmania* species,[25] the causative agents of Chagas disease, African sleeping sickness, and different forms of leishmaniasis, respectively, which collectively affect hundreds of millions of people, primarily the poor and underserved, and which have been designated by the WHO and NIH as neglected tropical diseases (NTDs). CYP51 is essential in *T. cruzi*, as inhibition of its enzymatic activity is lethal for the replicative intracellular clinical amastigote stage.[26] Susceptibility to CYP51 inhibitors in *Leishmania* is species-specific and depends on the disease type. Drugs that are potent in the treatment of cutaneous leishmaniasis caused by *Leishmania tropica* or *Leishmania major* are useless in cases of visceral leishmaniasis caused by *Leishmania infantum*.[27−30] The role of the endogenously synthesized sterols and their influence on cellular processes in agents of these diseases is poorly understood, even less so in the case of *T. brucei*. The bloodstream form of *T. brucei* is highly dependent on an exogenous supply of host cholesterol incorporated via receptor-mediated endocytosis,[31] while endogenous sterol biosynthesis is important for distinct biological functions in the insect form of the *T. brucei* parasite, where decreased levels of endogenously synthesized sterols have deleterious effect on proliferation and growth.[32]

Although the sterol biosynthesis pathway is not present in major agents of human tropical diseases such as worms and *Plasmodium*,[5] *T. cruzi* and at least some *Leishmania* species remain major validated targets for CYP51 inhibitors outside traditional antifungal drug discovery programs. CYP51 may be essential in free-living amoebas, *Acanthamoeba* and *Naegleria*, and thus should be viewed as a potential therapeutic target in these organisms. Growth inhibition by systemic fungicides, tridemorph and fenpropimorph, targeting several reactions in sterol biosynthesis in fungi and plants, has been reported in *Acanthamoeba polyphaga* and *Naegleria lovaniensis*.[22,23] Because tropical diseases elicit scant attention from the pharmaceutical industry owing to the absence of economic incentives, university laboratories, private research organizations, and public−private product development partnerships such as the Drugs for Neglected Disease Initiatives (DND*i*) lead the NTD drug discovery efforts. Reviewed in this article are advances in repurposing of classic antifungal azoles and their analogues for treatment of human infections caused by kinetoplastid parasites, as well as modern trends to identify structurally diversified lead compounds with entirely new chemical scaffolds specifically targeting *T. cruzi* CYP51.

2. CATALYTIC AND BIOLOGICAL FUNCTIONS OF CYP51

2.1. Catalytic Function of CYP51

CYP51 catalyzes a complex reaction sequence consisting of three successive monooxygenation steps to cleave the C−C bond at C-14 and remove the C-32 methyl group of sterol substrates (**1**) (Figure 1A).[33−37] The reaction mechanism

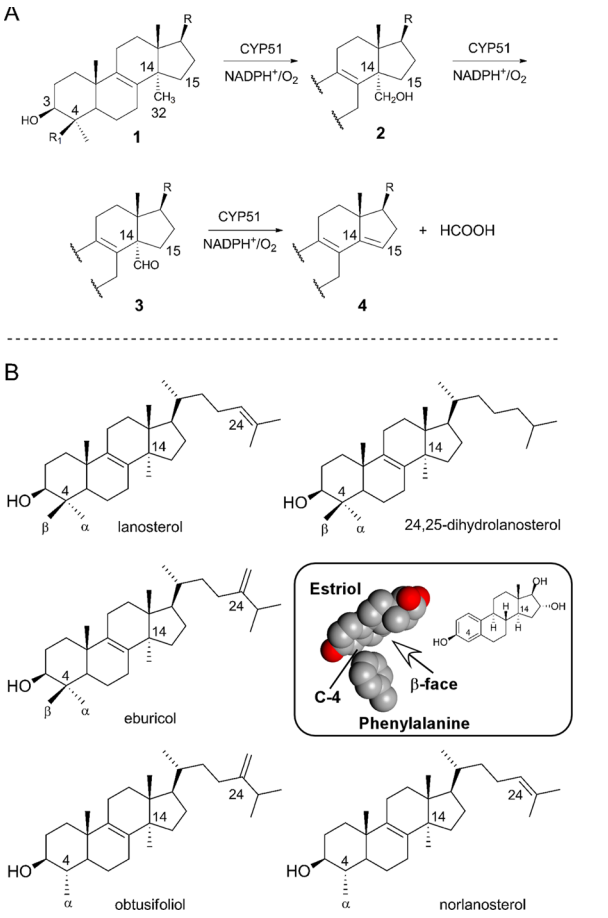

Figure 1. 14α-Demethylation of sterols. (A) Reaction sequence catalyzed by CYP51. (B) The structures of known CYP51 substrates. Insert: The Phe[105] equivalent in *M. tuberculosis* approaches at van der Waals distance to the C-4 atom at the estriol β-face (PDB ID 1X8V).[45] This disposition is consistent with the *M. tuberculosis* CYP51 preference to obtusifoliol.[14,46]

follows the fundamental chemistry well-characterized for other P450 enzymes,[38] with qualification that three enzyme turn over cycles are required to complete the entire transformation: (i) formation of the oxysterol intermediates **2** (C-32 alcohol) and (ii) **3** (C-14 aldehyde) and (iii) removal of the C-32 methyl group in the form of formic acid with concomitant formation of the C14−C15 double bond in the final product (**4**). Three oxygen molecules, six protons, and six reducing equivalents delivered by NADPH-dependent cytochrome P450-reductase are consumed in the course of the reaction. The deformylation step proceeds via an iron peroxo intermediate.[39−41] Altogether, five closely related sterols have been identified as CYP51 substrates in different species (Figure 1 **B**). Lanosterol, 24,25-dihydrolanosterol, and eburicol are CYP51 substrates in fungi, *T. cruzi*, yeast, and vertebrates, while obtusifoliol and

dx.doi.org/10.1021/cr5003134 | *Chem. Rev.* 2014, 114, 11242−11271

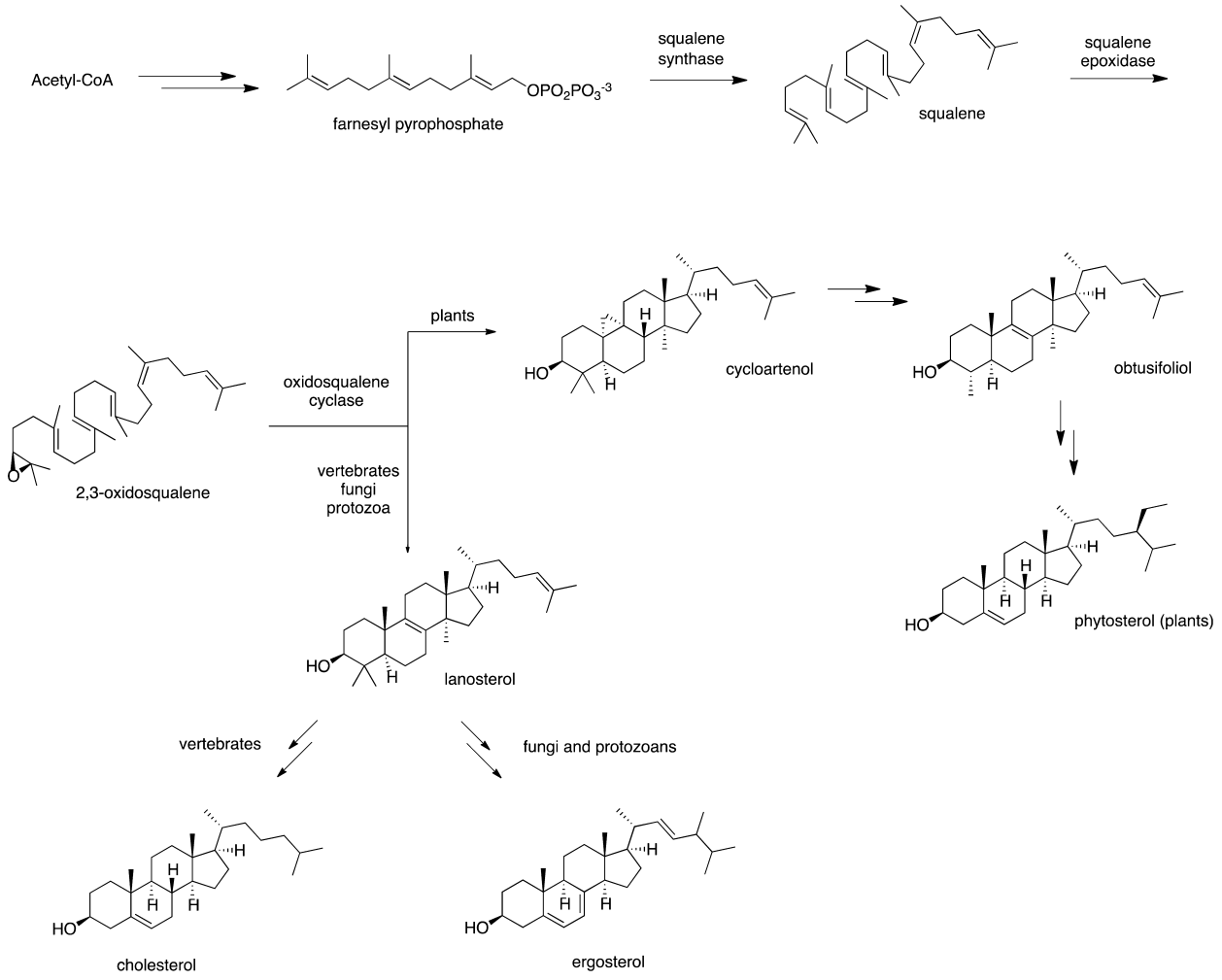

Figure 2. Sterol biosynthesis from acetyl-CoA to cholesterol (vertebrates), ergosterol (fungi and protozoa), and phytosterol (plants).

norlanosterol are substrates in plants, *Leishmania infantum*, and *T. brucei*.[42−44]

This complex reaction sequence hinges on the catalytic histidine residue in the CYP51 active site, His[294] (residue numbering adheres to the *T. cruzi* sequence), which in the primary sequence invariantly precedes a conserved threonine involved in the H-bond network supplying protons for the O_2 reduction step.[47,48] Thus, the A/G-G-XX-T sequence that is conserved across the P450 family[49] is reduced in CYP51 to the signature motif A/G-G-XH-T. The 4β-methyl group in lanosterol, 24,25-dihydrolanosterol, and eburicol is discriminated from the 4β-H atom in obtusifoliol and norlanosterol by phenylalanine at the 105 position, which otherwise is occupied by leucine, except for *T. cruzi* CYP51, which has isoleucine at position 105. On the basis of the X-ray structure of the estriol-bound *M. tuberculosis* CYP51, phenylalanine at position equivalent 105 sterically interferes with the methyl group in the 4β-configuration (Figure 1B, insert).[45] Despite the close similarity of CYP51 substrates, the CYP51 amino acid sequences have diverged substantially and have sequence identity below 30% between evolutionarily distant species. These differences enable development of selective drugs with a wide therapeutic window targeting CYP51 in human pathogens.

2.2. Sterol Biosynthesis Pathway

Sterols are indispensable constituents of eukaryotic cells. They maintain membrane fluidity and permeability, and modulate activity of membrane-bound proteins and ion channels. In addition, sterols are precursors of many biologically important molecules, which play roles in the regulation of growth and development. The biosynthesis of sterols in eukaryotic organisms is highly diversified, resulting in distinct but structurally related membrane components such as cholesterol in vertebrates, ergosterol in fungi and protozoans, and phytosterols in plants (Figure 2).

Sterol biosynthesis starts as an anaerobic process with a simple precursor, acetyl-CoA, as the foundational building block. In the mevalonate-isoprenoid part of the pathway, which is conserved within eukaryotic organisms, isopentenyl-5-pyrophosphate and dimethylallyl pyrophosphate are coupled to generate geranyl pyrophosphate which then leads to farnesyl pyrophosphate, a product of farnesyl diphosphate synthase. Squalene synthase then combines two molecules of farnesyl pyrophosphate into squalene, which is then oxidized by squalene epoxidase, which inserts an oxygen atom from molecular oxygen into the terminal double bond to yield 2,3-oxidosqualene. The 2,3-oxidosqualene is transformed into lanosterol in vertebrates, fungi, and protozoa, while in plants, it leads to phytosterol via cycloartenol and obtusifoliol as key intermediates.[50,51] The 19-step biosynthesis of cholesterol from

dx.doi.org/10.1021/cr5003134 | *Chem. Rev.* 2014, 114, 11242−11271

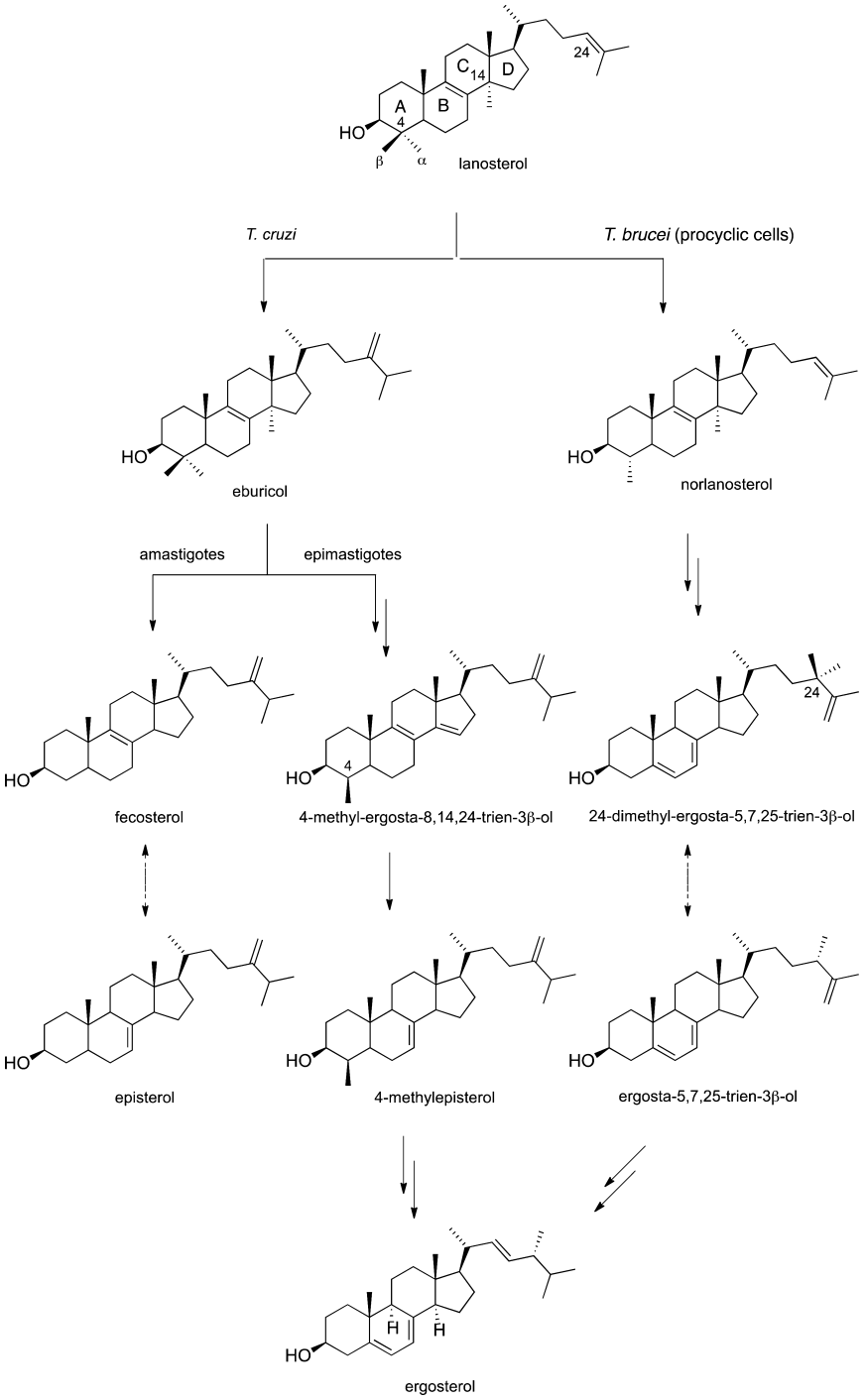

Figure 3. Conversion of lanosterol to 24-alkyl sterols in *T. cruzi* and *T. brucei*. The pathways are partially deduced on the basis of GC/MS and isotope labeling techniques.

lanosterol, catalyzed by nine different enzymes, is reviewed elsewhere.[52]

The biosynthesis of ergosterol in fungi and protozoa varies depending on strain and species, and details of the biosynthetic pathway still need more investigation. However, both fungi and kinetoplastids rely on ergosterol and related 24-alkyl sterols for growth and viability, which distinguishes their metabolism from that of the mammalian host.[28,53] Cholesterol and ergosterol have the same overall shape and structure−activity relationships in cellular membranes, including the essential role of 3β-OH hydroxyl group.[54] Cholesterol has a saturated side chain, while ergosterol has a $\Delta^{22,23}$-unsaturated side chain with an additional β-methyl group at C-24. The B rings also differ, with cholesterol having one double bond ($\Delta^{5,6}$), while ergosterol has two conjugated double bonds ($\Delta^{5,6}$ and $\Delta^{7,8}$) (Figure 3).

The main sterols of trypanosomatids include members of the ergostane and stigmastane family, which have 24-methyl or ethyl side chains, respectively.[55] On the basis of the analysis of sterol composition by chromatographic and mass spectroscopic methods, sterol biosynthetic pathways in *T. cruzi* amastigotes and epimastigotes were partially constructed (Figure 3).[56,57] A distinct sterol pathway has been proposed in *T. brucei* on the

dx.doi.org/10.1021/cr5003134 | *Chem. Rev.* 2014, 114, 11242−11271

basis of the GC/MS analysis and ^{2}H and ^{13}C labeling studies, indicating that the biosynthesis proceeds both from lanosterol and norlanosterol to ergosta-5,7,25,trien-3β-ol and 24-dimethyl ergosta-5,7,25-trien-3β-ol and thence to ergosterol.[58] However, only trace amounts of 24-alkyl sterols are observed in the membranes of the *T. brucei* bloodstream form.[31,58,59]

Extracellular epimastigotes and intracellular amastigotes in *T. cruzi* contain different sterol compositions (Figure 3). The former comprises ~40% of ergosterol and ergost-5,7-dien-3β-ol and ~30% of stigmasta-5,7-dien-3β-ol and stigmasta-5,7,22-trien-3β-ol in sterol content, while the latter contains ergosta-7-en-3β-ol, 24-ethylidinecholest-7-en-3β-ol, and smaller amounts of episterol, implying the absence of Δ^{5}- and Δ^{22}-desaturase activities in *T. cruzi* amastigotes.[54,57] In the other studies, fecosterol (ergosta-8,24,(24′)-dien-3β-ol) and its Δ8-Δ7 isomer episterol were identified as two principal sterols in amastigotes, while epimastigotes again revealed a pool of sterols richer than that found in amastigotes.[56] In contrast to *T. cruzi*, *Leishmania* amastigotes and promastigotes include 5-dehydroepisterol as a major sterol component along with a small amount of episterol and ergosterol.[54,60,61] In *T. brucei* procyclic cells, ergosterol is the predominant component in cells cultured on full-growth medium, while cholesta-5,7,24-trienol, ergosta-5,7,25-trienol, and ergosta-5,7,24-trienol are major components in cells cultured on cholesterol-depleted media.[50,62]

2.3. Sterol Biosynthesis: Drug Targets for Neglected Tropical Diseases

The sterol biosynthetic pathway in Trypanosomatidae is an attractive target for the development of antiparasitic agents because ergosterol and related 24-alkyl sterols are essential components of parasite cell membranes. Among enzymes constituting the sterol biosynthetic pathway, several targets have been studied for the development of therapeutic agents that interfere with sterol biosynthesis in humans and fungal infections.[54,63] For instance, HMG-CoA reductase (targeted by statins), farnesyl diphosphate synthase (bisphosphonates), squalene synthase (aryloxyethyl thiocyanate and quinuclidine derivatives), squalene epoxidase (terbinafine), oxidosqualene cyclase (pyridinium-ion-based mimetics), sterol 14α-demethylase (azoles), and sterol 24-methyl transferase (azasterols) have been validated as potential therapeutic targets in humans and fungal infections.[63] These inhibitors have been tested against parasite infections *in vitro* and *in vivo*, as stand-alone agents and in combination with others.[63]

Among proven sterol biosynthetic targets, CYP51 is one of the most extensively exploited for the development of antiparasitic agents. Inhibition of CYP51 alone or in combination with other sterol biosynthesis inhibitors[27,32,64] not only blocks the generation of ergosterol, which is vital for parasite growth, but also leads to accumulation of methylated toxic intermediates, resulting in the arrest of cell growth and cell death. Therefore, CYP51 constitutes a highly attractive, target for the development of new therapeutics for fungal and parasitic infections, including life-threatening NTDs prevalent in areas with poor living conditions and inadequate health care infrastructure.

3. CYP51: TARGET OF ANTIFUNGAL DRUGS

3.1. Antifungal Azoles Targeting CYP51

CYP51 is the therapeutic target of antifungal azole drugs of the "conazole" pedigree (Figures 4–6). High efficacy against a broad spectrum of fungal pathogens make the azoles

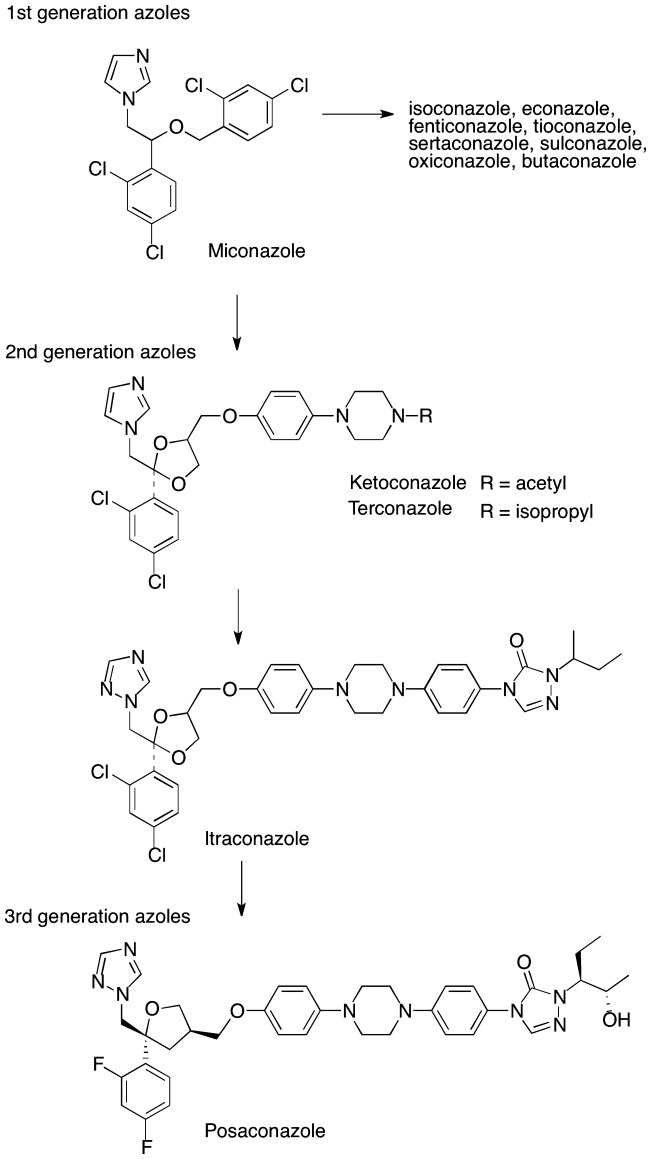

Figure 4. Antifungal drugs of "conazole" pedigree: from miconazole to posaconazole.

indispensable tools for controlling fungal infections in human and crop plants. Current and emerging azole antifungal agents have been reviewed,[19,65−71] including an in-depth historical overview by Heeres et al.[72] of the analogue-based drug discovery path leading from miconazole to posaconazole and isavuconazole.

Since miconazole was first launched, eight analogues (isoconazole, econazole, fenticonazole, tioconazole, sertaconazole, sulconazole, oxiconazole, and butaconazole) have been marketed as first generation conazole fungicides. Most of these first generation agents were accessible from a common key intermediate, 2-(imidazolyl)-acetophenone, and showed a broad range of antifungal activity against dermatophytes, pathogenic yeasts, and filamentous fungi. Interestingly, it was found that derivatives containing a dioxolane unit, the protected ketone derivative used in the course of miconazole synthesis, also displayed broad antifungal activity. This observation later led to the discovery of the first orally active broad-spectrum antifungal agent, ketoconazole (Figure 4).[73] In addition, terconazole, possessing an alkyl group and triazole

dx.doi.org/10.1021/cr5003134 | *Chem. Rev.* 2014, 114, 11242−11271

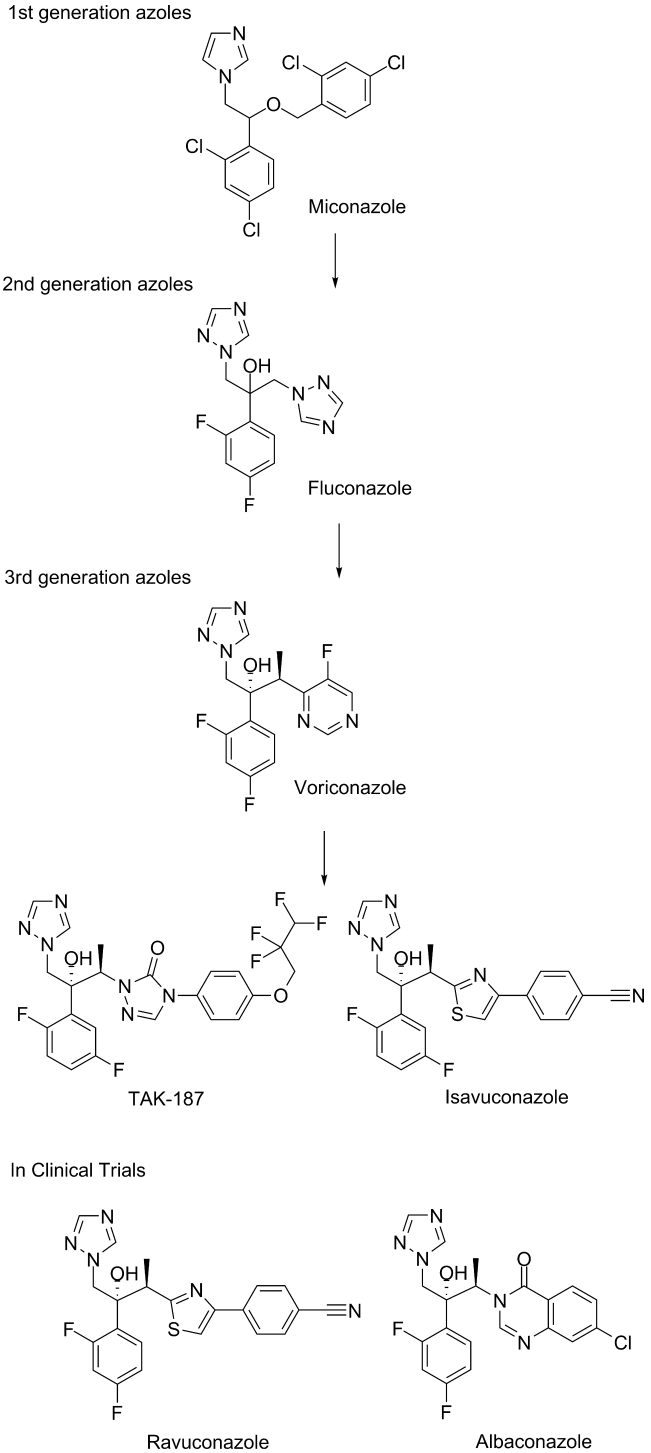

Figure 5. Antifungal drugs of "conazole" pedigree: from miconazole to isavuconazole.

ring rather than the acyl and imidazole groups of ketoconazole, showed enhanced topical activity against superficial fungal infections.[74] Substituted aryl groups at the N-position of the terminal piperazine ring in ketoconazole and terconazole were tolerated in terms of antifungal activity, a finding which led to the development of the highly orally active itraconazole.[75] This second generation conazoles showed very high potency against skin candidiasis, dermatophytosis, vaginal candidiasis, disseminated candidiasis, and aspergillosis in experimental animal models.[75]

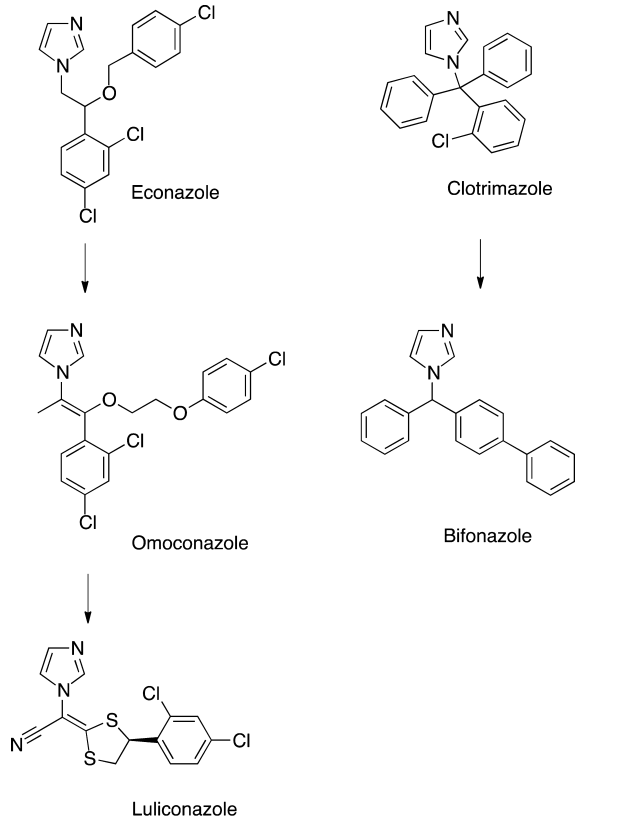

Figure 6. Antifungal drugs of "conazole" pedigree: from econazole to luliconazole.

Next came posaconazole (SCH-56592), whose single enantiomer form was developed by Schering-Plough through further structural modification of itraconazole followed by isolation and characterization of a circulating metabolite of an earlier lead (Figure 4).[76,77] Posaconazole displayed broader spectrum antifungal activity than itraconazole, although these two compounds are structurally very similar.[78] Posaconazole has activity against all of the organisms covered by the other triazoles such as itraconazole, fluconazole, and voriconazole, in addition to activity against *Scedosporium* spp. and *Zygomycetes*, which are refractory to the previous generation triazoles.[79−82] In addition, positive clinical outcomes against CNS fungal infections and cryptococcal meningitis, which were insensitive to conventional therapies, were achieved by posaconazole.[83]

Fluconazole and voriconazole, developed by Pfizer, are another pair of conazoles derived from the miconazole scaffold (Figure 5). These new antifungal agents were derived from the miconazole scaffold by shifting the benzyl moiety from the oxygen to the α-carbon. However, the *in vivo* efficacy of the initial imidazolyl carbinols was not significantly improved from that of ketoconazole. In subsequent studies, the metabolically vulnerable imidazole ring and aryl group were replaced with 1,2,4-triazole rings, leading to a symmetrical triazole analogue fluconazole, which possessed significantly improved pharmacokinetic properties.[84,85] Fluconazole displays significantly increased *in vivo* antifungal activity in murine systemic candidiasis and superficial infection models due to pharmacokinetic properties which are superior to those of ketoconazole.[85] Since fluconazole showed poor efficacy against aspergillosis, this compound was further optimized in the development of next-

dx.doi.org/10.1021/cr5003134 | *Chem. Rev.* 2014, 114, 11242−11271

generation agents possessing a broader spectrum of antifungal activity, particularly for use against aspergillus infections.

Further structural modification of fluconazole, including introduction of a methyl group and replacement of one of the triazole units with 5-fluoropyrimidine, resulted in voriconazole which gained *in vitro* potency against *Aspergillus*, *Fusarium*, and *Scedosporium apiospermum* species. Voriconazole was subsequently approved for the treatment of life-threatening fungal infections in immunocompromised patients, serious infections caused by the aforementioned fungi, and even fluconazole-resistant invasive candida infections.[86] Very recently (December 2013), the FDA approved isavuconazole, developed by Basilea Pharmaceutica, as a qualified infectious disease product (QIDP) for the treatment of invasive aspergillosis. In addition to these marketed conazoles, ravuconazole (BMS) and albaconazole (Actavis) are in clinical studies for the treatment of fungal infections in patients undergoing allogeneic stem cell transplantation, and onychomycosis, candidiasis vulvaginitis, and tinea pedis, respectively.

Other azole antifungal drugs with the same mechanism of action, such as bifonazole, clotrimazole, omoconazole, and luliconazole, are also available (Figure 6). Discovery of clotrimazole by Bayer AG in the late 1960s led to the development of bifonazole, a halogen-free imidazole antifungal agent that is very lipophilic and has poor aqueous solubility.[87] Bifonazole has broad-spectrum *in vitro* antifungal activity and is an effective and well-tolerated treatment for superficial fungal infections of the skin.[88,89] Siegfried (Pennsville, NJ) developed the antimycotic azole agent, omoconazole, from econazole.[90] Lastly, the FDA approved luliconazole to treat fungal infections in late 2013. Luliconazole displays broad-spectrum topical antifungal potency against the dermatophytes that cause 90% of onychomycosis.[91,92]

3.2. Antifungal Azoles as Antileishmaniasis Drugs

The most common off-label use of azoles is associated with their antiparasitic activity.[65] A number of antifungal azoles were tested against various parasitic diseases especially leishmaniasis and trypanosomiasis.[28−30] Antileishmanial activity is the most comprehensively studied for azoles. There are reports on miconazole,[93] fluconazole,[94,95] ketoconazole,[96,97] itraconazole,[98] and posaconazole[98,99] activity in *Leishmania* species. Although the proliferation of many species of *Leishmania* is inhibited *in vitro* or in animal models by azole antifungals, the effect of ketoconazole and itraconazole in the treatment of human infections has been equivocal, ranging from high efficacy in *Leishmania mexicana* and *Leishmania major* infections to little or no activity against *Leishmania braziliensis* and *Leishmania donovani*[100] infections. Successful treatment of cutaneous leishmaniasis has been reported by posaconazole[101] and itraconazole,[102,103] although the results of studies on the chemotherapy of cutaneous leishmaniasis may be difficult to interpret due to the self-curing nature of cutaneous lesions.[28] Randomized clinical trials are needed to provide stronger evidence on their therapeutic efficacy.[104] Azoles in general have not been shown to be effective against visceral leishmaniasis, also known as kala-azar (black sickness), predominantly caused by *L. donovani* and *L. infantum*.[105] Ketoconazole and itraconazole are also not effective against post kala-azar dermal leishmanaisis, a recurrence of kala-azar that may appear on the skin of affected individuals up to 20 years after being untreated, partially treated, or even adequately treated.[106] Ketoconazole and itraconazole are less effective than antimonial agents in reducing hepatic parasites in murine model of *L. infantum* visceral leishmaniasis.[107]

The variability in azole action against the etiological agents of leishmaniasis could be partially related to the pharmacokinetic profile of the drugs. However, natural resistance arises from the biochemical differences between *Leishmania* spp. at the level of specific sterol requirements. Thus, lack of azole activity against naturally resistant *L. braziliensis* strain 2903 is due to the ability of downstream C-4 demethylase to act on the C-14 methylated substrates, thus preventing accumulation of the C-4/C-14 methylated toxic intermediate 14α-methyl-ergosta-8,24(24^1)-3β,6α-diol.[27]

3.3. Antifungal Azoles as Anti-Chagasic Drugs

Chagas disease, a parasitic disease prevalent in Latin America, is caused by infection by the protozoan parasite *Trypanosoma cruzi*, which is transmitted by an insect vector (the so-called "kissing bug") of the family *Triatominae*.[108] *T. cruzi* colonizes the heart, gastrointestinal tract and nervous system, causing progressive inflammation which results in chronic human cardiopathy and/or gastrointestinal dysfunctions.[109] According to the World Health Organization (WHO),[110] *T. cruzi* infects around 7−8 million people worldwide. International travel, infected blood transfusions, coinfection with HIV, and migration of the insect vector that spreads *T. cruzi* all help to drive up the number of cases and push the incidence outside its historic geographic range.[111] With no vaccine available, Chagas disease is now seen in Europe, North America, and Asia, and seems set to become an urgent public health issue in countries far beyond its source in South America.

Though at any stage it can prove fatal, Chagas disease can be asymptomatic in both the acute stage following initial infection and the subsequent chronic stage. As a result, infected people may not seek treatment in a timely fashion. Until recently, antiparasitic treatment was not recommended for chronic patients due to the prevailing hypothesis of an autoimmune origin of the disease.[112] The standard of practice has changed recently, however, and treatment is now recommended for all acute and chronic patients.[113,114] An important caveat is that current treatments can be unsafe. The only available drugs, the nitro heterocyclic compounds nifurtimox and benznidazole, both developed more than 40 years ago, carry the risk of grave side effects,[115] probably due to oxidative or reductive damage to host tissues. Neither drug is approved by the FDA for use in the United States. Against the initial acute stage these drugs are about 80% effective, but in the much longer and epidemiologically prevalent chronic stage their efficacy is controversial.[116] To complicate matters still further, some *T. cruzi* strains are naturally resistant or have developed resistance to these old drugs.[117−121] Consequently, it is clear that new ways of treating Chagas disease must be a research priority.

In a shift in anti-Chagas disease strategy, the azole drugs fluconazole, ketoconazole, and posaconazole have been used to target CYP51 in *T. cruzi*-infected mammalian cells.[112,122−124] Originally developed for pathogenic fungal infections, these drugs have been shown to inhibit the same target in fungal and parasitic infections: the biosynthesis of ergosterol and related 24-alkyl sterols, essential components of cell membranes in both fungi and protozoa. The anti-Chagasic potency of posaconazole has been demonstrated in an animal model of *T. cruzi* infection[125−127] and has a precedent of successfully curing a patient with chronic Chagas disease and systemic lupus erythematosus.[128,129] The MIC of posaconazole versus *T. cruzi*

is 0.3 nM in cultured Vero cells.[126] Parasitological, serological, and PCR analyses confirmed 90−100% cure of animals (85−100% survived) in a murine model of acute *T. cruzi* infection treated with 10 mg/kg posaconazole daily.[126] In addition, posaconazole led to 60−70% cure of the animals (75−85% survived) in a chronic Chagas disease model. These curative activities were remarkable, since ketoconazole displayed only a 20% cure rate among 60% survivals at 30 mg/kg daily dose in the acute model and no cure in the chronic Chagas disease model.[126]

In vitro and *in vivo* anti-*T. cruzi* activities of ravuconazole were also investigated. This drug displayed very potent inhibition against the extracellular epimastgote and intracellular amastigote forms with MIC of 300 and 1 nM, respectively.[130] However, curative trypanocidal activity of ravuconaozle was restricted to a murine model of acute Chagas disease such as nitrofuran/nitroimidazole-susceptible (CL) and partially drug-resistant (Y) strains of *T. cruzi*, and no curative activity was observed in the fully drug-resistant Colombiana strain.[130] Furthermore, in a canine model of acute Chagas disease, ravuconazole significantly suppressed parasite level, but did not show curative potency against the Y and Berenice-78 *T. cruzi* strains.[131]

Another antifungal agent in clinical trials, albaconazole (Figure 5), displayed very effective suppression of parasite proliferation in animals infected with the Berenice-78 strain, but its curative activity was negligible even in the longer treatment period (150 doses).[132] TAK-187 (Figure 5), possessing a long half-life (35.6 h in mice and 87 h in monkeys), was studied in animal models of *T. cruzi* infection, and showed 100% survival rate of mice infected with the CL, Y, and Colombiana strains.[133] Complete parasitological cure was also achieved against the CL strain, while TAK-187 induced 50−70% cure rate against Y and Colobmiana strains at 20 mg/kg daily or e.o.d.[133] In addition, 80−100% cures of survivors (80−100%) were attained in both acute and chronic models of *T. cruzi* infection at 10−20 mg/kg e.o.d.[133] It was also reported that *T. cruzi*-induced cardiac damage was more effectively prevented by TAK-187 than benznidazole.[134]

Repurposing existing drugs is the quickest way to fill NTD clinical pipelines to bring forward drugs for those in need. The CYP51 inhibitors posaconazole and ravuconazole, which have undergone extensive pharmacological and toxicological optimization in antifungal programs, and demonstrated efficacy and curative activity in animal models of Chagas disease, have been recently tested in clinical trials.[135−137] Lack of curative effect has been reported for both compounds.[138,139] At the end of the ravuconazole treatment in the E1224/benznidazole trial (Bolivia),[137] all treatment groups had high percentages of parasite clearance in blood (79−91%, defined as parasite levels below the limit of detection by quantitative-PCR (qPCR)). After one year follow-up, patients receiving ravuconazole at low dose (200 mg/week, 8 weeks) or short dose (400 mg/week, 4 weeks) progressively relapsed, and their parasite levels by qPCR reached values indistinguishable from those receiving placebo. Patients receiving ravuconazole at high dose (400 mg/week for 8 weeks) or benznidazole (5 mg/kg for 60 days) had 30% or 81%, respectively, of parasitemia clearance. For the relapsed patients, the parasite levels were statistically indistinguishable among the two treatments, and very close to the limit of detection.[138] Further trials, at different doses or in combination with benznidazole, are thus indicated.

Significantly more patients in the posaconazole groups than in the benznidazole group had treatment failure during follow-up in the CHAGASAZOL Trial (Spain).[136,139] Antiparasitic activity was assessed by testing for the presence of *T. cruzi* DNA, using real-time-PCR (rt-PCR), during the treatment period and 10 months after the end of treatment; all the drugs were administered for 60 days. During the treatment period, all but two patients tested negative for *T. cruzi* DNA. During the follow-up period, in the per-protocol analysis, 90% of the patients receiving low-dose posaconazole (100 mg twice daily) and 80% of those receiving high-dose posaconazole (400 mg twice daily), as compared with 6% receiving benznidazole (150 mg twice daily), tested positive in the rt-PCR assay.

Factors explaining the disappointing efficacy of ravuconazole and posaconazole in humans may include the folowing: (1) Intracellular localization of *T. cruzi* parasites in chronic infection, largely in heart, gut, and skeletal muscles, requires drugs with different pharmacokinetic profiles. Large volume of distribution and long terminal half-life are two key parameters of drug efficacy in Chagas disease chemotherapy.[112,130,131,140] (2) The stochastic nature of the *T. cruzi* infection[141] may require longer drug exposure. (3) Finally, sequence/structural differences between the *T. cruzi* and fungi CYP51 targets potentially attenuate the activity of the antifungal CYP51 inhibitors against the *T. cruzi* enzyme. On the basis of these considerations, it is expected that targeted inhibitors, optimized specifically by structure-based drug-design and close monitoring of PK parameters, will be more effective against human *T. cruzi* infections than the repurposed antifungal agents.

4. CYP51 AS A DRUG TARGET FOR CHAGAS DISEASE

4.1. X-ray Structures of CYP51

A drug target in several human pathogens, CYP51 has been intensively studied over the past decade. Significant progress has been made in characterization of CYP51 orthologues from *Mycobacterium tuberculosis*,[45,142−145] kinetoplastids, including *Trypanosoma cruzi*,[146−152] *Trypanosoma brucei*,[146,153−156] and *Leishmania infantum*,[42] *Saccharomyces cerevisiae*,[157] as well as the human host[158] (Table 1). This accumulated knowledge supports structure-aided drug development against protozoan parasites, including *T. cruzi*. It also advances antifungal drug discovery research programs by providing templates for molecular modeling of fungal CYP51 drug targets and also laying the groundwork for understanding azole resistance phenomena.[159]

Eukaryotic P450 enzymes associated with the ER, including CYP51, are divided into an N-terminal transmembrane domain and a catalytic core composed of a four-helix bundle with a trigonal prism-shaped structure. The N-terminal transmembrane domain important for subcellular localization and tethering to the ER is usually removed from the recombinant protein constructs to facilitate catalytic domain expression and purification. *S. cerevisiae* CYP51 is the only characterized full-length P450 enzyme with amphipathic and transmembrane helices resolved in the X-ray structure.[157] Rigid interactions between the transmembrane anchor and the catalytic domain serve to precisely orient the substrate entry channel relative to the lipid bilayer.[157] Topologically, P450 catalytic core folds as a single domain. Structurally, it is subdivided into two subdomains, the α-helical and β-sheet-rich domain.[160,161] The subdomain interface serves as a substrate binding site, with size and topology modulated by the concerted motion of the BC-

Table 1. CYP51 Drug–Target Complexes in PDB Databank as Assessed in June 2014

Organism	Ligand chemical structure	Small-molecule ID	PDB ID	Res.	Ref.	Organism	Ligand chemical structure	Small-molecule ID	PDB ID	Res.	Ref.
T. cruzi	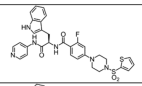	T9H	4COH	2.08 Å	151	*T. brucei*	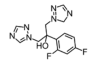	TPF	2WV2	2.70 Å	146
T. cruzi	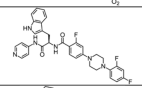	WVN	4C0C	2.04 Å	152	*T. brucei*	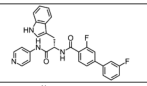	18I	4BJK	2.67 Å	154
T. cruzi	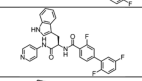	TU1	4BMM	2.84 Å	152	*T. brucei*	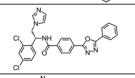	VNI	3GW9	1.87 Å	153
T. cruzi	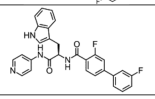	5PS	4BY0	3.10 Å	147	*T. brucei*	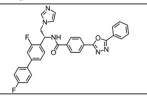	VFV	4G7G	2.05	N/A[d]
T. cruzi	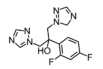	TPF	2WX2	2.27 Å	146	*T. brucei*	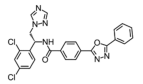	VNT	4G3J	1.83	N/A[d]
			2WUZ	2.35 Å	146						
			3KHM[a]	2.85 Å	148	*T. brucei*	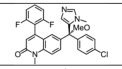	JKF	3TIK	2.05 Å	156
T. cruzi	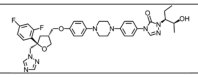	POZ	3K1O[b]	2.89 Å	148	*T. brucei*	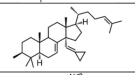	LNP	3P99[c]	3.00 Å	155
T. cruzi	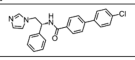	VNF	3KSW	3.03 Å	148	*L. infantum*		TPF	3L4D[a]	2.75 Å	42
T. cruzi	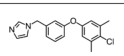	NEE	4H6O	2.80 Å	149	Human	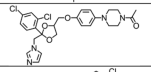	KKK	3LD6	2.80 Å	158
T. cruzi	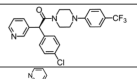	UDO	3ZG2	2.80 Å	150	Human	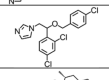	ECL/ ECN	3JUS	2.90 Å	158
T. cruzi	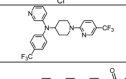	UDD	3ZG3	2.90 Å	150	*S. cerevisiae*	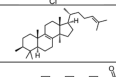	LAN	4LXJ	1.90 Å	157
T. brucei	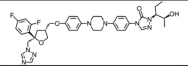	X2N	2X2N	2.60 Å	146	*S. cerevisiae*	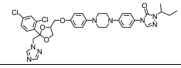	1YN	4K0F	2.19 Å	157

[a]A nitrogen atom in the triazole ring of fluconazole is refined in sp^3 instead of sp^2 electronic configuration. [b]One of the stereocenters in posaconazole is erroneously assigned. [c]Lanosterol derivative LNP is in a bent conformation of the 5β-skeleton, in contrast to the flat shape of the biogenic sterol lanosterol. [d]N/A: structure available in PDB only.

dx.doi.org/10.1021/cr5003134 | Chem. Rev. 2014, 114, 11242−11271

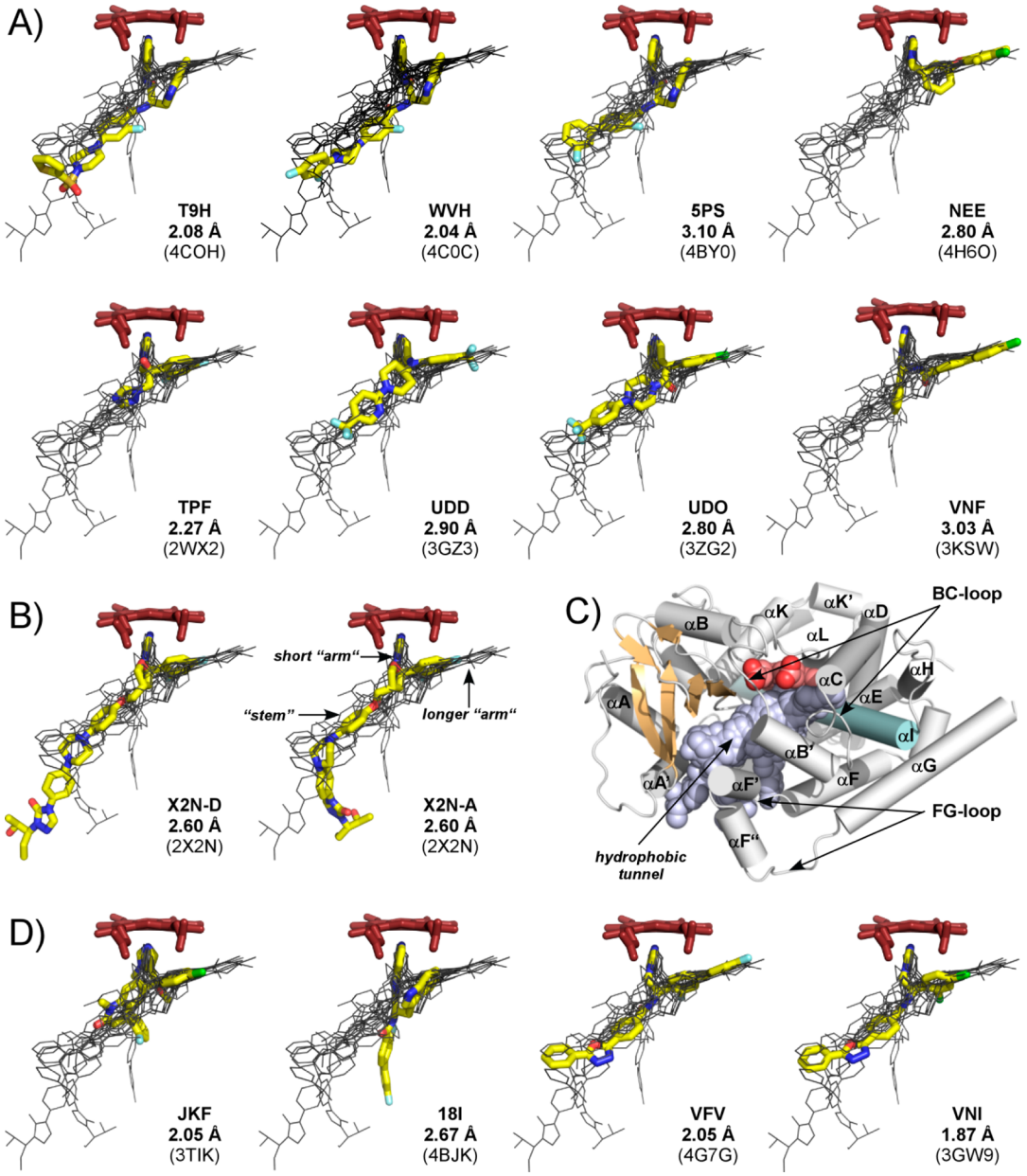

Figure 7. Y-shaped inhibitor envelope in CYP51. Inhibitor envelope derived from the 3-D alignments of eight *T. cruzi* (A) and six *T. brucei* (B, D) CYP51 drug−target complexes. All superimposed ligands are shown in black lines. The inhibitor highlighted in yellow is labeled by the small-molecule code, followed by resolution and the PDB ID of the corresponding structure (in parentheses); heme is in red sticks. (B) Two different posaconazole conformers as observed in 2X2N structure. (C) Inhibitor envelope delineated by the van der Waals spheres of the superimposed inhibitors (light blue) is shown in the same orientation surrounded by the protein secondary structure elements with helices represented by cylinders. The I-helix, longest in P450, is in cyan, and β-sheets are in wheat; heme is in pink, and oxygen atoms of propionate groups are in red. Reprinted with permission from ref 151 (Copyright 2014 Wiley-VCH Verlag GmbH & Co. KGaA, Weinheim).

and FG-loops, the F- and G-helices, and bending of the central (and longest) P450 α-helix, the I-helix, which runs over the distal surface of the heme across the entire protein structure.[49,160,161] Secondary structure nomenclature is according to the generally accepted scheme introduced by Poulos et al. for bacterial P450cam.[162] Extra helices, designated prime or double-prime, are typical within the longer BC- and FG-loops of the eukaryotic P450s. Thus, B′ and F′/F″ helical structures directly interact with the inhibitors in the eukaryotic CYP51 (Figure 7).

The soluble bacterial CYP51 orthologue from *Mycobacterium tuberculosis* lacking the N-terminal transmembrane domain demonstrates the extreme solvent exposure of the heme prosthetic group due to the bent I-helix and the unusual conformation of the BC-loop, which remains wide open even when inhibitors[142,143,145] or substrate analogues[45,144] are bound in the active site. In eukaryotic CYP51, the substrate binding site is shaped as a tunnel buried in the protein interior leading from the protein surface to the heme group (Figure 7).[146,158] Essentially the same ground-state closed conformation is observed in low-resolution structures of the CYP51 drug−target complexes,[148,150] while higher resolution structures demonstrate the fit induced by 4-aminopyridyl-based inhibitors bound in the active site.[151,152]

T. cruzi CYP51 belongs to a category of proteins whose crystallization propensity depends on interactions with the

dx.doi.org/10.1021/cr5003134 | *Chem. Rev.* 2014, 114, 11242−11271

ligand bound in the active site. The accuracy of low-resolution structures largely relies on the topology/parameter restraints used during refinement, particularly as they pertain to new small-molecule ligands, which are not included in default computer databases used by structure determination software. Yet, if not misinterpreted, low-resolution structures can deliver information on high scientific and practical value. A complicating factor, however, can be misinterpretations of electron density associated with inaccurate restraint refinement against low-resolution data, as has occurred with the erroneous assignment of sp^3 rather than sp^2 configurations to nitrogen atoms of the triazole ring, resulting in deformed fluconazole ligands in the 3KHM[148] and 3L4D[42] CYP51 structures; a related error is the assignment of the absolute configuration of one of the stereocenters of posaconazole in 3K10.[148]

4.2. Inhibitor and Substrate Envelopes

The large hydrophobic CYP51 active site promiscuously permits small-molecule binding.[163] The inhibitor envelope deduced from superimposed CYP51 drug−target complexes branches into a Y-shape with an elongated "stem" and two shorter "arms" (Figure 7).[151] The shortest arm orthogonal to the heme macrocycle invariantly binds to coordinate to the heme iron with the aromatic nitrogen atom on the azole or pyridyl/pyrimidyl moiety, while the longer arm, consisting of one or two fused aromatic functionalities, binds at an angle to the heme plane. The stem of the envelope is much longer, allowing as many as four linearly fused rings to bind in the hydrophobic tunnel, as exemplified by posaconazole (X2N). Each of the inhibitors only partially utilizes the binding envelope. Three inhibitors, VNF, VFV, and NEE, extend into the longer arm of the envelope arguably occupied by the sterol aliphatic side chain;[164] fluconazole (TPF) and tipifarnib (JKF) largely utilize the central space adjacent to the heme group, while VNI, VNF, and posaconazole (X2N) explore the stem of the envelope. The particularly long posaconazole moiety extends into the exterior space, adopting alternative conformations at the terminal unit (Figure 7B). Inhibitor nomenclature is according to small-molecule codes associated with each molecule in the PDB databank.

In contrast to the inhibitor envelope deduced from the 3-D alignments of multiple drug−target complexes, the substrate envelope is yet to be convincingly defined in CYP51. The cocrystal structure featuring the substrate analogue methyl-enecyclopropyl-Δ7-24,25-dihydrolanosterol (LNP) bound to *T. brucei* CYP51 (PDB ID 3P99)[155] depicts, at resolution of >3 Å, this sterol derivative with an unnatural 5β-configuration of the H atom at the C-5 bridgehead position, which is not consistent with the 5α-configuration of the lanosterol precursors used in the synthesis of the substrate analogue.[155,165,166] This causes the sterol tetracycle in LNP to adopt a bent conformation of the 5β-skeleton (Figure 8A), in contrast to the flat shape of the biogenic sterol precursor, lanosterol, which has 5α-configuration (Figure 8B).[167] While these structural differences are functionally significant in nature, difference in shapes of the two sterol skeletons was not commented on by the authors.[155] We infer that the inconsistence may be again an artifact of refinement against low-resolution data. Furthermore, the binding orientation of LNP in the active site of *T. brucei* CYP51 is opposite to that of lanosterol in fungal CYP51. Lanosterol substrate is flipped in *S. cerevisiae* CYP51 (4LXJ),[157] with the aliphatic side chain pointing in an opposite direction from that of *T. brucei* CYP51

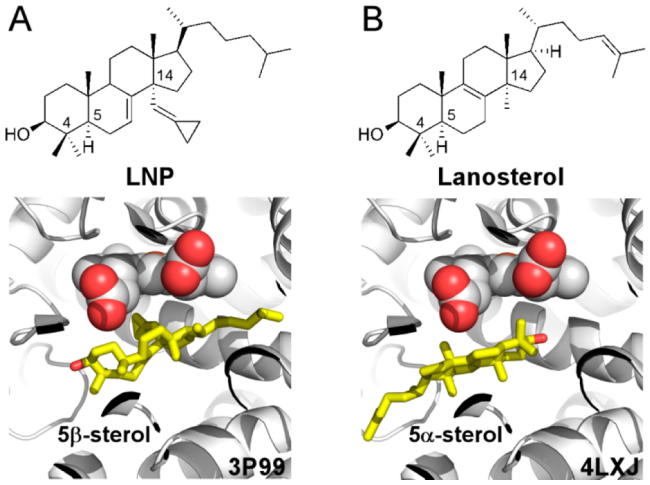

Figure 8. Substrate binding controversy in CYP51. Opposite orientations of the sterol molecules featured in the *T. brucei* (A) and *S. cerevisiae* (B) CYP51 structures. Bent conformation of the 5β-skeleton in 3P99 (A) contrasts to the flat shape of lanosterol in 4LXJ (B) Inhibitors are shown in yellow sticks, and heme is in van der Waals spheres; protein is represented by a ribbon. Heteroatoms are colored according to the atom types: nitrogen in blue, oxygen in red. Images here and throughout are generated using PYMOL[168] unless specified otherwise.

(Figure 8).[157] However, electron density for the sterol molecules lacks sufficient detail in either structure to convincingly resolve the controversy. For comparison, the unambiguous orientation of the estriol molecule lacking the aliphatic side chain in *M. tuberculosis* CYP51 (resolution 1.55 Å; PDB ID 1X8V)[45] is consistent with the sterol orientation suggested by the *T. brucei* 3P99 structure.

4.3. High-Throughput Hit Identification

4.3.1. Phenotypic Screens. Resent success in acquiring structurally diverse compounds for hit-to-lead optimization programs aiming at Chagas disease hinges on modern drug discovery strategies, including probing *T. cruzi* parasites or the CYP51 target in high-throughput format with diverse libraries of compounds, including those developed for different therapeutic applications. A major hit-generating effort to discover new *T. cruzi* inhibitors involves screening of compound libraries using robust phenotypic whole-cell parasite assays which fall into two categories: high-content image-based assays pioneered by Engel and coauthors[169] and colorimetric assays using the *T. cruzi* Tulahuen strain transfected by the β-galactosidase gene utilizing chlorophenol red β-D-galactopyranoside as a substrate, developed by Buckner and coauthors.[170] The *T. cruzi* luc strain expressing firefly luciferase is a complementary HTS drug discovery platform, which allows rapid assessment of compound performance *in vivo*.[152,171] In phenotypic assays, compounds are screened for their ability to inhibit replication of intracellular *T. cruzi* amastigotes inside host cells. Depending on the order of adding parasites and inhibitors, phenotype screening can be a "catch-all" method identifying compounds that kill extracellular trypomastigotes, inhibit host cell invasion, or inhibit parasite development inside the cells. However, the β-galactosidase-based assay does not readily provide information about toxicity of the compounds for host cells. The image-based assay distinguishes between the cell and parasite toxicity, but requires more sophisticated instrumentation and large data storage capacities. Both

dx.doi.org/10.1021/cr5003134 | *Chem. Rev.* 2014, 114, 11242−11271

phenotypic assays select compounds for cell permeability but do not provide information on mechanism of action, which distinguishes them from target-based assays.

Phenotypic screening of over 300 000 compounds at the Broad Research Institute gave momentum to follow-up efforts, including hit triage and early lead optimization studies by DNDi focusing on two promising inhibitor series, CM74 and CM100 (Figure 9).[172] Selected compounds in the CM100

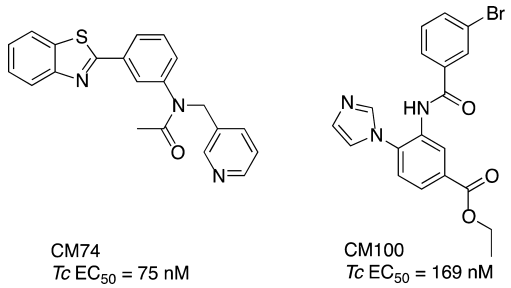

Figure 9. Structures of CM74 and CM100.

series demonstrated *in vivo* efficacy upon oral administration at 20 mg/kg, b.i.d. There were 60% of the mice who survived parasite-free in blood following b.i.d. treatment for 20 days, but they were not cured as determined by PCR analysis of tissues. On the basis of the structures consisting of a heterocycle and two additional lipophilic or aromatic motifs in a trigonal or tetragonal arrangement around a central atom, these compounds are recognized as potential CYP51 inhibitors, although their mechanism of action has not been confirmed.

Compounds containing known antifungal pharmacophores and compounds likely to be CYP51 inhibitors based on structural similarity with previously reported CYP51 inhibitors have been discovered in screens of other compound collections.[173] Eight such compounds available from a small laboratory library were identified in a screen against *T. brucei*, *T. cruzi*, and *L. donovani* (Figure 10). These azole derivatives showed moderate inhibition against *T. brucei* and *L. donovani* in micromolar range IC_{50}s.[173] However, *in vitro* anti-*T. cruzi* activity of compounds **5**, **6**, **7**, and **8** were in the low nanomolar range with about 1000-fold selectivity against rat myogenic L6 cells.[173] Enantiomerically pure compounds were prepared,[174,175] and it was found that *S*-enantiomers had better inhibition potency against *T. cruzi* than the *R*-enantiomers. No information on the utility of these compounds in animal models is yet available.

A phenotypic screen of Broad Institute's diversity-oriented synthesis (DOS) collection singled out compound ML341 for low nanomolar growth-inhibition activity versus *T. cruzi* and trypanocidal at 40 nM.[176] Compared to commercial vendor libraries, DOS compounds have distinct ring architectures, contain several stereocenters, and have a higher content of sp^3-hybridized carbon atoms. SAR data generated for ML341 point at the indispensable role of the aromatic heterocycle for inhibitory potential, particularly favoring 4-pyridyl analogue (**9**, IC_{50} = 1 nM) over the 3-pyridyl (**10**, 45 nM) and the sterically hindered 2-pyridyl (**11**, 344 nM) analogues (Figure 11). These data are consistent with the potential for these compounds to coordinate to heme iron and serve as CYP51 inhibitors, although the molecular target of ML341 has not been identified. However, since compounds **12**, **13**, and **14**, which do not include iron coordinating units, also show low

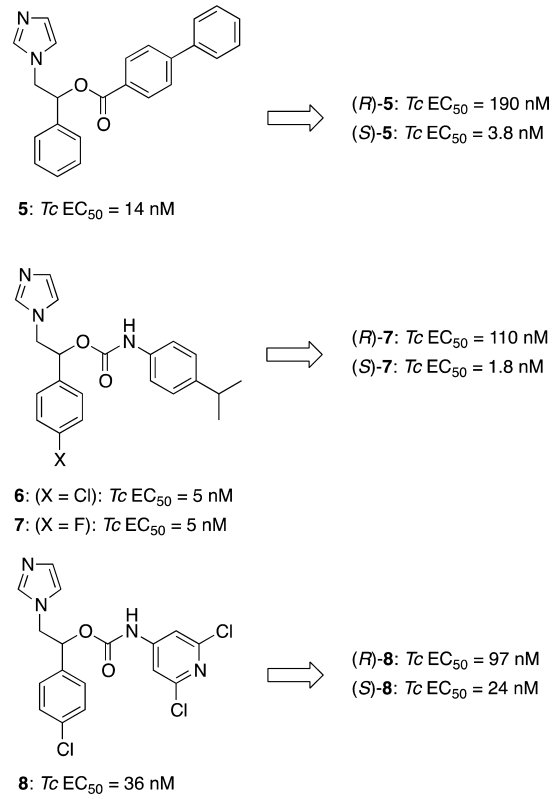

Figure 10. Potent anti-*T. cruzi* hits from small compound collection.

micromolar inhibition potency, there might be other unknown targets of these ML341 analogues.

4.3.2. Target-Based Screens. Screening of CYP51 against a library of synthetic small molecules was performed, first using *M. tuberculosis* CYP51 orthologue[177] and then recombinant *T. cruzi* CYP51 in order to identify structurally diverse CYP51 inhibitors.[163] The property of the ferric heme iron Soret band of the P450 enzyme to shift in response to ligand binding was utilized to select chemotypes with high binding affinity to the CYP51 target.[163,177] Thus, the 4-aminopyridyl-based chemotype **15** was identified.[143] On the basis of potency in cell-based assays and in a mouse model of *T. cruzi* infection,[143,145] the *N*-indolyl-oxopyridinyl-4-aminopropanyl analogue, LP10 (**16**, Figure 12), was selected as a starting point for hit-to-lead optimization. Rounds of analogue design, compound synthesis, testing, and analysis of structure–activity and structure–property relationships led to substantially improved inhibitors,[147,151,152,154] as discussed in section 5.2.

Through a series of high-throughput screening and cross-validation steps, Gunatilleke and coauthors[163] have identified a diverse array of low molecular weight submicromolar and low micromolar hits, demonstrating that CYP51 in *T. cruzi* is a rather permissive target for small molecules (Figure 13). Cheminformatic analysis of hits using an algorithm implemented in the Similarity Ensemble Approach (SEA) online research tool[178] indicates CYP51's similarity to other P450 drug targets, including thromboxane synthase (CYP5), fatty acid ω-hydroxylases (CYP4), 17α-hydroxylase/17,20-lyase (CYP17), and aromatase (CYP19). These enzymes have been targeted by the pharmaceutical industry for cardiovascular disease,[179] metabolic disorders of lipid metabolism and inflammation,[180] prostate cancer,[181] and estrogen receptor-positive breast cancer,[182] respectively. Cheminformatic searching in the SEA

dx.doi.org/10.1021/cr5003134 | *Chem. Rev.* 2014, 114, 11242–11271

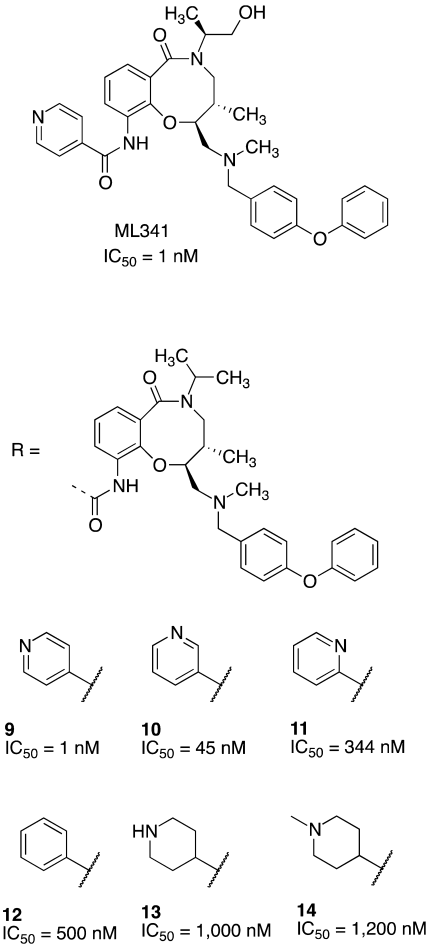

Figure 11. ML341 and its analogues from a screen of a diversity oriented synthesis-derived compound collection.

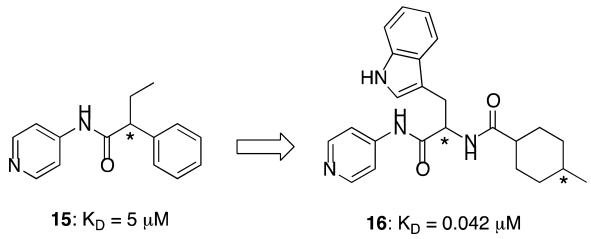

Figure 12. 4-Aminopyridyl hits from target-based screen.

databases revealed the unexpected resemblance of the highly scored hits, **17**–**19**, to inhibitors of glutaminyl-peptide cyclotransferase, an enzyme unrelated to the CYP family either by sequence or structure. Human glutaminyl-cyclase which catalyzes pyroglutamic acid formation at the N-terminus of amyloid peptides, is potentially involved in the development and progression of neurodegenerative disorders.[183]

A target-based high-throughput screen against *T. cruzi* CYP51 by the research group at Vanderbilt identified the amide form of indomethacin (COX-2 inhibitor), which displayed modest binding affinity to CYP51 and antiparasitic potency against *T. cruzi* in cell-based assay (Figure 14).[184] The most potent hit in this class, compound **28**, possessed submicromolar EC_{50} against *T. cruzi* amastigotes, leading to a decrease in the number of intracellular parasites. In addition, compound-**28**-treated *T. cruzi* cells produced altered sterol composition, compared to untreated parasites.

The unexpected promiscuity of CYP51 revealed by target-based screens may potentially be utilized in a piggyback strategy for identifying a chemical starting point (e.g., glutamyl-peptidyl cyclotransferase inhibitors) for antiparasitic therapy development, while structure–activity relationships derived from parasite assays could lead to disease-specific clinical candidates. Diversification of leads for CYP51 inhibitors should offer the medicinal chemist new choices in terms of chemical accessibility and prospects for lead optimization. In addition, multiple leads lower the risk of drug attrition in the case of undesirable ADMET properties.

5. *T. CRUZI* CYP51 INHIBITORS

Promising activity of repurposed azole drugs in *in vitro* and *in vivo* animal models of *T. cruzi* infection has triggered research on parasite-specific CYP51 inhibitors focused exclusively on anti-*T. cruzi* activity. These efforts are aimed to overcome two major limitations to the piggyback approach: (i) structural differences between the parasites and fungi CYP51 molecular targets potentially limiting the potency and specificity for *T. cruzi* CYP51, and (ii) differences in pharmacokinetic drug profiles due to intracellular localization of *T. cruzi* parasites in deep tissues.[112,140] It seems reasonable that targeted inhibitors, optimized by using structure-based drug-design with monitoring of PK parameters and inhibition of human CYPs involved in metabolism of xenobiotics, will be more effective in developing efficacious treatments of human *T. cruzi* infections compared to use of repurposed antifungal agents.

Compounds inhibiting CYP51 belong to chemically distinct classes such as imidazole, triazole, pyridine, and pyrimidine derivatives. This classification is based on the structure of the heme Fe-coordinating aromatic heterocycle present in each inhibitor. Although the electronic properties of the nitrogen atoms in the heterocyclic rings differ significantly, no bias for any particular Fe-coordinating group was observed in a target-based high-throughput screen, where distribution of the heme Fe-coordinating heterocycles among the approximate 200 hits reflects the frequency of each group in the small-molecule library.[163] This observation suggests a significant role for the rest of the inhibitor molecule in defining specificity and selectivity to the molecular drug target by means of multiple drug–target interactions. Nevertheless, the role of the heterocycle seems indispensable in CYP51 inhibitors. For instance, reducing the Fe-coordinating capacity of the 4-aminopyridyl-based analogues abolishes inhibition of CYP51.[185] Given the promiscuity of the rest of the binding site to small-molecule structures,[163] the method of classification of CYP51 inhibitors by Fe-coordinating heterocycles has demonstrable utility. In this review, we adopt this method; compounds which do not form a coordination bond to the heme iron are referred to as substrate mimetics. Imidazole and triazole CYP51 inhibitors constituting a conazole class of the antifungal drugs[72] are also known under the combined name of the azole inhibitors. Some of the *T. cruzi*-specific CYP51 inhibitors which have been developed recently fit this combined azole category, while others are grouped as pyridine/pyrimidine derivatives.

5.1. Azole Derivatives

5.1.1. Tipifarnib: "Piggybacking" on Anticancer Drug Development. A popular approach in drug discovery against parasitic diseases is to piggyback on pharmaceutical industry

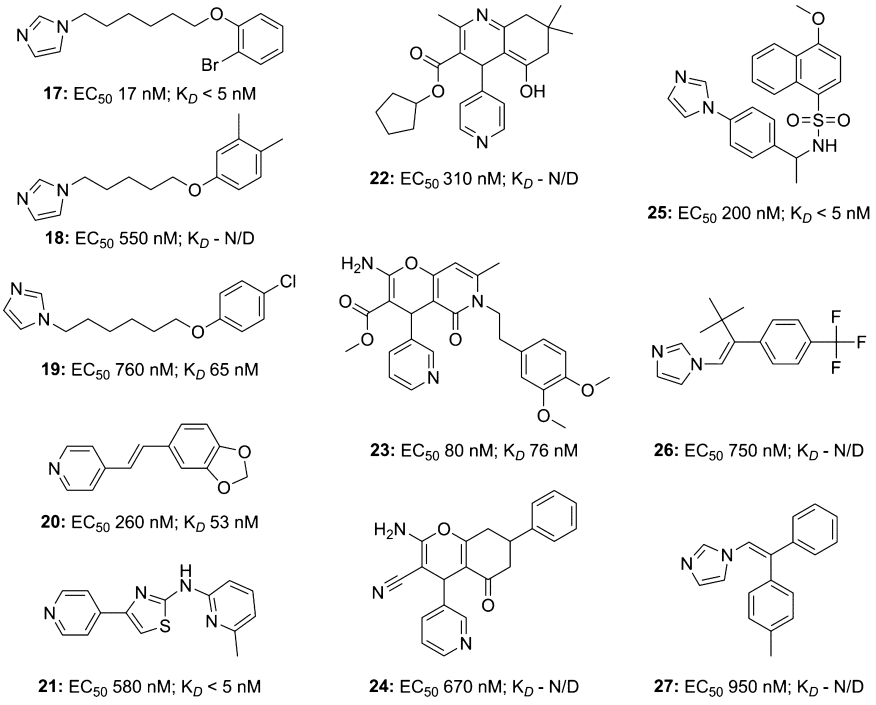

Figure 13. Top hits from target-based screen against *T. cruzi* CYP51. Compounds selected for low-nanomolar binding affinity in the HTS assay. Depending on compound availability, K_D values (shown) have been confirmed in manual assays. EC_{50} values obtained against *T. cruzi* parasites in image-based whole-cell assay.[163]

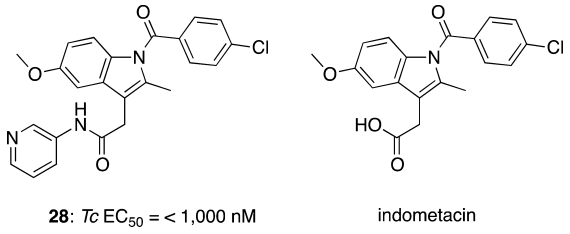

Figure 14. Indomethacin amide analogues as *T. cruzi* CYP51 inhibitors.

research efforts directed at development of drugs against other diseases.[186] For example, the cancer clinical drug candidate tipifarnib (**29**), an inhibitor of human protein farnesyltransferase (hPFT),[187,188] was found to efficiently block endogenous ergosterol biosynthesis in *T. cruzi* by binding to CYP51.[189,190] A series of tipifarnib analogues were generated in the course of hit-to-lead optimization to reduce inhibition of hPFT and enhance efficacy against *T. cruzi* (Figure 15).[191−193] The chlorine atom in the *para*-position of ring 1 and the methoxy group at the chiral center provided optimal contacts of the tipifarnib analogue with CYP51, but disabled interactions with hPFT. Combined with the methyl group at C-2 of ring 2, these modifications led to a 7-fold increase of potency in compound **30** compared to tipifarnib, while reducing inhibition of hPFT more than 10 000-fold.[193] Inhibitor **30** was subjected to efficacy studies in mice infected by the Tulahuen strain. Administered by oral gavage beginning day 7 postinfection, first at 100 mg/kg, b.i.d., for 6 days, and then followed by 50 mg/kg, b.i.d., for 20 days, **30** suppressed parasitemia to microscopically undetectable levels through day 100 postinfection. However, parasitological cure was not achieved; surviving parasites were recoverable by hemoculture.

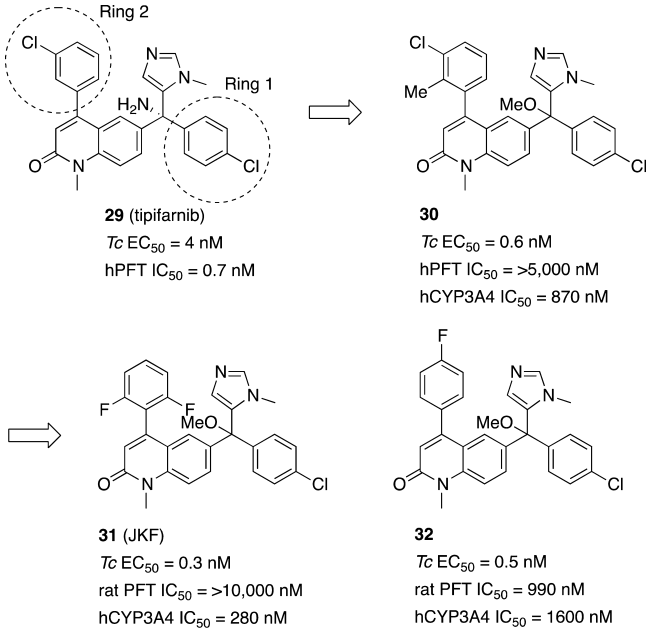

Figure 15. Tipifarnib and its *T. cruzi*-specific analogues.

Compound **30** is a mixture of quinolone ring atropisomers, which could complicate drug development. Thus, analogues **31** and **32**, possessing a C_2-symmetric ring 2 or a ring 2 lacking ortho substitution (substitution patterns that not subject to atropisomerism), were synthesized and showed to have similar to **30** inhibition potency and selectivity against *T. cruzi* amastigotes cultured in mammalian cells.[192] The pharmacokinetic profile and potency of racemic inhibitor **32** was superior to **31**, but **32** failed to cure mice infected by *T. cruzi* Y strain when administered at 40 mg/kg for 20 days. The plasma concentration of **32** was significantly less than that of

dx.doi.org/10.1021/cr5003134 | *Chem. Rev.* 2014, 114, 11242−11271

posaconazole (C_{max} = 4.7 vs 14.3 μM; AUC_{inf} = 22.9 vs 509 μM × h); the estimated $C_{av,ss}$ (average steady-state concentration) values on day 20 of **32** and posaconazole are 1.9 and 141 μM, respectively. Thus, throughout the treatment period, the concentration of posaconazole remained high (>30 μM for the full 20-day), while the concentration of **32** was below 10 μM, which probably contributed to the lower efficacy of **32** compared to posaconazole. The two enantiomers of **32**, separated by chiral HPLC, differ significantly in potency *in vitro*. The enantiomer with longer retention time, 185.4 min, is less potent (EC_{50} = 26.3 nM and K_d = 3800 nM) than the enantiomer with shorter retention time, 164.3 min (EC_{50} = 0.31 nM and K_d = 180 nM). The absolute stereochemistry was not established, but on the basis of the cocrystal structure of *T. brucei* CYP51 with analogue **31** (Figure 16), it was assumed

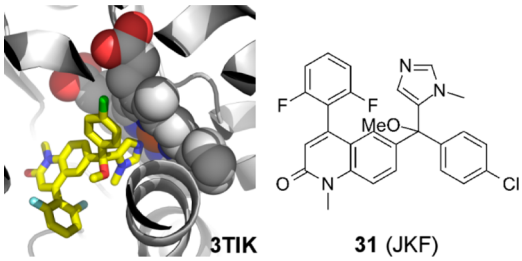

Figure 16. Tipifarnib analogue **31** (JKF) in *R*-configuration bound in the active site of *T. brucei* CYP51 (PDB ID 3TIK).

that the isomer with *R*-configuration was more potent,[156] with qualification that *T. brucei* CYP51 has 85% sequence identity to the *T. cruzi* orthologue. However, *in vivo* efficacy studies of single enantiomer **32** have not been reported yet.

5.1.2. Dialkylimidazole Analogues: From Protein Farnesyl Transferase to CYP51 Inhibitors. Dialkylimidazole analogues have been developed as structurally simple inhibitors of CYP51 by the same research laboratory where tipifarnib analogues were developed. Through an academic–industrial research partnership, FTI-2220 (**33**) was identified as a mimetic of the tetrapeptide substrate of protein farnesyltransferase (PFT), Cys-Val-Ile-Met (Figure 17).[194] FTI-2220 showed strong inhibition of *T. brucei* PFT (with IC_{50} = 8 nM). The methyl ester prodrug (**34**) was less potent against *T. brucei* (ED_{50} = 500 nM) in cell culture.[194] Interestingly, compounds like **35** which lack the methionine residue of **33** were highly potent against *T. cruzi* in cell-based assays (ED_{50} = 0.5 nM), even though most inhibitory activity against *T. cruzi* PFT disappeared. Further studies on *T. cruzi* labeled with ^{3}H-mevalonolactone showed accumulation of lanosterol and complete blockade of downstream sterol synthesis with this class of inhibitors.[189] Since the methyl ester of **35** is susceptible to hydrolysis in mouse serum, analogues **36** and **37** were used in efficacy studies in a murine model of Chagas disease. Mice were treated with 50 mg/kg of each inhibitor twice daily by oral gavage for 14 days. Up to 99% parasitemia levels were suppressed in treated mice groups, and all mice in these groups survived to 101 days postinfection. In contrast, all of the untreated mice succumbed to overwhelming infection by day 18.[189] Due to promising *in vivo* efficacy along with the relatively simple synthesis of compounds **36** and **37**, extensive SAR studies were performed in order to further increase potency against *T. cruzi*. Introduction of an *ortho*-amino group in the 1,4-biaryl moiety led to about 10-fold increase in potency

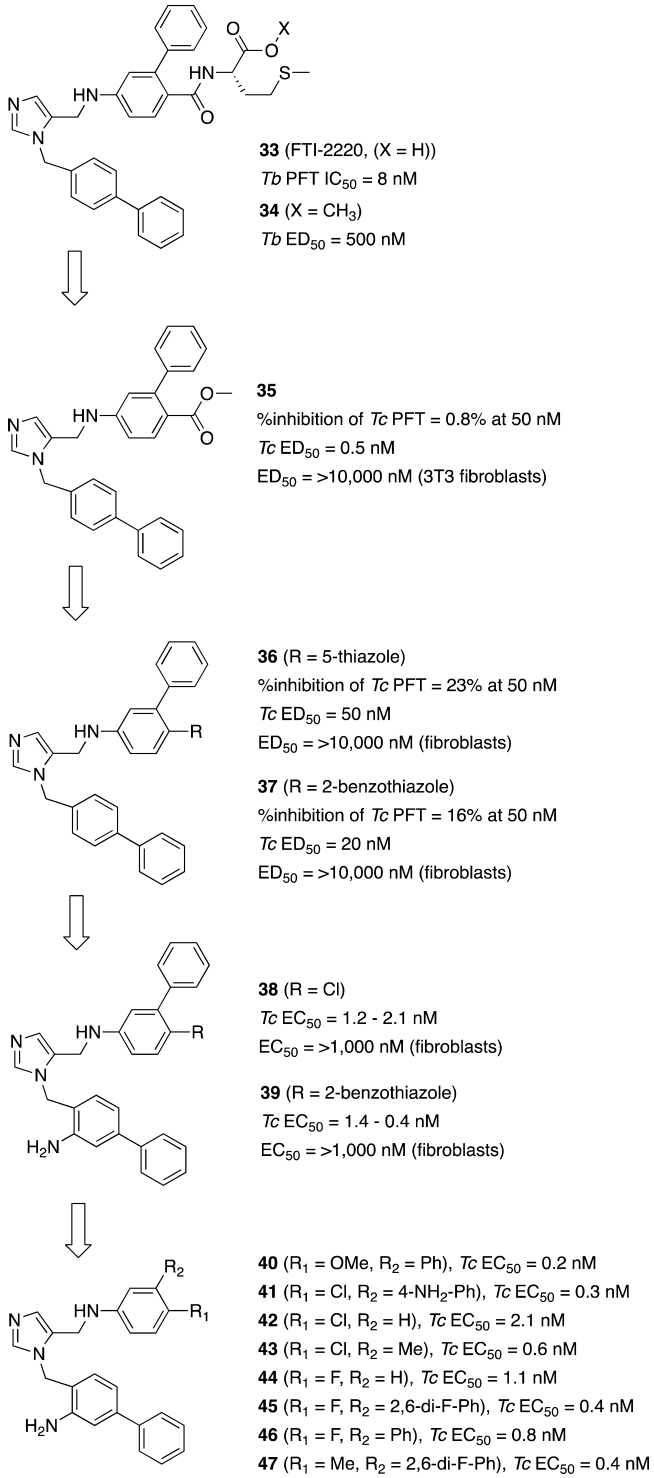

Figure 17. Dialkylimidazole analogues and their inhibition potency against *T. cruzi*.

against *T. cruzi* and retained a good pharmacokinetic profile: AUC_{0-5h} (**38** and **39**) = 6.3 and 28.7 μg × h/mL. Compounds **38** and **39** were subjected to an *in vivo* efficacy study using the Tulahuen strain at 50 and 20 mg/kg, b.i.d, po, for 20 days. Parasitemia decreased to microscopically undetectable levels without apparent side effects, and the treated mice exhibited gradual weight gain. However, PCR blood test at day 100 postinfection was positive in 2 of 6 mice treated with compound **39** at 50 mg/kg, and in all six mice treated with

compound **38** at 50 mg/kg. Systematic modifications of **39** were carried out to gain potency and reduce molecular weight and lipophilicity. Of the 75 dialkylimidazole-based inhibitors that were tested in cell-based assay, eight inhibitors (**40**–**47**) possessed similar or only slightly improved potency against *T. cruzi* as well as reduced molecular weight and lipophilicity, compared to **39**.[195] However, follow-up *in vivo* studies have not yet been reported for these dialkylimidazole-based inhibitors.

5.1.3. NEU321: Phenotypic Screen Hit. Screening of 2000 compounds from the DIVERSet library (ChemBridge Corporation, San Diego, CA) chosen for pharmacophore diversity led to identification of the imidazole-based *T. cruzi* inhibitor, compound **48**, which showed strong trypanocidal activity (EC_{50} of 23 nM) manifested in lysis of the intracellular amastigote membranes.[196] Screening of >300 000 more compounds[171] led to the identification of hits **49**–**51** with long flexible aliphatic linkers connecting the Fe-coordinating imidazole moiety with a second aromatic functionality, as well as a ring-constrained analogue **52** (Figure 18). Compounds

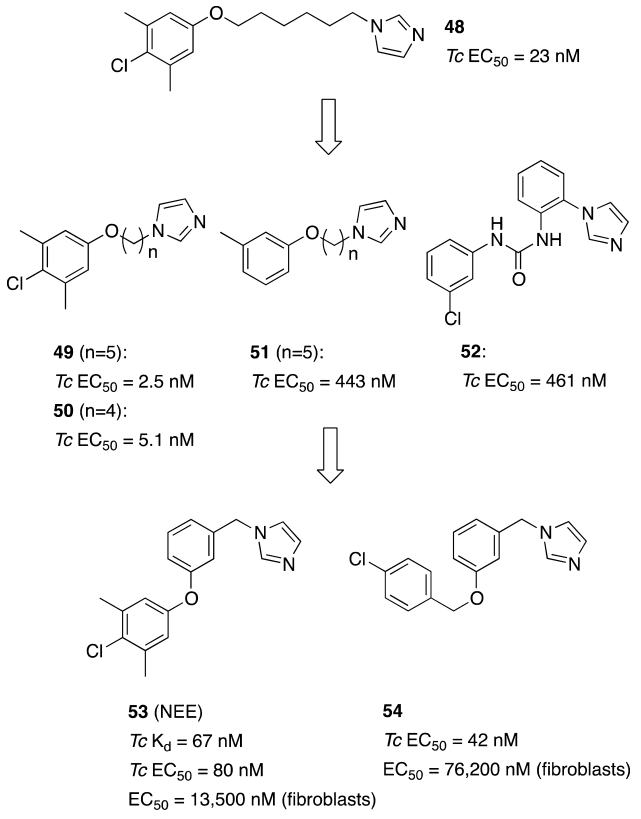

Figure 18. NEU321 derived from phenotypic screening hits and optimized analogues.

48–**51** resemble the target-based hits **17**–**19** identified in the spectral assay against *T. cruzi* CYP51 (Figure 12).[163] An unusually long aliphatic chain distinguishes these derivatives from the trigonal- and tetragonal-chemical group arrangement in canonic CYP51 inhibitors. The cell death phenotype exhibited by **48**[196] and the spectral behavior demonstrated by **17**[163] suggest interaction of this chemotype with the *T. cruzi* CYP51 target. Follow-up optimization of **49**–**51**[149] led to replacement of the alkyl linker, which was implicated in poor bioavailability and poor metabolic properties, with more rigid structural elements inspired by compound **52**. A hybrid structure **53** combining the structural features of **51** and **52** resulted in increased potency against cultured *T. cruzi* amastigotes, but attenuated stability. Even in the presence of quinidine and ketoconazole, which are inhibitors of drug-metabolizing CYP2D6 and CYP3A4, respectively, 29–39% of compound **53** was metabolized in 20 min. Given high binding to plasma proteins (>99.8%) and strong inhibition of the hERG ion channel (94% at 10 μM), **53** has poor predicted prognosis for bioavailability and cardiotoxicity.[149]

Binding of **53** to the *T. cruzi* CYP51 target was confirmed by characteristic UV–vis spectra and by X-ray structure analysis of the drug–target complex (Figure 19).[149] Compound **53** (small-

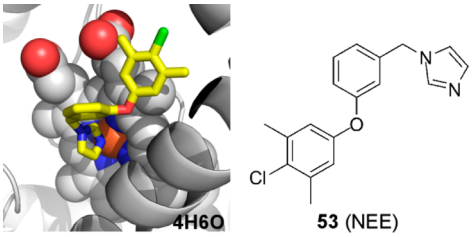

Figure 19. NEU321 (**53**, small-molecule code NEE) in the active site of *T. cruzi* CYP51 (PDB ID: 4H6O).

molecule ID NEE) has a distinct binding mode with the 4-chloro-3,5-dimethylphenoxybenzyl moiety extending into the hydrophobic pocket between the BC-loop and the N-terminus of the I-helix, constituting the short arm of the Y-shape inhibitor binding envelope (Figures 7). This makes **53** the only structurally characterized CYP51 inhibitor that does not utilize the hydrophobic tunnel between the α- and β-domains.

5.1.4. VNI/VNF: Vitamin D Hydroxylase Inhibitor Analogues. Probing of enzymatic activity of *T. cruzi* and *T. brucei* CYP51 *in vitro* with imidazole derivatives from the Novartis Research Institute collection of vitamin D hydroxylase inhibitors singled out two structurally related compounds, **55** and **56** (VNF), as strong inhibitors of CYP51 catalytic function (Figure 20).[197] Both compounds showed moderate potency against procyclic and bloodstream forms of *T. brucei* (EC_{50} of 1.3–7.0 μM) but somewhat improved potency against *T. cruzi* trypomastigotes and amastigotes (less than 1 μM EC_{50} and EC_{95}).[197] On the basis of the common structural motif of **55** and **56**, VNI (compound **57**) was subsequently developed.[164,198] VNI displayed moderate inhibition at the enzyme level, but its antiparasitic potency against *T. cruzi* amastigotes infecting cardiomyocytes exceeded that of posaconazole or ravuconazole. Thus, *T. cruzi* was cleared from host cells at 7.5 nM VNI, while more than 30 nM of posaconazole or ravuconazole was required to achieve similar effect. The C_{max} of VNI is about 40 μM (25 mg/kg, po), which is at least 2 fold and >10-fold higher than posaconazole and ravuconazole, respectively. Twice daily oral dosing of VNI in an acute murine model of *T. cruzi* infection (Tulahuen strain) at 25 mg/kg for 30 days (treatment begun 24 h postinfection) resulted in a 100% cure rate and 100% survival.[198] In a chronic model of Chagas disease, blood and tissue of the VNI-treated mice were PCR-negative after a 30-day treatment followed by 6 rounds of immunosuppression.[198] However, at the same treatment regimen, all VNI-treated mice infected by the benznidazole-resistant Colombiana strain showed relapse after three cycles of cyclophosphamide administration, and most (5 out of 6) died during the immunosuppression procedure.[199] Treatment of benznidazole-resistant *T. cruzi* Y strain with VNI also has not

dx.doi.org/10.1021/cr5003134 | *Chem. Rev.* 2014, 114, 11242–11271

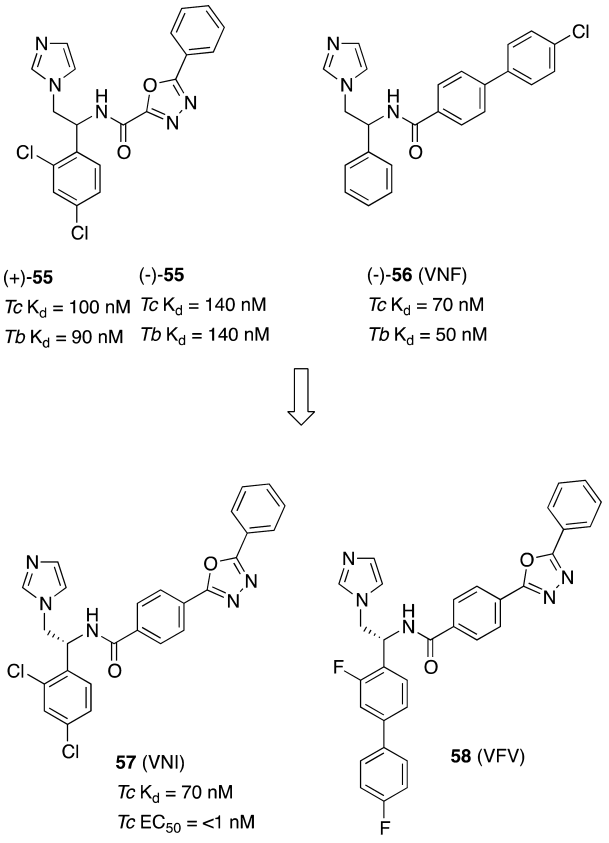

Figure 20. VNI and VNF.

attained parasitological cure but led to >80% decrease in circulating parasites.[199] Two genes are present for Colombiana *T. cruzi* CYP51 with 7 and 8 amino acid differences compared to the Tulaheun *T. cruzi* CYP51. Thus, high abundance of CYP51 enzyme and/or involvement of the altered amino acids for CYP51 function could possibly cause decreased susceptibility of the Colombiana strain to VNI.

The cocrystal structures for both VNI (and its triazole analogue VNT) and VNF inhibitors have been reported with the *T. brucei* and *T. cruzi* CYP51 orthologues, reaspectively,[148,153] as has been the structure of the VNF/VNI chimera, VFV, with *T. brucei* CYP51 (Figure 21).

5.2. Pyrimidine and Pyridine Derivatives

5.2.1. Fenarimol: An Agricultural Fungicide. The plant fungicide fenarimol (**59**) was identified in a screen of a diverse set of agrochemicals against *T. cruzi* Tulahuen strain transfected with the β-galactosidase gene.[200] It also has notable activity against *Leishmania* spp.[201] Fenarimol belongs to the pyrimidine class of CYP51 inhibitors. The mechanism of fenarimol action against *T. cruzi* CYP51 was determined,[150] and hit-to-lead optimization was conducted to obtain potent fenarimol analogues with curative activity in a mouse model of *T. cruzi* infection.[202] The simple structure and uncomplicated synthesis made fenarimol an attractive starting point for developing an anti-*T. cruzi* drug by the product development partnership DNDi. Use of structure−activity (SAR) and structure−property relationship (SPR) design criteria followed by *in vivo* evaluation of compounds in a mouse model focused on improving potency and establishing *in vivo* efficacy of analogues (Figure 22). Significant improvement of inhibition potency was achieved by replacing the original 5-pyrimidinyl group with 3-pyridinyl and the ring 1 *ortho*-chlorophenyl with a 4-trifluoromethylphenyl moiety as in **60**. The 4-trifluoromethyl substituent in ring 1 was particularly beneficial for metabolic stability while maintaining potency.[200] Oral dosing of compound **62** showed 95% bioavailability due to high solubility (50−100 μg/mL) and low clearance (18.9 mL/min/kg). However, a daily dose of **62** at 100 mg/kg for 5 days led to significantly (>95%) decreased blood parasitemia, but dosing at lower levels (50 or 20 mg/kg) was less effective (65%) or ineffective, respectively. Another analogue, compound **61**, which possesses lower bioavailability (68%), lower solubility (6.3−12.5 μg/mL), and higher clearance (24.4 mL/min/kg), suppressed parasitemia to microscopically undetectable levels following daily oral dosing at 50 mg/kg for 10 days in mice infected with *T. cruzi* Tulahuen strain. After a 10-day rest period, which allowed parasites in tissues to re-enter the blood from sanctuary sites, PCR analysis of blood samples showed >99% parasitemia reduction. However, parasites re-emerged in blood after a third cycle of cyclophosphamide-induced immunosuppression.[200]

Chemical diversity of the fenarimol SAR series was expanded by replacing one aromatic ring of the triaryl structure with a piperazine unit, to give new analogues possessing [phenyl-(pyridine-3-yl)methyl] piperazine scaffolds.[202] Analogue **63** suppressed parasite levels up to 96%, 95%, and 73% with once daily oral doses of 100, 50, and 20 mg/kg for 5 days, respectively. Analogue **63** also showed improved survival rates (80−100%) on day 30 postinfection. Further follow-up scaffold modifications were undertaken to improve DMPK properties and achieve higher efficacy.[203] Replacement of the central chiral carbon atom of compound **63** with a nitrogen atom gave rise to an achiral template represented by compound **64**. SAR was investigated by generating analogues with various aryl groups attached to *N*-piperidine; several analogues with this scaffold were as potent as posaconazole. The need to fill the void space in the active site of CYP51 required the aryl substituent of the *N*-arylpiperidine unit to extend further into hydrophobic tunnel

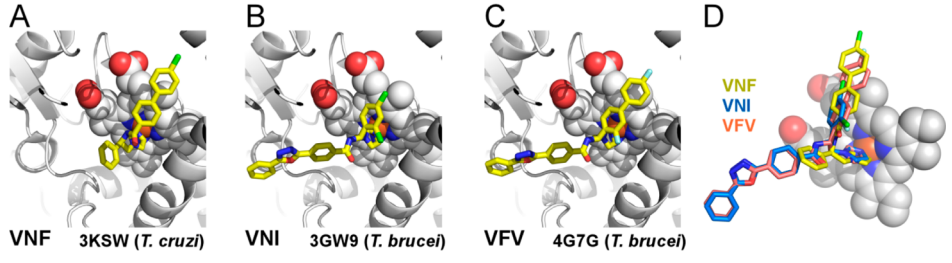

Figure 21. Binding of the **56** (VNF) (A), **57** (VNI) (B), and **58** (VFV) (C) analogues in *T. cruzi* or *T. brucei* CYP51. (C) Chimeric VFV structure combines features of both parental analogues, VNF (A) and VNI (B). (D) All three inhibitors are shown superimposed.

dx.doi.org/10.1021/cr5003134 | *Chem. Rev.* 2014, 114, 11242−11271

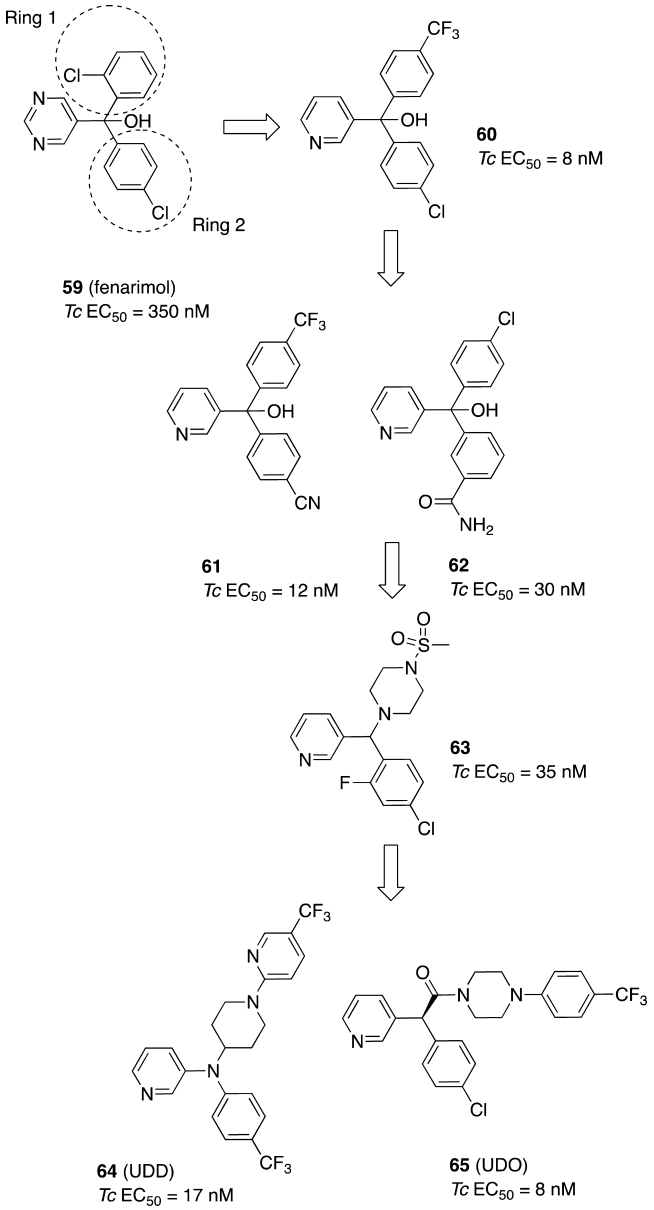

Figure 22. Fenarimol analogues with potent anti-*T. cruzi* activity *in vivo*.

of the binding site (Figure 7). The choice of the aryl group in the *N*-arylpiperidine unit had a major impact on microsomal stability in the series of analogues represented by compound **64**.[203] In addition, an acetamide unit was introduced in an attempt to lead to a new SAR series represented by compound **65**. This resulted in high potency (EC_{50} = 8 nM) and moderate stability (microsome predicted hepatic extraction ratio, E_H = 0.5). Both highly optimized lead compounds **64** and (*S*)-**65** had overall 50−60% cure rate of *T. cruzi*-infected mice (Tulahuen strain), confirmed by PCR analysis of tissue and blood of mice treated at 10−20 mg/kg/day for 20 days, followed by three cycles of immunosuppression.[203] The plasma concentration of **64** and (*S*)-**65** at 24 h were 0.79 and 0.65 μM for 20 mg/kg dosing (vs C_{24h} of **61** = 0.03 μM at 20 mg/kg dosing). Thus, these results suggest *in vivo* efficacy is related to an extended drug exposure over the full dosing interval in addition to *in vitro* inhibition potency (EC_{50}).

Both highly optimized inhibitors **64** and **65** were structurally characterized in complex with the *T. cruzi* CYP51 target.[150] The role of the pyridine heterocycle in coordinating to the heme Fe-iron in fenarimol-like inhibitors is consistent with the role of the 5-membered heterocycle in the azole series (Figure 23). However, the pyridy-3-yl Fe-coordinating group forces aryl ring 2 of both **64** and **65** virtually into a sandwich conformation with the heme macrocycle, maximizing overlap of the π systems. This configuration is less stable compared to offset parallel or perpendicular geometries, which is consistent with the relative rarity of the sandwich orientation in X-ray crystal data. Repulsive interactions, which are normally reduced by offsetting one of the aromatic rings in the parallel displaced conformation, may be a factor responsible for the weakened Fe−N coordination bond in the CYP51 complexes with compound **64** (2.31 Å) and particularly compound **65** (2.35 Å), the latter carrying the larger 4-trifluoromethylphenyl substituent on ring 2.

5.2.2. *N*-Indolyl-oxopyridinyl-4-aminopropanyl Derivatives: From Screening Hit to Lead Optimization. The *N*-indolyl-oxopyridinyl-4-aminopropanyl-based CYP51 inhibitors originated from a target-based screen,[143,145] and evolved through an iterative approach involving rounds of SAR and SPR analysis, compound synthesis, testing, and biological and structural evaluation.[147,151,154] Medicinal chemistry efforts improved the EC_{50} of these inhibitors in *T. cruzi* cell-based assay by up to 4 orders of magnitude, compared to that of parental hit (Figure 24).[147] Initial efforts were focused on the *S*-enantiomer because of better binding affinity and inhibition potency of LP10 analogues, **66** and **67**, generated early in the development cycle, as demonstrated in spectral and cell-based assays. The X-ray cocrystal structure of **68** with *T. brucei* CYP51 allowed comparative molecular modeling which led to the development of **69** which possesses significantly increased potency in cell-based assay. The orientation of the biaryl units of **69** in the CYP51 active site changed dramatically compared to **68** (Figure 25), resulting in a >1000-fold improved inhibition potency against *T. cruzi*.[147] On the basis of consistently superior potency, the *R*-configuration of this class of the inhibitors was used in subsequent optimization efforts.

Analogues **70**−**73** and their derivatives were further explored by docking and comparative molecular modeling using the X-ray structure of **69** bound to *T. cruzi* CYP51. Most of these derivatives displayed strong inhibitory potency to *T. cruzi* with single digit nanomolar EC_{50} or less.[154] In addition, **70** and **72** showed significantly improved *in vitro* microsomal stability (compared to **66** and **67**) by replacing the cyclohexyl unit with an aromatic ring of which potential susceptible sites are blocked with halogen atoms and/or an additional aromatic ring. Furthermore, **72** showed significantly decreased inhibition against human CYP1A2, CYP2C9, CYP2D6, and CYP3A4 enzymes with −26%, 41%, −17%, and 15% percent inhibition at 1 μM, respectively.

Inspired by the SAR and SPR analysis and aided by the X-ray structures and docking models, orally bioavailable and highly potent *in vivo* agents **74**−**77** were developed.[152] Inhibitors **74**−**77** showed considerably enhanced *in vitro* microsomal stability ($t_{1/2}$ = 22−58 min), and possessed enhanced *in vivo* pharmacokinetic properties and tissue exposure when delivered as a single 50 mg/kg oral dose in a Kolliphor formulation rather than in HPβCD, except for **75** which was comparable in both vehicles. To avoid downstream disconnect between *in vitro* activity and *in vivo* efficacy that may arise when SAR studies are

dx.doi.org/10.1021/cr5003134 | *Chem. Rev.* 2014, 114, 11242−11271

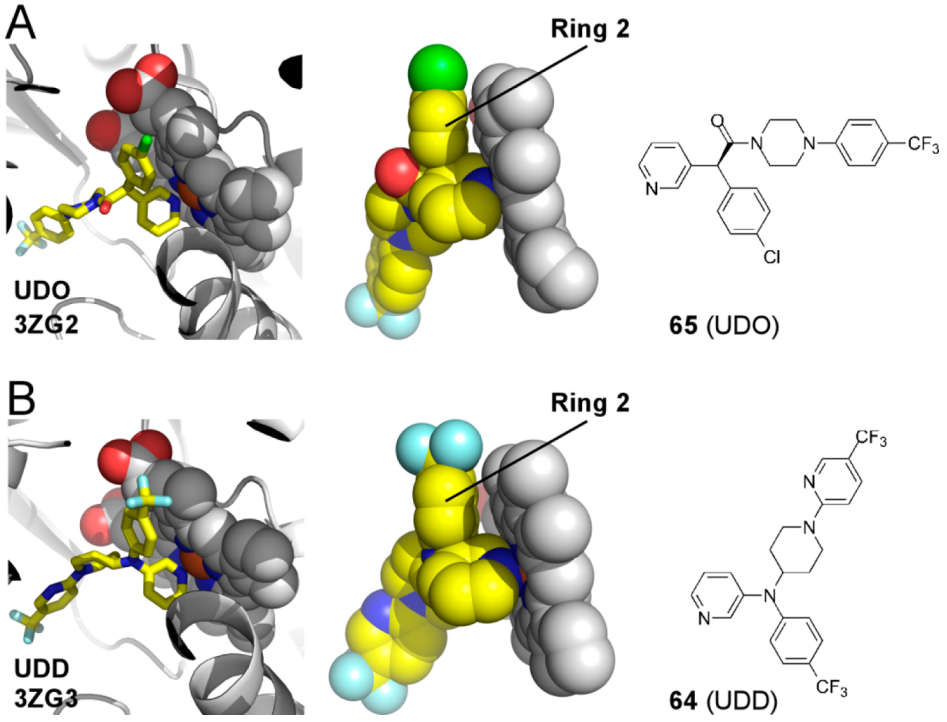

Figure 23. Fenarimol analogues **65** (UDO) (A) and **64** (UDD) (B) in the active site of *T. cruzi* CYP51.

driven by target-based or cell-based assays, a 4-day mouse model using infection with a transgenic *T. cruzi* luc strain expressing firefly luciferase[171] was used in the early stages of the SAR efforts. In this animal model, compounds **74**−**77** displayed 97−99% suppression of *T. cruzi* parasitemia upon twice daily dosing at 50 mg/kg for four consecutive days.[152] It is also noteworthy that **75** and **76**, which possess good *in vivo* half-lives (4.4 and 3.1 h) and AUC_{last} (30 and 84 μM × h), showed superior efficacy (89% and 90% *T. cruzi* growth suppression) at 25 mg/kg po dosing. Rounds of molecular modeling and inhibitor synthesis to improve stability, selectivity, and potency ultimately led to enhanced binding to the *T. cruzi* CYP51 target, enabling high-resolution crystal structures to be obtained for this therapeutic target (Figure 26).[151,152] For the first time resolution of the *T. cruzi* CYP51 drug−target complexes approached the 2 Å barrier (Table 1), deepening the level of atomic information available for structure-aided drug discovery. These high-resolution structures demonstrate that the binding site is modulated in response to an incoming inhibitor and characterize CYP51 as a flexible rather than a rigid template, as reported by the other group.[164] This observation contradicts the previously assumed CYP51 rigidity[164,204] and suggests that compounds binding CYP51 by an induced fit mechanism likely form tighter complexes which generate higher resolution crystal structures.

Although both *N*-indolyl-oxopyridinyl-4-aminopropanyl-based and fenarimol analogues utilize a 6-membered pyridine heterocycle to coordinate the heme iron, the two pyridine-based scaffolds have significant differences defining their interactions with the target (Figure 27). First, the 4-pyridyl Fe-coordinating moiety of the *N*-indolyl-oxopyridinyl-4-amino-propanyl-based analogues contrasts with the 3-pyridyl moiety of the fenarimol analogues. Second, the structure branching point in the fenarimol analogues is positioned three bond-lengths closer to the Fe-coordinating nitrogen atom compared to that in the *N*-indolyl-oxopyridinyl-4-aminopropanyl-based analogues. Both factors synergize to impose spatial constraints on the interactions of the fenarimol analogues with the heme macrocycle. Structurally, it translates to energetically more favorable T-shape $\pi-\pi$ stacking interactions between the indole ring and heme macrocycle in the *N*-indolyl-oxopyridinyl-4-aminopropanyl-based inhibitors, as opposed to spatial hindrance caused by the proximity of virtually coplanar aromatic systems of heme and fenarimol analogues (Figure 27). This steric hindrance rather than electronic effects of the pyridine group likely explains a weakened Fe−N coordination bond in the fenarimol analogue−CYP51 complexes, which is >0.2 Å longer than in the *N*-indolyl-oxopyridinyl-4-amino-propanyl-based complexes and >0.3 Å longer than in azoles.[150] Attenuated metal-binding is believed to improve the selectivity and safety profile of the fenarimol analogues, compared to the azole antifungal inhibitors, by increasing the contributions to binding affinity by specific drug−protein interactions at the expense of nonspecific drug−metal interactions.

5.3. Substrate Mimetics

Several attempts have been carried out to develop lanosterol-based inhibitors of human and fungal CYP51 for cholesterol-lowering and antifungal drugs.[205,206] However, few successful results have been reported probably because of the limited range of structural modifications possible for lanosterol, and the minimal amount of structural information on lanosterol binding in the active site of CYP51. 14α-Methylenecyclopropyl-Δ7-24,25-dihydrolanosterol (LNP) was reported as a substrate-based analogue, which tightly binds to all protozoan CYP51 but acts as a suicide substrate for *T. cruzi* CYP51, providing an example of a mechanism-based CYP51 inhibitor.[155] EC_{50} of 5 μM has been reported for LNP to parasites in mammalian cells;[155] efficacy in animal models of infection has not been reported. The X-ray cocrystal structure of LNP-bound *T. brucei* CYP51 features the sterol molecule in un-natural 5β-configuration (PDB ID 3P99, Figure 8A) (discussed in section

dx.doi.org/10.1021/cr5003134 | *Chem. Rev.* 2014, 114, 11242−11271

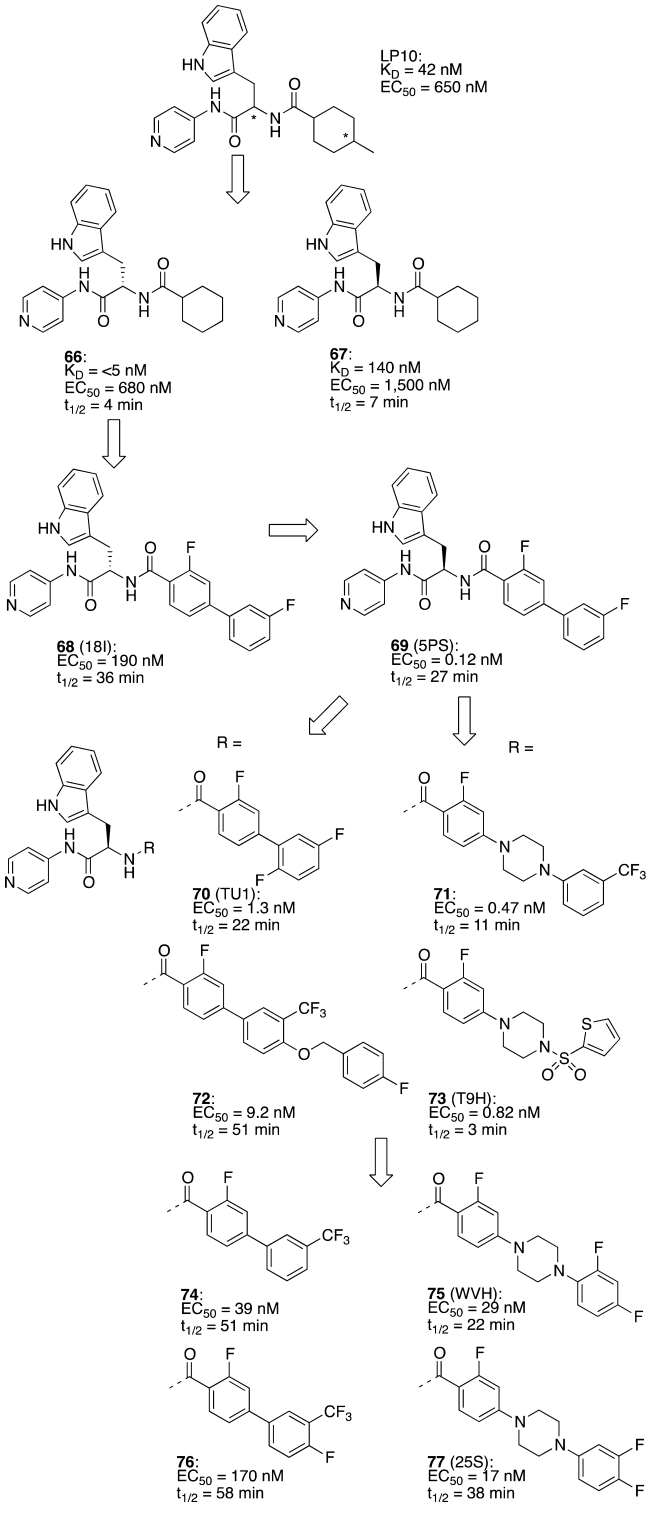

Figure 24. Optimization of 4-aminopyridyl-based CYP51 inhibitors. EC_{50} values are from a *T. cruzi* cell-based assay; half-life of compounds, $t_{1/2}$, was assessed in mouse liver microsomes.

4.2). We infer that the un-natural sterol configuration may be an artifact of refinement against low-resolution data, which calls into question the conclusions drawn in the cited article.[155]

6. ISSUES TO ADDRESS

6.1. Azole Resistance

Fungal species have evolved a multitude of mechanisms to survive exposure to antifungal agents. These are divided into several categories including (i) increased levels of the cellular target, either by upregulation or duplication of the gene encoding for CYP51 (referred to as *erg11* in all fungi from which it was cloned); (ii) decreased affinity of drugs to the cellular target, sterol 14-demethylase, CYP51; (iii) reduced intracellular accumulation of antifungals largely by upregulation of genes encoding efflux transporters; (iv) alteration of ergosterol biosynthesis affecting permeability of the cell membrane or enabling downstream conversion of otherwise toxic intermediates; and, finally, specific to fungi, (v) the capacity to build biofilm creating a physical barrier against the efficient penetration of antifungal agents.[65,207,208] To complicate matters even further, more than one mechanism may operate simultaneously, and different mechanisms may dominate in different pathogens and toward different drugs. Azole resistance can be CYP51-mediated (categories i–ii) or not CYP51-mediated (categories iii–v). A shift between the potential resistance mechanisms is not well-understood.

Although >140 amino acid mutations have been identified in *Candida albicans* CYP51 (half found in isolates with reduced susceptibility to fluconazole),[209,210] the drug efflux route dominates azole resistance in this pathogen.[211] Clinical isolates harbor several amino acid substitutions in CYP51 that may be acquired sequentially in the course of long-term azole therapy and have additive or synergistic effects in azole susceptibility.[212,213] Quantitative effects of the CYP51 amino acid substitutions vary considerably for different azoles, which likely results from the alteration of specific drug–target point contacts as judged by molecular docking.[214] The arsenal of X-ray structure templates for modeling drug–target interactions has recently been amplified with the structure of the *S. cerevisiae* CYP51,[157] which carries higher sequence homology to fungal pathogens than the bacterial sequence, or to its kinetoplastid or human counterparts. Other CYP51-mediated mechanisms reducing *C. albicans* susceptibility to antifungal azole drugs include increase of *erg11* transcript level, resulting from a gain-of-function mutation in the transcription factor,[215] or increased copy number of *cyp51* due to chromosomal aberrations.[216,217]

Uptake of azole antifungal drugs is believed to be via passive diffusion through the cell wall[207] and is affected by modification of cell wall structure by altering the glycosylation of surface proteins.[218] Mutation of *erg6* (sterol methyltransferase in the ergosterol biosynthesis pathway) also enhances permeability of the cell membrane to different growth inhibitors, including azoles.[219] Finally, azole resistant *Candida* spp. and *Cryptococcus neoformans* may also originate as a result of mutation to other genes in the ergosterol biosynthesis pathway, e.g., *erg2* and *erg3*, encoding for C-8 sterol isomerase and C-5 sterol desaturase, downstream of CYP51.[220−222] Activity of these downstream enzyme mutants alleviates toxic effects of 14α-methyl-ergosta-8,24(28)-dien-3β,6α-diol, which accumulates as a result of CYP51 inhibition and arrests fungal growth.[223]

However, a major route of azole resistance in *C. albicans* and the related yeast pathogens, *C. tropicalis, C. grabata*, and *C. dubliniensis*, is enhanced drug efflux resulting in decreasing intracellular drug concentration.[207] The multidrug efflux transporters in plasma membranes of fungal cells are responsible for expelling from cells a large variety of

dx.doi.org/10.1021/cr5003134 | *Chem. Rev.* 2014, 114, 11242−11271

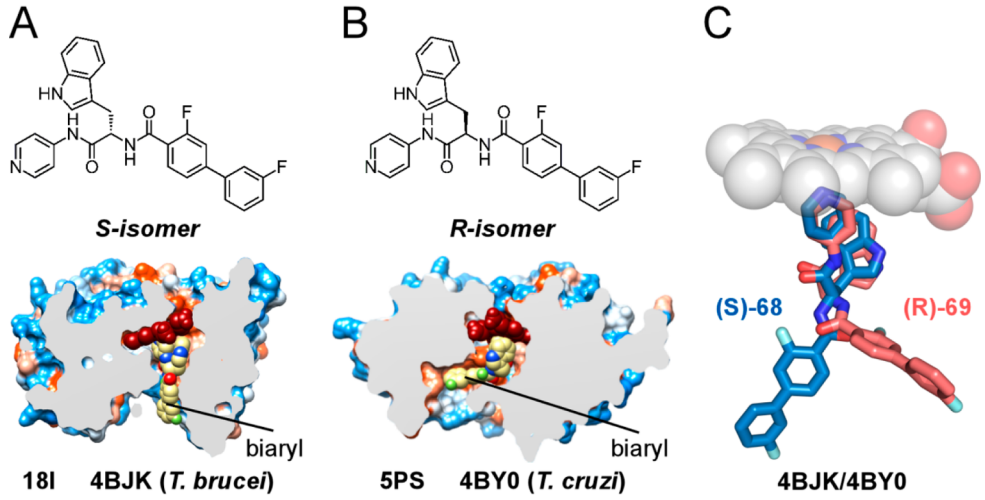

Figure 25. Orientation of the biaryl moiety of the *S*- and *R*-stereoisomers, **68** and **69**. Compounds **68** (18I) (A) and **69** (5PS) (B) are shown as van der Waals spheres, with carbon atoms highlighted in yellow, in the CYP51 active sites clipped by a plane. Active site surface indicates hydrophobicity, ranging from orange (lipophilic) to blue (hydrophilic). Heme is shown as red spheres. (C) Superimposition of **68** (blue sticks) and **69** (red sticks) highlights the differences in binding of the biaryl moieties. Heme is in van der Waals spheres.

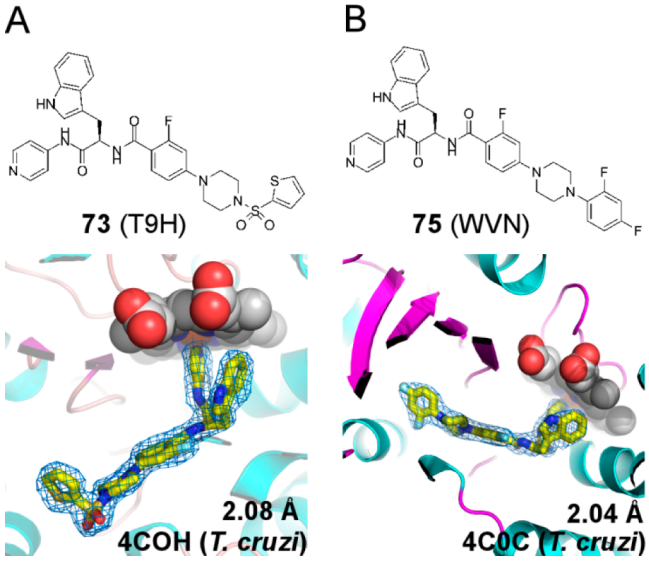

Figure 26. High-resolution structures for the *T. cruzi* CYP51 drug–target complexes. Compounds **73** (T9H) (A) and **75** (WVN) (B) are shown in yellow sticks fitted in the electron density (blue mesh).

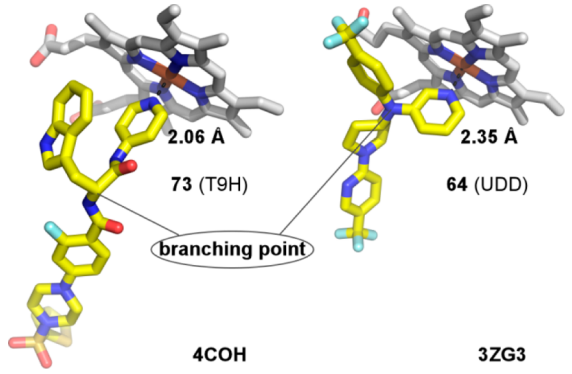

Figure 27. Binding modes of pyridinyl-based CYP51 inhibitors. Energetically more favorable T-shape $\pi-\pi$-stacking mode and lack of steric interference with the heme macrocycle result in a much shorter Fe–N coordination bond, 2.06 Å, in the *N*-indolyl-oxopyridinyl-4-aminopropanyl-based inhibitors (**73**, T9H, left) compared to 2.35 Å in the fenarimol analogue (**64**, UDD, right).

compounds. The two main classes of pumps are the ATP-binding cassette (ABC) and the major facilitator superfamily (MFS). The overexpression of the MDR1 (multidrug resistance 1) gene (MFS family) is responsible for specific resistance to fluconazole. Overexpression of efflux transporter genes of the ABC class, CDR1 and CDR2 (Candida drug resistance 1 and 2), is associated with cross-resistance to different azole drugs, including fluconazole, itraconazole, and ketoconazole.[207,208] In *Aspergillus fumigatus,* itraconazole induces an ABC-transporter gene, *atrF*, although the detailed role of this gene in resistance is not known.[224]

In contrast to yeast pathogens, intrinsic resistance of the opportunistic human pathogen *Aspergillus fumigatus* to fluconazole is associated with the duplication of the erg11 gene encoding two CYP51 isoforms, CYP51A and CYP51B, found in *A. fumigatus* and related *Aspergillus* spp.[225] Sporadic cases of itraconazole resistance occasionally observed in *A. fumigatus* in the late 1990s and early 2000s were associated with the altered affinity of CYP51A due to point mutations developed in patients initially infected with susceptible strains. Mutational hotspots at codons 54, 220, and 98 have been reported by multiple research laboratories[226−228] (residue numbering adheres to the *A. fumigatus* CYP51A sequence). Late in the past decade, the frequency of itraconazole resistance dramatically increased, and CYP51 mutations notably diversified under selective pressure of long-term azole treatment of patients with chronic and allergic aspergillosis.[229] In the culture collection of the mycology laboratory in Manchester, 18 amino acid alterations were found in the CYP51 enzyme, different mutations were found in the same strain, and cross-resistance between azole drugs was dependent on position and type of amino acid substitution within CYP51.[229] A list of CYP51A mutations identified in other studies is summarized in a comprehensive review by Becher and Wirsel.[159]

Resistance to posaconazole in *A. fumigatus* occurs mainly by a mechanism involving mutations in CYP51A.[229−231] Posaconazole is less susceptible to the efflux pumps that confer resistance to other azoles in *Candida* spp.[212,231,232] Mapping

dx.doi.org/10.1021/cr5003134 | *Chem. Rev.* 2014, 114, 11242−11271

amino acid substitutions identified in CYP51A in clinical posaconazole resistant isolates on the *T. cruzi* CYP51 structure points to the substrate tunnel entrance as a mutation hotspot: G54, P216, and M220 map directly to the tunnel mouth.[146] Substitution of glycine at codon 54 to arginine or tryptophane associates with moderate and high levels of resistance, and confers cross-resistance between itraconazole and posaconazole.[228] Mutations of M220 confer cross-resistance to four tested azole drugs including itraconazole, voriconazole, ravuconazole, and posaconazole.[233,234]

In recent years, cases of invasive aspergillosis due to pan-azole-resistant strains of *A. fumigatus* have been reported, where resistance was attributed to one predominant mechanism, referred to as TR_{34}/L98H.[235] This mechanism relies on a tandem repeat of 34 bases in the promoter of the CYP51A gene leading to enhanced expression, combined with a leucine to histidine amino acid substitution at codon 98.[236,237] Substitution of methionine 220 or a duplication in tandem of 34-bp fragment in the CYP51A promoter combined with L98H substitution confers cross-resistance to all azole drugs tested.[234] A similar TR_{46}/Y121F/T289A mechanism is associated with voriconazole therapy failure with moderately attenuated susceptibility to itraconazole and posaconazole.[238] In contrast to the "in-patient" route, an environment fungicide-driven development has been suggested for the TR_{34}/L98H and TR_{46}/Y121F/T289A mechanisms. This occurs when *A. fumigatus* became resistant in the environment due to the use of azole fungicides for crop protection and patients are believed to inhale azole-resistant *A. fumigatus* spores.[239−241]

Azole resistance phenomenon has being explored in other clinically significant pathogenic fungi, including *Histoplasma capsulatum* and *Cryptococus neoformans*. *H. capsulatum* belongs to the Pezizomycotina and causes pulmonary histoplasmosis, a frequent opportunistic infection in endemic countries, with an annual incidence about 5% per year in HIV-infected individuals, and high mortality rates.[242] Therapy with less active fluconazole fails at higher proportion than with itraconazole.[243] As with *A. fumigatus*, *H. capsulatum* encodes two CYP51 isoforms, with CYP51A involved in azole resistance.[244] Unlike *A. fumigatus*, only one CYP51A substitution, Y136F (corresponding to Y132H in *C. albicans*), has been identified in fluconazole-resistant clinical isolates.

C. neoformans belongs to Basidiomycota and is the most common cause of life-threatening fungal infections in HIV-infected individuals, and also can cause disease in immunocompetent individuals. Fluconazole is a drug of choice for long-term maintenance therapy of cryptococcal meningitis in HIV-infected patients.[221,245] Mutations of the CYP51 drug target play a minor role in acquiring resistance. Only two have been identified in fluconazole-resistant isolates: G484A[246] and Y145F (corresponding to Y132H in *C. albicans*).[247] Chromosome duplication is suggested to play a more important role for failing azole therapy.[248] The ABC transporter gene *CnArf1* carried by this same chromosome also contributes to fluconazole resistance.[249]

Occurrence of naturally resistant *T. cruzi* strains may be one of the most important factors explaining the low rate of cure of chagasic patients with benznidazole and nefurtimox in some endemic areas.[117−120] The strategy of using azole chemotypes against Chagas disease may also be complicated by development of resistance to azoles. The alarming perspective emerging from antifungal therapy efforts must be taken in consideration when designing anti-Chagasic drugs targeting CYP51. *T. cruzi* resistance to azoles was rapidly induced *in vitro* by serial passage of mammalian-stage parasites in the presence of fluconazole (which has low potency against *T. cruzi* compared to posaconazole) for 4 months.[250] These parasites were cross-resistant to the other azoles, ketoconazole, miconazole, and itraconazole, but remained susceptible to benznidazole and amphotericin B. The azole-resistant phenotype was stable for more than 2 months of *in vitro* serial passage without fluconazole. In addition, these parasites resisted treatment in mice receiving ketoconazole.[250]

The issues of drug resistance attributed to the azole class of molecules has led to a general believe that nonazole inhibitors will lack this disadvantage. Realistically, it is unlikely that transition from the azole Fe-coordinating moiety to a nonazole heme-binding unit can alone significantly affect propensity for drug resistance. Some of the same mechanisms which reduce susceptibility of pathogenic fungi to azole drugs may operate in kinetoplastid parasites. Solution to the problem is in enhancing potency of new drugs to shorten course of treatment, ensure patient's compliance, and achieve parasitological cure. An advantage to the development of CYP51 inhibitors targeting CYP51 via structure-based drug-discovery is that the Fe-coordinating module is only part of the inhibitor structure. Specificity and potency of CYP51 inhibitors are largely defined by the rest of the molecule through multiple drug−target interactions which now can be specifically tailored to precisely fit the active site of a specific target.

6.2. Genetic Heterogeneity of *T. cruzi*

An additional challenge for drug resistance in Chagas disease programs is the genetic heterogeneity of *T. cruzi* which at present is subdivided into six phylogenetically discrete typing units (DTUs).[251,252] *T. cruzi* DTUs display different virulence and pathogenic characteristics. Members of all DTUs are infective to humans and capable of causing Chagas disease. However, DTUs TcI, TcII, TcV, and TcVI are the main agents of human Chagas disease.[253] Some degree of correlation between DTUs and clinical manifestations of chronic disease has been observed; however, this association may originate from geographical overlap between specific *T. cruzi* DTUs and human populations.[251] All four, TcI, TcII, TcV, and TcVI, are capable of causing cardiomyopathy; however, only TcII, TcV, and TcVI have been so far associated with chronic digestive syndromes.[251] Ideally, new chemotherapy developed for Chagas disease should be active against all circulating genotypes of the parasite.

Efficacy of current chemotherapy with benznidazole and nifurtimox varies according to geographic area, probably due to differences in drug susceptibility among different *T. cruzi* strains.[252] A recent survey has found 10-fold variation in benznidazole sensitivity in *T. cruzi* parasites isolated from a variety of biological and geographical backgrounds.[121] Laboratory-adapted CL-Brener and Tulahuen *T. cruzi* strains (both TcVI) are known to be drug-sensitive, while *T. cruzi* strains Y (TcII) and Colombiana (TcI) display medium and high resistance to benznidazole and nefurtimox, respectively.[117,254,255] The same pattern of resistance has been observed in these laboratory strains for antifungal inhibitors, including posaconazole[256] and the experimental inhibitor VNI.[199]

Available data on correlation between drug susceptibility and phylogenetic distances between different DTUs are controversial. Lack of statistically significant correlation was reported

for benznidazole *in vitro*,[257] whereas partial correlation for both benznidazole and itraconazole was observed for three out of six DTUs *in vivo*.[258] Finally, a cluster tree generated on the basis of the epimastigote susceptibility to a new macrolide antibiotic from *Streptomyces diastaticus* resembled phylogenies of *T. cruzi* lineages derived from genetic data.[259] A recent study on the most advanced antichagasic leads and clinical compounds against a panel of *T. cruzi* strains representing all current DTUs challenges previous reports on variable responses to nitro heterocyclic compounds among different *T. cruzi* strains.[260] The same study suggests that drug susceptibility may be an action-specific mechanism. This later observation highlights the need for caution in relying on standardized assays applied to the drugs with different mechanisms of action.

6.3. Selectivity against Human CYP Enzymes

Cytochrome P450 enzymes catalyze the oxidation of xenobiotics and endogenous substances, leading to elimination of foreign compounds and maintaining endocrine homeostasis in humans. Most antiparasitic agents targeting CYP51 are heme-iron coordinating compounds with potential to interact also with human CYPs, partially via nonspecific drug-metal binding, which can lead to various drug safety issues. Hepatotoxicity and hepatic tumors related to antifungal azole therapies correlating with induced expression of liver CYP enzymes and lipid peroxidation have been reported.[261] In addition, reproductive impairment, alterations in sexual differentiation, delayed growth and development, and hormone-related cancers can be caused by disruption of steroid biosynthesis.[262] For instance, ketoconazole led to a demasculinizing effect on male fetuses in pregnant Wistar rats,[263] and to decreased testosterone and cortisol levels in the plasma of humans.[264,265] Thus, it is imperative to address selectivity issues against human CYP enzymes in the course of inhibitor development to avoid metabolism-induced drug−drug interactions, to minimize hepatotoxicity, and to preserve the balance of host steroid hormones.

Attenuated metal-binding is believed to improve the selectivity and safety profile of CYP inhibitors, compared to azole antifungal drugs, by increasing contributions of specific drug−protein interactions in binding affinity at the expense of nonspecific drug−metal interactions via less avid metal-binding groups. This paradigm has been used to achieve highly selective CYP17A1 inhibitors, potential treatment for prostate cancer,[266] and broad-spectrum CYP51 inhibitors that are more selective for fungal enzymes than for human drug-metabolizing CYPs.[267]

As discussed in this review, structure guided lead development has proven to be a productive strategy for generating highly potent antiparasitic CYP51 inhibitors. Lead selectivity can also be assessed *in silico* at early stages of drug discovery via molecular docking and comparative modeling of newly designed inhibitors against the structures for human CYP enzymes. Currently, the X-ray structures of various human CYP enzymes such as CYP1A2, CYP2C9, CYP2C19, CYP2D6, and CYP3A4, the major metabolic enzymes in humans, are available in the PDB database. In addition, structures of cytochrome P450 enzymes involved in steroid hormone biosynthesis in humans, such as CYP19 (aromatase), CYP11A (cholesterol side-chain cleavage enzyme), CYP21 (steroid 21-hydroxylase), CYP11B2 (aldosterone synthase), CYP17 (steroid 17α-hydroxylase), and CYP51 (sterol 14-demethylase), are also accessible.

Human CYP51 is a potential alternate target for antifungal azoles and antiparasitic drug candidates targeting CYP51. Although sequence identities between the CYP51 orthologues in eukaryotic species are low (about 25%), amino acids constituting the substrate binding sites are far more conserved.[152,204] Comparative binding affinities reported for azole inhibitors toward *C. albicans* and human CYP51 suggest that chances to hit human CYP51 for some azole drugs are higher than for the others.[268,269] Thus, fluconazole and voriconazole bind human CYP51 weakly (K_d = 30 000 nM and 2300 nM, respectively), whereas clotrimazole, itraconazole, and ketoconazole have much higher binding affinities (K_d = 55 nM, 92 nM, and 42 nM, respectively). This brings selectivity index for clotrimazole, itraconazole, and ketoconazole down to 5, whereas fluconazole and voriconazole are 200−500-fold more selective for *C. albicans* compared to human CYP51.[269]

7. CONCLUDING REMARKS

The cytochrome P450 enzyme CYP51 is a promising therapeutic target for neglected tropical diseases such as Chagas disease and leishmaniasis, which are caused by the kinetoplastid protozoa *T. cruzi* and various *Leishmania* species, respectively. CYP51 plays a central role in the biosynthesis of ergosterol and related 24-alkyl sterols, key sterol components of fungi and protozoan membranes, specifically catalyzing the oxidative removal of the C-32 methyl group of lanosterol. CYP51 is a clinically validated target in fungi. Drugs of the azole class have been developed as antifungal agents for human diseases. Substantial efforts have been made to repurpose approved antifungal azole drugs for treatment of Chagas disease. However, recently completed clinical trials of posaconazole and ravuconazole have shown that neither drug is superior to benznidazole. The quest for anti-Chagas cure must continue.

Alternative strategies toward development of anti-Chagas drugs discussed in this review involve optimization of lead compounds specifically targeting parasite CYP51. It is likely that parasite-specific inhibitors, optimized by structure-based drug-design criteria with close monitoring of PK parameters and inhibition of human drug-metabolizing CYPs, will be more effective in developing efficacious treatments of human *T. cruzi* and other protozoan infections than the antifungal agents. Starting points for these efforts have been identified by screening of compound collections, either in phenotypic cell-based assays or in biochemical target-based assays. Promising lead compound series have emerged from efforts at Vanderbilt (VNI/VNF), DNDi (fenarimol analogues), the UCSF−Scripps Florida collaboration (*N*-indoyloxypyridinyl-4-aminopropanyl derivatives), Northeastern (NEU321), and the Broad Institute (ML341), among others, that are discussed in this review. An intriguing opportunity pursued at Washington University involves piggybacking on the development efforts for the cancer clinical drug candidate tipifarnib targeting human protein farnesyltransferase (hPFT) which has emerged as a CYP51 inhibitor.

Ultimately, the long-term success of these efforts will depend on the ability to develop potent therapeutic agents ensuring parasitological cure with minimal or no harm to the human host. Off-target effects are an obvious concern, given the similarity of CYP51 to other cytochrome P450 enzymes that play critical roles in human tissues. This issue can be addressed, at least in part, by incorporating molecular modeling and appropriate selectivity screens in early stages of drug develop-

ment to minimize interactions with human CYPs. The potential for development of resistance to new CYP51 inhibitors is yet another concern, especially given the widespread development of resistance to clinically used antifungal agents. A potential solution to this problem is sufficient drug potency to ensure short treatment courses, which will maximize patient compliance and attain parasitological cure.

AUTHOR INFORMATION

Corresponding Authors

*E-mail: larissa.podust@ucsf.edu.
*E-mail: roush@scripps.edu.

Notes

The authors declare no competing financial interest.

Biographies

Jun Yong Choi (born 1974) received the Bachelors Degree in Chemistry and the Masters Degree in Physical Chemistry from the Inha University, South Korea, in 2000 and 2002, respectively, where he performed computational studies such as quantum mechanics and molecular modeling with Professor Chan Kyung Kim. After moving to the United States in 2003, he received his Ph.D. degree in Chemistry from SUNY at Stony Brook in 2009 under the direction of Professor Dale G. Drueckhammer and Professor Richard Z. Lin. His Ph.D. studies focused on bioorganic chemistry by developing chemical agents, which selectively target mTOR. He started his postdoctoral training in the Roush Laboratory at Scripps Florida as Pfizer-Scripps Florida postdoctoral fellow in 2009, and then he was promoted to Senior Research Associate in 2012. His research focuses on medicinal chemistry and chemical biology by applying organic synthesis combined with computer-aided molecular design techniques such as docking, homology modeling, virtual screening, library design and screening, cheminformatics, QSAR, and quantum mechanics under the supervision of Professor William R. Roush. He was an NIDDK scholarship winner at Keystone Symposia in 2007, and he received a travel award from the ACS Medicinal Chemistry Division in 2007.

Larissa M. Podust (born 1960) earned her Ph.D. in Chemistry from the Novosibirsk State University, Russia, in 1994. She completed postdoctoral training in enzymology of DNA replication first at the University Zurich-Irchel, Switzerland, under the direction of Professor U. Hubsher, and then in protein x-ray crystallography at Vanderbilt University, in the laboratory of Professor Y. Kim. After an additional four years as a Research Assistant Professor at the Department of Biochemistry at Vanderbilt, she moved to University of California at San Francisco in 2006, to join Paul Ortiz de Montellano's laboratory as an Adjunct Assistant Professor. Currently, she serves as a group leader for X-ray Crystallography at the Center for Discovery and Innovation in Parasitic Diseases (CDIPD) at UCSF, directed by Professor J. McKerrow. Her research is focused on the enzymatic mechanisms of oxidative reactions in bacterial biosynthetic systems producing antibiotics, and on structure-aided drug discovery for diseases representing global health problems. She received the Dr. Philip J. Browning Memorial Award (2004) from the Vanderbilt-Meharry Center for AIDS Research and Target of the Year Award (2009) from the Center for Emerging Neglected Diseases (CEND), UC—Berkeley.

William R. Roush (born 1952) received the Bachelors Degree in Chemistry, Summa Cum Laude, from the University of California at Los Angeles in 1974, where he performed undergraduate research with Professor Julius Rebek, and the Ph.D. Degree in Chemistry from Harvard University in 1977 under the direction of Professor R. B. Woodward. After an additional year as a postdoctoral associate in Woodward's laboratory, he joined the Massachusetts Institute of Technology as Assistant Professor. He moved to Indiana University in 1987, and was promoted to the rank of Professor in 1989 and Distinguished Professor in 1995. In 1997 he moved to the University of Michigan as the Warner Lambert/Parke Davis Professor of Chemistry. He served as Chair of the Department of Chemistry, University of Michigan, from 2002 to 2004, and then moved to the new Scripps Research Institute in Jupiter, Florida, as Professor of

dx.doi.org/10.1021/cr5003134 | Chem. Rev. 2014, 114, 11242−11271

Chemistry, Executive Director of Medicinal Chemistry, and Associate Dean of Scripps' Graduate Program 2005. His research interests focus on the total synthesis of natural products and the development of new synthetic methodology. Since moving to Scripps Florida in 2005, his research program has expanded into new areas of chemical biology and medicinal chemistry. Dr. Roush has received numerous awards and honors, including the 1994 Arthur C. Cope Scholar Award of the American Chemical Society, the 2002 Paul G. Gassman Distinguished Service Award of the American Chemical Society Division of Organic Chemistry, and in the 2004 the ACS Ernest Guenther Award in the Chemistry of Natural Products. In 2006, Dr. Roush was elected Fellow of the American Association for the Advancement of Science, and in 2009 he was elected to the inaugural class of Fellows of the American Chemical Society.

ACKNOWLEDGMENTS

We thank James McKerrow and Potter Wickware for critical reading and proofreading of the manuscript, and Iosune Ibiricu Urriza for providing the EM image included in the cover art. This research was generously supported by NIH R01 Grant AI095437.

ABBREVIATIONS

ABC	ATP-binding cassette
Acetyl-CoA	acetyl coenzyme A
ADMET	absorption, distribution, metabolism, excretion, and toxicity
CDR1/CDR2	candida drug resistance 1/2
COX-2	cyclooxygenase 2
CYP1A2	cytochrome P450 1A2
CYP2C9	cytochrome P450 2C9
CYP2D6	cytochrome P450 2D6
CYP3A4	cytochrome P450 3A4
CYP51	cytochrome P450 isoform 51
DMPK	drug metabolism and pharmacokinetics
DNDi	drugs for neglected disease Initiatives
DOS	diversity oriented synthesis
DTU	discrete typing units
EC_{50}	half maximal effective concentration
ED_{50}	half maximal effective dose
E_H	microsome predicted hepatic extraction ratio
ER	endoplasmic reticulum
FDA	food and drug administration
GC/MS	gas chromatography/mass spectrometry
hERG	human ether-a-go-go-related gene
HMG-CoA	3-hydroxy-3-methylglutaryl-coenzyme A
hPFT	human protein farnesyltransferase
HTS	high-throughput screening
IC_{50}	half maximal inhibition constant
K_D	dissociation constant
MDR1	multidrug resistance 1
MFS	major facilitator superfamily
NTD	neglected tropical disease
PCR	polymerase chain reaction
PDB	protein data bank
PFT	protein farnesyltransferase
PK	pharmacokinetics
QIDP	qualified infectious disease product
SAR	structure activity relationship
SEA	similarity ensemble approach
SPR	structure property relationship
Tb	*Trypanosoma brucei*
Tc	*Trypanosoma cruzi*
WHO	World Health Organization

REFERENCES

(1) Nelson, D. R. *Arch. Biochem. Biophys.* **1999**, *369*, 1.
(2) Aoyama, Y. *Front. Biosci.* **2005**, *10*, 1546.
(3) Aoyama, Y.; Noshiro, M.; Gotoh, O.; Imaoka, S.; Funae, Y.; Kurosawa, N.; Horiuchi, T.; Yoshida, Y. *J. Biochem.* **1996**, *119*, 926.
(4) Rezen, T.; Debeljak, N.; Kordis, D.; Rozman, D. *J. Mol. Evol.* **2004**, *59*, 51.
(5) Desmond, E.; Gribaldo, S. *Genome Biol. Evol.* **2009**, *1*, 364.
(6) Summons, R. E.; Bradley, A. S.; Jahnke, L. L.; Waldbauer, J. R. *Philos. Trans. R. Soc., B* **2006**, *361*, 951.
(7) Volkman, J. K. *Appl. Microbiol. Biotechnol.* **2003**, *60*, 495.
(8) Bird, C. W.; Lynch, J. M.; Pirt, F. J.; Reid, W. W. *Nature* **1971**, *230*, 473.
(9) Pearson, A.; Budin, M.; Brocks, J. J. *Proc. Natl. Acad. Sci. U.S.A.* **2003**, *100*, 15352.
(10) Bode, H. B.; Zeggel, B.; Silakowski, B.; Wenzel, S. C.; Reichenbach, H.; Muller, R. *Mol. Microbiol.* **2003**, *47*, 471.
(11) Kohl, W.; Gloe, A.; Reichenbach, H. *J. Gen. Microbiol.* **1983**, *129*, 1629.
(12) Jackson, C. J.; Lamb, D. C.; Marczylo, T. H.; Warrilow, A. G. S.; Manning, N. J.; Lowe, D. J.; Kelly, D. E.; Kelly, S. L. *J. Biol. Chem.* **2002**, *277*, 46959.
(13) Aoyama, Y.; Horiuchi, T.; Gotoh, O.; Noshiro, M.; Yoshida, Y. *J. Biochem. (Tokyo)* **1998**, *124*, 694.
(14) Bellamine, A.; Mangla, A. T.; Nes, W. D.; Waterman, M. R. *Proc. Natl. Acad. Sci. U.S.A.* **1999**, *96*, 8937.
(15) Pietila, M. P.; Vohra, P. K.; Sanyal, B.; Wengenack, N. L.; Raghavakaimal, S.; Thomas, C. F., Jr. *Am. J. Respir. Cell Mol. Biol.* **2006**, *35*, 236.
(16) Brezna, B.; Kweon, O.; Stingley, R. L.; Freeman, J. P.; Khan, A. A.; Polek, B.; Jones, R. C.; Cerniglia, C. E. *Appl. Microbiol. Biotechnol.* **2006**, *71*, 522.
(17) Keber, R.; Motaln, H.; Wagner, K. D.; Debeljak, N.; Rassoulzadegan, M.; Acimovic, J.; Rozman, D.; Horvat, S. *J. Biol. Chem.* **2011**, *286*, 29086.
(18) Bard, M.; Lees, N. D.; Turi, T.; Craft, D.; Cofrin, L.; Barbuch, R.; Koegel, C.; Loper, J. C. *Lipids* **1993**, *28*, 963.
(19) Sheehan, D. J.; Hitchcoch, C. A.; Sibley, C. M. *Clin. Microbiol. Rev.* **1999**, *12*, 40.
(20) Baldwin, B. C. *Biochem. Soc. Trans.* **1990**, *18*, 61.
(21) Raederstorff, D.; Rohmer, M. *Biochem. J.* **1985**, *231*, 609.
(22) Raederstorff, D.; Rohmer, M. *Eur. J. Biochem.* **1987**, *164*, 421.
(23) Raederstorff, D.; Rohmer, M. *Eur. J. Biochem.* **1987**, *164*, 427.
(24) Visvesvara, G. S. *Handb. Clin. Neurol.* **2013**, *114*, 153.
(25) El-Sayed, N. M.; Myler, P. J.; Blandin, G.; Berriman, M.; Crabtree, J.; Aggarwal, G.; Caler, E.; Renauld, H.; Worthey, E. A.; Hertz-Fowler, C.; Ghedin, E.; Peacock, C.; Bartholomeu, D. C.; Haas, B. J.; Tran, A. N.; Wortman, J. R.; Alsmark, U. C.; Angiuoli, S.; Anupama, A.; Badger, J.; Bringaud, F.; Cadag, E.; Carlton, J. M.; Cerqueira, G. C.; Creasy, T.; Delcher, A. L.; Djikeng, A.; Embley, T. M.; Hauser, C.; Ivens, A. C.; Kummerfeld, S. K.; Pereira-Leal, J. B.; Nilsson, D.; Peterson, J.; Salzberg, S. L.; Shallom, J.; Silva, J. C.; Sundaram, J.; Westenberger, S.; White, O.; Melville, S. E.; Donelson, J. E.; Andersson, B.; Stuart, K. D.; Hall, N. *Science* **2005**, *309*, 404.
(26) Buckner, F. S.; Urbina, J. A. *Int. J. Parasitol.: Drugs Drug. Resist.* **2012**, *2*, 236.
(27) Rangel, H.; Dagger, F.; Hernandez, A.; Liendo, A.; Urbina, J. A. *Antimicrob. Agents Chemother.* **1996**, *40*, 2785.
(28) Roberts, C. W.; McLeod, R.; Rice, D. W.; Ginger, M.; Chance, M. L.; Goad, L. J. *Mol. Biochem. Parasitol.* **2003**, *126*, 129.
(29) Mishra, J.; Saxena, A.; Singh, S. *Curr. Med. Chem.* **2007**, *14*, 1153.
(30) Croft, S. L.; Barrett, M. P.; Urbina, J. A. *Trends Parasitol.* **2005**, *21*, 508.
(31) Coppens, I.; Courtoy, P. J. *Annu. Rev. Microbiol.* **2000**, *54*, 129.

(32) Perez-Moreno, G.; Sealey-Cardona, M.; Rodrigues-Poveda, C.; Gelb, M. H.; Ruiz-Perez, L. M.; Castillo-Acosta, V.; Urbina, J. A.; Gonzalez-Pacanowska, D. *Int. J. Parasitol.* **2012**, *42*, 975.
(33) Aoyama, Y.; Yoshida, Y.; Sonoda, Y.; Sato, Y. *J. Biol. Chem.* **1989**, *264*, 18502.
(34) Fischer, R.; Trzaskos, J.; Magolda, R.; Ko, S.; Brosz, C.; Larsen, B. *J. Biol. Chem.* **1991**, *266*, 6124.
(35) Fischer, R. T.; Stam, S. H.; Johnson, P. R.; Ko, S. S.; Magolda, R. L.; Gaylor, J. L.; Trzaskos, J. M. *J. Lipid Res.* **1989**, *30*, 1621.
(36) Trzaskos, J.; Fischer, R.; Favata, M. *J. Biol. Chem.* **1986**, *261*, 16937.
(37) Shyadehi, A. Z.; Lamb, D. C.; Kelly, S. L.; Kelly, D. E.; Schunck, W. H.; Wright, J. N.; Corina, D.; Akhtar, M. *J. Biol. Chem.* **1996**, *271*, 12445.
(38) Ortiz de Montellano, P. R. *Cytochrome P450: Structure, Mechanism, and Biochemistry*, 3rd ed.; Kluwer Academic/Plenum Publishers: New York, 2005.
(39) Gibbons, G. F.; Pullinger, C. R.; Mitropoulos, K. A. *Biochem. J.* **1979**, *183*, 309.
(40) Sen, K.; Hackett, J. C. *J. Am. Chem. Soc.* **2010**, *132*, 10293.
(41) Patra, T.; Manna, S.; Maiti, D. *Angew. Chem., Int. Ed.* **2011**, *50*, 12140.
(42) Hargrove, T. Y.; Wawrzak, Z.; Liu, J.; Nes, W. D.; Waterman, M. R.; Lepesheva, G. I. *J. Biol. Chem.* **2011**, *286*, 26838.
(43) Lamb, D. C.; Kelly, D. E.; Kelly, S. L. *FEBS Lett.* **1998**, *425*, 263.
(44) Lepesheva, G. I.; Zaitseva, N. G.; Nes, W. D.; Zhou, W.; Arase, M.; Liu, J.; Hill, G. C.; Waterman, M. R. *J. Biol. Chem.* **2006**, *281*, 3577.
(45) Podust, L. M.; Yermalitskaya, L. V.; Lepesheva, G. I.; Podust, V. N.; Dalmasso, E. A.; Waterman, M. R. *Structure* **2004**, *12*, 1937.
(46) Bellamine, A.; Mangla, A. T.; Dennis, A. T.; Nes, W. D.; Waterman, M. R. *J. Lipid Res.* **2001**, *42*, 128.
(47) Schlichting, I.; Berendzen, J.; Chu, K.; Stock, A. M.; Maves, S. A.; Benson, D. E.; Sweet, R. M.; Ringe, D.; Petsko, G. A.; Sligar, S. G. *Science* **2000**, *287*, 1615.
(48) Nagano, S.; Poulos, T. L. *J. Biol. Chem.* **2005**, *280*, 31659.
(49) Podust, L. M.; Sherman, D. H. *Nat. Prod. Rep.* **2012**, *29*, 1251.
(50) Nes, W. D.; Song, Z.; Dennis, A. L.; Zhou, W.; Nam, J.; Miller, M. B. *J. Biol. Chem.* **2003**, *278*, 34505.
(51) Rees, H. H.; Goad, L. J.; Goodwin, T. W. *Biochem. J.* **1968**, *107*, 417.
(52) Risley, J. M. *J. Chem. Educ.* **2002**, *79*, 377.
(53) Urbina, J. A. *Parasitology* **1997**, *114* (Suppl), S91.
(54) de Souza, W.; Rodrigues, J. C. *Interdiscip. Perspect. Infect. Dis.* **2009**, *2009*, 642502.
(55) Urbina, J. A. *Trypanosomatid Diseases: Molecular Routes to Drug Discovery*; Jager, T., Koch, O., Flohe, L.; Wiley-Blackwell: Weinheim, Germany, 2013; pp 489−514.
(56) Doyle, P. S.; Chen, C. K.; Johnston, J. B.; Hopkins, S. D.; Leung, S. S.; Jacobson, M. P.; Engel, J. C.; McKerrow, J. H.; Podust, L. M. *Antimicrob. Agents Chemother.* **2010**, *54*, 2480.
(57) Liendo, A.; Visbal, G.; Piras, M. M.; Piras, R.; Urbina, J. A. *Mol. Biochem. Parasitol.* **1999**, *104*, 81.
(58) Nes, C. R.; Singha, U. K.; Liu, J.; Ganapathy, K.; Villalta, F.; Waterman, M. R.; Lepesheva, G. I.; Chaudhuri, M.; Nes, W. D. *Biochem. J.* **2012**, *443*, 267.
(59) Coppens, I.; Baudhuin, P.; Opperdoes, F. R.; Courtoy, P. J. *Proc. Natl. Acad. Sci. U.S.A.* **1988**, *85*, 6753.
(60) Goad, L. J.; Holz, G. G., Jr.; Beach, D. H. *Mol. Biochem. Parasitol.* **1984**, *10*, 161.
(61) Rodrigues, J. C.; Attias, M.; Rodriguez, C.; Urbina, J. A.; Souza, W. *Antimicrob. Agents Chemother.* **2002**, *46*, 487.
(62) Zhou, W.; Cross, G. A.; Nes, W. D. *J. Lipid Res.* **2007**, *48*, 665.
(63) Sanchez-Sancho, F.; Campillo, N. E.; Paez, J. A. *Curr. Med. Chem.* **2010**, *17*, 423.
(64) Shang, N.; Li, Q.; Ko, T. P.; Chan, H. C.; Li, J.; Zheng, Y.; Huang, C. H.; Ren, F.; Chen, C. C.; Zhu, Z.; Galizzi, M.; Li, Z. H.; Rodrigues-Poveda, C. A.; Gonzalez-Pacanowska, D.; Veiga-Santos, P.; de Carvalho, T. M.; de Souza, W.; Urbina, J. A.; Wang, A. H.; Docampo, R.; Li, K.; Liu, Y. L.; Oldfield, E.; Guo, R. T. *PLoS Pathog.* **2014**, *10*, e1004114.
(65) Musiol, R.; Kowalczyk, W. *Curr. Med. Chem.* **2012**, *19*, 1378.
(66) DiDomenico, B. *Curr. Opin. Microbiol.* **1999**, *2*, 509.
(67) Paiva, J. A.; Pereira, J. M. *Curr. Opin. Infect. Dis.* **2013**, *26*, 168.
(68) Castelli, M. V.; Butassi, E.; Monteiro, M. C.; Svetaz, L. A.; Vicente, F.; Zacchino, S. A. *Expert Opin. Ther. Pat.* **2014**, *24*, 323.
(69) Gupta, A. K.; Tomas, E. *Dermatol. Clin.* **2003**, *21*, 565.
(70) Hossain, M. A.; Ghannoum, M. A. *Expert Opin. Investig. Drugs* **2000**, *9*, 1797.
(71) Geronikaki, A.; Fesatidou, M.; Kartsev, V.; Macaev, F. *Curr. Top. Med. Chem.* **2013**, *13*, 2684.
(72) Heeres, J.; Meerpoel, L.; Lewi, P. *Molecules* **2010**, *15*, 4129.
(73) Heeres, J.; Backx, L. J.; Mostmans, J. H.; Van Cutsem, J. *J. Med. Chem.* **1979**, *22*, 1003.
(74) Heeres, J.; Hendrickx, R.; Van Cutsem, J. *J. Med. Chem.* **1983**, *26*, 611.
(75) Heeres, J.; Backx, L. J.; Van Cutsem, J. *J. Med. Chem.* **1984**, *27*, 894.
(76) Bennett, F.; Saksena, A. K.; Lovey, R. G.; Liu, Y. T.; Patel, N. M.; Pinto, P.; Pike, R.; Jao, E.; Girijavallabhan, V. M.; Ganguly, A. K.; Loebenberg, D.; Wang, H.; Cacciapuoti, A.; Moss, E.; Menzel, F.; Hare, R. S.; Nomeir, A. *Bioorg. Med. Chem. Lett.* **2006**, *16*, 186.
(77) Nomeir, A. A.; Pramanik, B. N.; Heimark, L.; Bennett, F.; Veals, J.; Bartner, P.; Hilbert, M.; Saksena, A.; McNamara, P.; Girijavallabhan, V.; Ganguly, A. K.; Lovey, R.; Pike, R.; Wang, H.; Liu, Y. T.; Kumari, P.; Korfmacher, W.; Lin, C. C.; Cacciapuoti, A.; Loebenberg, D.; Hare, R.; Miller, G.; Pickett, C. *J. Mass. Spectrom.* **2008**, *43*, 509.
(78) Schiller, D. S.; Fung, H. B. *Clin. Ther.* **2007**, *29*, 1862.
(79) Mellinghoff, I. K.; Winston, D. J.; Mukwaya, G.; Schiller, G. J. *Clin. Infect. Dis.* **2002**, *34*, 1648.
(80) Greenberg, R. N.; Mullane, K.; van Burik, J. A.; Raad, I.; Abzug, M. J.; Anstead, G.; Herbrecht, R.; Langston, A.; Marr, K. A.; Schiller, G.; Schuster, M.; Wingard, J. R.; Gonzalez, C. E.; Revankar, S. G.; Corcoran, G.; Kryscio, R. J.; Hare, R. *Antimicrob. Agents Chemother.* **2006**, *50*, 126.
(81) Raad, I. I.; Graybill, J. R.; Bustamante, A. B.; Cornely, O. A.; Gaona-Flores, V.; Afif, C.; Graham, D. R.; Greenberg, R. N.; Hadley, S.; Langston, A.; Negroni, R.; Perfect, J. R.; Pitisuttithum, P.; Restrepo, A.; Schiller, G.; Pedicone, L.; Ullmann, A. J. *Clin. Infect. Dis.* **2006**, *42*, 1726.
(82) Cacciapuoti, A.; Loebenberg, D.; Corcoran, E.; Menzel, F., Jr.; Moss, E. L., Jr.; Norris, C.; Michalski, M.; Raynor, K.; Halpern, J.; Mendrick, C.; Arnold, B.; Antonacci, B.; Parmegiani, R.; Yarosh-Tomaine, T.; Miller, G. H.; Hare, R. S. *Antimicrob. Agents Chemother.* **2000**, *44*, 2017.
(83) Pitisuttithum, P.; Negroni, R.; Graybill, J. R.; Bustamante, B.; Pappas, P.; Chapman, S.; Hare, R. S.; Hardalo, C. J. *J. Antimicrob. Chemother.* **2005**, *56*, 745.
(84) Richardson, K.; Cooper, K.; Marriott, M. S.; Tarbit, M. H.; Troke, P. F.; Whittle, P. J. *Rev. Infect. Dis.* **1990**, *12* (Suppl 3), S267.
(85) Troke, P. F.; Andrews, R. J.; Pye, G. W.; Richardson, K. *Rev. Infect. Dis.* **1990**, *12* (Suppl 3), S276.
(86) Herbrecht, R. *Expert Rev. Anti-Infect. Ther.* **2004**, *2*, 485.
(87) Plempel, M.; Bartmann, K.; Buchel, K. H.; Regel, E. *Antimicrob. Agents Chemother.* **1969**, *9*, 271.
(88) Plempel, M.; Regel, E.; Buchel, K. H. *Arzneim. Forsch.* **1983**, *33*, 517.
(89) Lackner, T. E.; Clissold, S. P. *Drugs* **1989**, *38*, 204.
(90) Zirngibl, L.; Fischer, J.; Jahn, U.; Thiele, K. *Ann. N.Y. Acad. Sci.* **1988**, *544*, 63.
(91) Koga, H.; Tsuji, Y.; Inoue, K.; Kanai, K.; Majima, T.; Kasai, T.; Uchida, K.; Yamaguchi, H. *J. Infect. Chemother.* **2006**, *12*, 163.
(92) Niwano, Y.; Kuzuhara, N.; Kodama, H.; Yoshida, M.; Miyazaki, T.; Yamaguchi, H. *Antimicrob. Agents Chemother.* **1998**, *42*, 967.
(93) Berman, J. D. *Am. J. Trop. Med. Hyg.* **1981**, *30*, 566.
(94) Emad, M.; Hayati, F.; Fallahzadeh, M. K.; Namazi, M. R. *J. Am. Acad. Dermatol.* **2011**, *64*, 606.
(95) Shakya, N.; Sane, S. A.; Gupta, S. *Parasitol. Res.* **2011**, *108*, 793.

(96) Shakya, N.; Sane, S. A.; Vishwakarma, P.; Bajpai, P.; Gupta, S. *Acta Trop* **2011**, *119*, 188.
(97) Gonzalez, U.; Pinart, M.; Rengifo-Pardo, M.; Macaya, A.; Alvar, J.; Tweed, J. A. *Cochrane Database of Systemic Reviews*; 2009; CD004834.
(98) de Macedo-Silva, S. T.; Urbina, J. A.; de Souza, W.; Rodrigues, J. C. *PLoS One* **2013**, *8*, e83247.
(99) Al-Abdely, H. M.; Graybill, J. R.; Loebenberg, D.; Melby, P. C. *Antimicrob. Agents Chemother.* **1999**, *43*, 2910.
(100) Navin, T. R.; Arana, B. A.; Arana, F. E.; Berman, J. D.; Chajon, J. F. *J. Infect. Dis.* **1992**, *165*, 528.
(101) Paniz Mondolfi, A. E.; Stavropoulos, C.; Gelanew, T.; Loucas, E.; Perez Alvarez, A. M.; Benaim, G.; Polsky, B.; Schoenian, G.; Sordillo, E. M. *Antimicrob. Agents Chemother.* **2011**, *55*, 1774.
(102) Baroni, A.; Aiello, F. S.; Vozza, A.; Vozza, G.; Faccenda, F.; Brasiello, M.; Ruocco, E. *Dermatol. Ther.* **2009**, *22* (Suppl 1), S27.
(103) White, J. M.; Salisbury, J. R.; Jones, J.; Higgins, E. M.; Vega-Lopez, F. *Pediatr. Dermatol.* **2006**, *23*, 78.
(104) Firooz, A.; Khatami, A.; Dowlati, Y. *Int. J. Dermatol.* **2006**, *45*, 1446.
(105) Berman, J. D. *Clin. Infect. Dis.* **1997**, *24*, 684.
(106) Zijlstra, E. E.; el-Hassan, A. M. *Trans. R. Soc. Trop. Med. Hyg.* **2001**, *95* (Suppl 1), S59.
(107) Gangneux, J. P.; Dullin, M.; Sulahian, A.; Garin, Y. J.; Derouin, F. *Antimicrob. Agents Chemother.* **1999**, *43*, 172.
(108) Chagas, C. *Mem. Inst. Oswaldo Cruz* **1909**, *1*, 159.
(109) Russi, A. J.; Russi, A.; Marin-Neto, J. A. *Lancet* **2010**, *375*, 1388.
(110) World Health Organization. *Fact Sheet 340: Chagas Disease (American trypanosomiasis)*; 2013. http://www.who.int/mediacentre/factsheets/fs340/en/.
(111) Lee, B. Y.; Bacon, K. M.; Bottazzi, M. E.; Hotez, P. J. *Lancet Infect. Dis.* **2013**, *13*, 342.
(112) Urbina, J. A.; Docampo, R. *Trends Parasitol.* **2003**, *19*, 495.
(113) Coura, J. R.; Borges-Pereira, J. *Mem. Inst. Oswaldo Cruz* **2011**, *106*, 641.
(114) Viotti, R.; de Noya, B. A.; Araujo-Jorge, T.; Grijalva, M. J.; Guhl, F.; Lopez, M. C.; Ramsey, J. M.; Ribeiro, I.; Schijman, A. G.; Sosa-Estani, S.; Torrico, F.; Gascon, J. *Antimicrob. Agents Chemother.* **2014**, *58*, 635.
(115) Castro, J. A.; de Mecca, M. M.; Bartel, L. C. *Hum. Exp. Toxicol.* **2006**, *25*, 471.
(116) Cancado, J. R. *Rev. Inst. Med. Trop. Sao Paulo* **2002**, *44*, 29.
(117) Filardi, L. S.; Brener, Z. *Trans. R. Soc. Trop. Med. Hyg.* **1987**, *81*, 755.
(118) Camandaroba, E. L.; Reis, E. A.; Goncalves, M. S.; Reis, M. G.; Andrade, S. G. *Rev. Soc. Bras. Med. Trop.* **2003**, *36*, 201.
(119) Moreno, M.; D'Avila, D. A.; Silva, M. N.; Galvao, L. M.; Macedo, A. M.; Chiari, E.; Gontijo, E. D.; Zingales, B. *Mem. Inst. Oswaldo Cruz* **2010**, *105*, 918.
(120) Teston, A. P.; Monteiro, W. M.; Reis, D.; Bossolani, G. D.; Gomes, M. L.; de Araujo, S. M.; Bahia, M. T.; Barbosa, M. G.; Toledo, M. J. *Trop. Med. Int. Health* **2013**, *18*, 85.
(121) Mejia, A. M.; Hall, B. S.; Taylor, M. C.; Gomez-Palacio, A.; Wilkinson, S. R.; Triana-Chavez, O.; Kelly, J. M. *J. Infect. Dis.* **2012**, *206*, 220.
(122) Urbina, J. A. *Curr. Opin. Infect. Dis.* **2001**, *14*, 733.
(123) Buckner, F. In *Drug Targets in Kinetoplastid Parasites*; Majumder, H. K., Ed.; Springer: New York, 2008; Vol. *625*.
(124) Urbina, J. A. *Mem. Inst. Oswaldo Cruz* **2009**, *104* (Suppl 1), 311.
(125) Urbina, J. A.; Payares, G.; Molina, J.; Sanoja, C.; Liendo, A.; Lazardi, K.; Piras, M. M.; Piras, R.; Perez, N.; Wincker, P.; Ryley, J. F. *Science* **1996**, *273*, 969.
(126) Urbina, J. A.; Payares, G.; Contreras, L. M.; Liendo, A.; Sanoja, C.; Molina, J.; Piras, M.; Piras, R.; Perez, N.; Wincker, P.; Loebenberg, D. *Antimicrob. Agents Chemother.* **1998**, *42*, 1771.
(127) Ferraz, M. L.; Gazzinelli, R. T.; Alves, R. O.; Urbina, J. A.; Romanha, A. J. *Antimicrob. Agents Chemother.* **2007**, *51*, 1359.
(128) Pinazo, M.-J.; Espinosa, G.; Gállego, M.; López-Chejade, P. L.; Urbina, J.; Gascón, J. *Am. J. Trop. Med. Hyg.* **2010**, *82*, 583.
(129) Clayton, J. *Nature* **2010**, *465*, S12.
(130) Urbina, J. A.; Payares, G.; Sanoja, C.; Lira, R.; Romanha, A. J. *Int. J. Antimicrob. Agents* **2003**, *21*, 27.
(131) Diniz Lde, F.; Caldas, I. S.; Guedes, P. M.; Crepalde, G.; de Lana, M.; Carneiro, C. M.; Talvani, A.; Urbina, J. A.; Bahia, M. T. *Antimicrob. Agents Chemother.* **2010**, *54*, 2979.
(132) Guedes, P. M.; Urbina, J. A.; de Lana, M.; Afonso, L. C.; Veloso, V. M.; Tafuri, W. L.; Machado-Coelho, G. L.; Chiari, E.; Bahia, M. T. *Antimicrob. Agents Chemother.* **2004**, *48*, 4286.
(133) Urbina, J. A.; Payares, G.; Sanoja, C.; Molina, J.; Lira, R.; Brener, Z.; Romanha, A. J. *Int. J. Antimicrob. Agents* **2003**, *21*, 39.
(134) Corrales, M.; Cardozo, R.; Segura, M. A.; Urbina, J. A.; Basombrio, M. A. *Antimicrob. Agents Chemother.* **2005**, *49*, 1556.
(135) *STOP CHAGAS Trial (Merck, Latin America and Spain): A Study of the Use of Oral Posaconazole (POS) in the Treatment of Asymptomatic Chronic Chagas Disease (P05267) (STOP CHAGAS)*; Merck Sharp & Dohme Corp. http://clinicaltrials.gov/. Identifier: NCT01377480.
(136) *CHAGASAZOL Trial (Posaconazole, Spain): Clinical Trial For The Treatment Of Chronic Chagas Disease With Posaconazole And Benznidazole (CHAGASAZOL)*; Hospital Universitari Vall d'Hebron Research Institute. http://clinicaltrials.gov/. Identifier: NCT01162967.
(137) *E1224/Benznidazole Trial (DNDi-Eisai, Bolivia): Proof-of-Concept Study of E1224 to Treat Adult Patients With Chagas Disease. Drugs for Neglected Diseases Initiative*. http://clinicaltrials.gov/. Identifier: NCT01489228.
(138) *Drug Trial for Leading Parasitic Killer of the Americas Shows Mixed Results but Provides New Evidence for Improved Therapy*; DNDi. http://www.dndi.org/media-centre/press-releases/1700-e1224.html.
(139) Molina, I.; Gomez i Prat, J.; Salvador, F.; Trevino, B.; Sulleiro, E.; Serre, N.; Pou, D.; Roure, S.; Cabezos, J.; Valerio, L.; Blanco-Grau, A.; Sanchez-Montalva, A.; Vidal, X.; Pahissa, A. *N. Engl. J. Med.* **2014**, *370*, 1899.
(140) Urbina, J. A. *Acta Trop.* **2010**, *115*, 55.
(141) Lewis, M. D.; Fortes Francisco, A.; Taylor, M. C.; Burrell-Saward, H.; McLatchie, A. P.; Miles, M. A.; Kelly, J. M. *Cell Microbiol.* **2014**, *16*, 1285.
(142) Podust, L. M.; Poulos, T. L.; Waterman, M. R. *Proc. Natl. Acad. Sci. U.S.A.* **2001**, *98*, 3068.
(143) Podust, L. M.; von Kries, J. P.; Nasser Eddine, A.; Kim, Y.; Yermalitskaya, L. V.; Kuehne, R.; Ouellet, H.; Warrier, T.; Altekoster, M.; Lee, J.-S.; Rademann, J.; Oschkinat, H.; Kaufmann, S. H. E.; Waterman, M. R. *Antimicrob. Agents Chemother.* **2007**, *51*, 3915.
(144) Nasser Eddine, A.; von Kries, J. P.; Podust, M. V.; Warrier, T.; Kaufmann, S. H.; Podust, L. M. *J. Biol. Chem.* **2008**, *283*, 15152.
(145) Chen, C.-K.; Doyle, P. S.; Yermalitskaya, L. V.; Mackey, Z. B.; Ang, K. K. H.; McKerrow, J. H.; Podust, L. M. *PLoS Neglected Trop. Dis.* **2009**, *3*, e372.
(146) Chen, C.-K.; Leung, S. S. F.; Guilbert, C.; Jacobson, M. P.; McKerrow, J. H.; Podust, L. M. *PLoS Neglected Trop. Dis.* **2010**, *4*, e651.
(147) Choi, J. Y.; Calvet, C. M.; Vieira, D. F.; Gunatilleke, S. S.; Cameron, M. D.; McKerrow, J. H.; Podust, L. M.; Roush, W. R. *ACS Med. Chem. Lett.* **2014**, *5*, 434.
(148) Lepesheva, G. I.; Hargrove, T. Y.; Anderson, S.; Kleshchenko, Y.; Furtak, V.; Wawrzak, Z.; Villalta, F.; Waterman, M. R. *J. Biol. Chem.* **2010**, *285*, 25582.
(149) Andriani, G.; Amata, E.; Beatty, J.; Clements, Z.; Coffey, B. J.; Courtemanche, G.; Devine, W.; Erath, J.; Juda, C. E.; Wawrzak, Z.; Wood, J. T.; Lepesheva, G. I.; Rodriguez, A.; Pollastri, M. P. *J. Med. Chem.* **2013**, *56*, 2556.
(150) Hargrove, T. Y.; Wawrzak, Z.; Alexander, P. W.; Chaplin, J. H.; Keenan, M.; Charman, S. A.; Perez, C. J.; Waterman, M. R.; Chatelain, E.; Lepesheva, G. I. *J. Biol. Chem.* **2013**, *288*, 31602.
(151) Vieira, D. F.; Choi, J. Y.; Roush, W. R.; Podust, L. M. *ChemBioChem* **2014**, *15*, 1111.

(152) Calvet, C. M.; Vieira, D. F.; Choi, J. Y.; Kellar, D.; Cameron, M. D.; Siqueira-Neto, J. L.; Gut, J.; Johnston, J. B.; Lin, L.; Khan, S.; McKerrow, J. H.; Roush, W. R.; Podust, L. M. *J. Med. Chem.* **2014**, *57*, 6989.
(153) Lepesheva, G. I.; Park, H. W.; Hargrove, T. Y.; Vanhollebeke, B.; Wawrzak, Z.; Harp, J. M.; Sundaramoorthy, M.; Nes, W. D.; Pays, E.; Chaudhuri, M.; Villalta, F.; Waterman, M. R. *J. Biol. Chem.* **2010**, *285*, 1773.
(154) Choi, J. Y.; Calvet, C. M.; Gunatilleke, S. S.; Ruiz, C.; Cameron, M. D.; McKerrow, J. H.; Podust, L. M.; Roush, W. R. *J. Med. Chem.* **2013**, *56*, 7651.
(155) Hargrove, T. Y.; Wawrzak, Z.; Liu, J.; Waterman, M. R.; Nes, W. D.; Lepesheva, G. I. *J. Lipid Res.* **2012**, *53*, 311.
(156) Buckner, F. S.; Bahia, M. T.; Suryadevara, P. K.; White, K. L.; Shackleford, D. M.; Chennamaneni, N. K.; Hulverson, M. A.; Laydbak, J. U.; Chatelain, E.; Scandale, I.; Verlinde, C. L.; Charman, S. A.; Lepesheva, G. I.; Gelb, M. H. *Antimicrob. Agents Chemother.* **2012**, *56*, 4914.
(157) Monk, B. C.; Tomasiak, T. M.; Keniya, M. V.; Huschmann, F. U.; Tyndall, J. D. A.; O'Connell, J. D., III; Cannon, R. D.; McDonald, J. G.; Rodriguez, A.; Finer-Moore, J. S.; Stroud, R. M. *Proc. Natl. Acad. Sci. U.S.A.* **2014**, *111*, 3865.
(158) Strushkevich, N.; Usanov, S. A.; Park, H. W. *J. Mol. Biol.* **2010**, *397*, 1067.
(159) Becher, R.; Wirsel, S. G. *Appl. Microbiol. Biotechnol.* **2012**, *95*, 825.
(160) Li, H.; Poulos, T. L. *Curr. Top. Med. Chem.* **2004**, *4*, 1789.
(161) Pochapsky, T. C.; Kazanis, S.; Dang, M. *Antioxid. Redox Signal.* **2010**, *13*, 1273.
(162) Poulos, T. L.; Finzel, B. C.; Howard, A. J. *J. Mol. Biol.* **1987**, *195*, 687.
(163) Gunatilleke, S. S.; Calvet, C. M.; Johnston, J. B.; Chen, C. K.; Erenburg, G.; Gut, J.; Engel, J. C.; Ang, K. K.; Mulvaney, J.; Chen, S.; Arkin, M. R.; McKerrow, J. H.; Podust, L. M. *PLoS Neglected Trop. Dis.* **2012**, *6*, e1736.
(164) Hargrove, T. Y.; Kim, K.; de Nazare Correia Soeiro, M.; da Silva, C. F.; Batista, D. D.; Batista, M. M.; Yazlovitskaya, E. M.; Waterman, M. R.; Sulikowski, G. A.; Lepesheva, G. I. *Int. J. Parasitol.: Drugs Drug Resist.* **2012**, *2*, 178.
(165) Parish, E. J.; Schroepfer, G. J., Jr. *J. Lipid Res.* **1981**, *22*, 859.
(166) Frye, L. L.; Robinson, C. H. *J. Org. Chem.* **1990**, *55*, 1579.
(167) Moss, G. P. *Nomenclature of Steroids*; Queen Mary College: London, 1989.
(168) DeLano, W. L. *The PyMOL Molecular Graphics System*; DeLano Scientific: San Carlos, CA, 2002.
(169) Engel, J. C.; Ang, K. K. H.; Chen, S.; Arkin, M. R.; McKerrow, J. H.; Doyle, P. S. *Antimicrob. Agents Chemother.* **2010**, *54*, 3326.
(170) Buckner, F. S.; Verlinde, C. L.; La Flamme, A. C.; Van Voorhis, W. C. *Antimicrob. Agents Chemother.* **1996**, *40*, 2592.
(171) Andriani, G.; Chessler, A. D.; Courtemanche, G.; Burleigh, B. A.; Rodriguez, A. *PLoS Neglected Trop. Dis.* **2011**, *5*, e1298.
(172) Keenan, M.; Alexander, P. W.; Chaplin, J. H.; Abbott, M. J.; Diao, H.; Wang, Z.; Best, W. M.; Perez, C. J.; Cornwall, S. M.; Keatley, S. K.; Thompson, R. C.; Charman, S. A.; White, K. L.; Ryan, E.; Chen, G.; Ioset, J. R.; von Geldern, T. W.; Chatelain, E. *Future Med. Chem.* **2013**, *5*, 1733.
(173) Friggeri, L.; Scipione, L.; Costi, R.; Kaiser, M.; Moraca, F.; Zamperini, C.; Botta, B.; Di Santo, R.; De Vita, D.; Brun, R.; Tortorella, S. *ACS Med. Chem. Lett.* **2013**, *4*, 538.
(174) De Vita, D.; Scipione, L.; Tortorella, S.; Mellini, P.; Di Rienzo, B.; Simonetti, G.; D'Auria, F. D.; Panella, S.; Cirilli, R.; Di Santo, R.; Palamara, A. T. *Eur. J. Med. Chem.* **2012**, *49*, 334.
(175) Lennon, I. C.; Ramsden, J. A. *Org. Process Res. Dev.* **2005**, *9*, 110.
(176) Dandapani, S.; Germain, A. R.; Jewett, I.; le Quement, S.; Marie, J.-C.; Muncipinto, G.; Duvall, J. R.; Carmody, L. C.; Perez, J. R.; Engel, J. C.; Gut, J.; Kellar, D.; Siqueira-Neto, J. L.; McKerrow, J. H.; Kaiser, M.; Rodriguez, A.; Palmer, M. A.; Foley, M.; Schreiber, S. L.; Munoz, B. *ACS Med. Chem. Lett.* **2014**, *5*, 149.
(177) von Kries, J. P.; Warrier, T.; Podust, L. M. *Current Protocols in Microbiology*; Wiley: New York, 2010; Vol. *16*, Unit 17.4.
(178) Keiser, M. J.; Roth, B. L.; Armbruster, B. N.; Ernsberger, P.; Irwin, J. J.; Shoichet, B. K. *Nat. Biotechnol.* **2007**, *25*, 197.
(179) Sakariassen, K. S.; Alberts, P.; Fontana, P.; Mann, J.; Bounameaux, H.; Sorensen, A. S. *Future Cardiol.* **2009**, *5*, 479.
(180) Hardwick, J. P. *Biochem. Pharmacol.* **2008**, *75*, 2263.
(181) Courtney, K. D.; Taplin, M. E. *Curr. Opin. Oncol.* **2012**, *24*, 272.
(182) Litton, J. K.; Arun, B. K.; Brown, P. H.; Hortobagyi, G. N. *Expert Opin. Pharmacother.* **2012**, *13*, 325.
(183) Schilling, S.; Wasternack, C.; Demuth, H. U. *Biol. Chem.* **2008**, *389*, 983.
(184) Konkle, M. E.; Hargrove, T. Y.; Kleshchenko, Y. Y.; von Kries, J. P.; Ridenour, W.; Uddin, M. J.; Caprioli, R. M.; Marnett, L. J.; Nes, W. D.; Villalta, F.; Waterman, M. R.; Lepesheva, G. I. *J. Med. Chem.* **2009**, *52*, 2846.
(185) Choy, J. W.; Bryant, C.; Calvet, C. M.; Doyle, P. S.; Gunatilleke, S. S.; Leung, S. S.; Ang, K. K.; Chen, S.; Gut, J.; Oses-Prieto, J. A.; Johnston, J. B.; Arkin, M. R.; Burlingame, A. L.; Taunton, J.; Jacobson, M. P.; McKerrow, J. M.; Podust, L. M.; Renslo, A. R. *Beilstein J. Org. Chem.* **2013**, *9*, 15.
(186) Nwaka, S.; Hudson, A. *Nat. Rev. Drug Discovery* **2006**, *5*, 941.
(187) Kohl, N. E.; Mosser, S. D.; deSolms, S. J.; Giuliani, E. A.; Pompliano, D. L.; Graham, S. L.; Smith, R. L.; Scolnick, E. M.; Oliff, A.; Gibbs, J. B. *Science* **1993**, *260*, 1934.
(188) Karp, J. E.; Kaufmann, S. H.; Adjei, A. A.; Lancet, J. E.; Wright, J. J.; End, D. W. *Curr. Opin. Oncol.* **2001**, *13*, 470.
(189) Buckner, F.; Yokoyama, K.; Lockman, J.; Aikenhead, K.; Ohkanda, J.; Sadilek, M.; Sebti, S.; Van Voorhis, W.; Hamilton, A.; Gelb, M. H. *Proc. Natl. Acad. Sci. U.S.A.* **2003**, *100*, 15149.
(190) Hucke, O.; Gelb, M. H.; Verlinde, C. L.; Buckner, F. S. *J. Med. Chem.* **2005**, *48*, 5415.
(191) Chennamaneni, N. K.; Arif, J.; Buckner, F. S.; Gelb, M. H. *Bioorg. Med. Chem. Lett.* **2009**, *19*, 6582.
(192) Kraus, J. M.; Tatipaka, H. B.; McGuffin, S. A.; Chennamaneni, N. K.; Karimi, M.; Arif, J.; Verlinde, C. L.; Buckner, F. S.; Gelb, M. H. *J. Med. Chem.* **2010**, *53*, 3887.
(193) Kraus, J. M.; Verlinde, C. L.; Karimi, M.; Lepesheva, G. I.; Gelb, M. H.; Buckner, F. S. *J. Med. Chem.* **2009**, *52*, 1639.
(194) Ohkanda, J.; Buckner, F. S.; Lockman, J. W.; Yokoyama, K.; Carrico, D.; Eastman, R.; de Luca-Fradley, K.; Davies, W.; Croft, S. L.; Van Voorhis, W. C.; Gelb, M. H.; Sebti, S. M.; Hamilton, A. D. *J. Med. Chem.* **2004**, *47*, 432.
(195) Suryadevara, P. K.; Racherla, K. K.; Olepu, S.; Norcross, N. R.; Tatipaka, H. B.; Arif, J. A.; Planer, J. D.; Lepesheva, G. I.; Verlinde, C. L.; Buckner, F. S.; Gelb, M. H. *Bioorg. Med. Chem. Lett.* **2013**, *23*, 6492.
(196) Bettiol, E.; Samanovic, M.; Murkin, A. S.; Raper, J.; Buckner, F.; Rodriguez, A. *PLoS Neglected Trop. Dis.* **2009**, *3*, e384.
(197) Lepesheva, G. I.; Ott, R. D.; Hargrove, T. Y.; Kleshchenko, Y. Y.; Schuster, I.; Nes, W. D.; Hill, G. C.; Villalta, F.; Waterman, M. R. *Chem. Biol.* **2007**, *14*, 1283.
(198) Villalta, F.; Dobish, M. C.; Nde, P. N.; Kleshchenko, Y. Y.; Hargrove, T. Y.; Johnson, C. A.; Waterman, M. R.; Johnston, J. N.; Lepesheva, G. I. *J. Infect. Dis.* **2013**, *208*, 504.
(199) Soeiro Mde, N.; de Souza, E. M.; da Silva, C. F.; Batista Dda, G.; Batista, M. M.; Pavao, B. P.; Araujo, J. S.; Aiub, C. A.; da Silva, P. B.; Lionel, J.; Britto, C.; Kim, K.; Sulikowski, G.; Hargrove, T. Y.; Waterman, M. R.; Lepesheva, G. I. *Antimicrob. Agents Chemother.* **2013**, *57*, 4151.
(200) Keenan, M.; Abbott, M. J.; Alexander, P. W.; Armstrong, T.; Best, W. M.; Berven, B.; Botero, A.; Chaplin, J. H.; Charman, S. A.; Chatelain, E.; von Geldern, T. W.; Kerfoot, M.; Khong, A.; Nguyen, T.; McManus, J. D.; Morizzi, J.; Ryan, E.; Scandale, I.; Thompson, R. A.; Wang, S. Z.; White, K. L. *J. Med. Chem.* **2012**, *55*, 4189.
(201) Zeiman, E.; Greenblatt, C. L.; Elgavish, S.; Khozin-Goldberg, I.; Golenser, J. *J. Parasitol.* **2008**, *94*, 280.
(202) Keenan, M.; Alexander, P. W.; Diao, H.; Best, W. M.; Khong, A.; Kerfoot, M.; Thompson, R. C.; White, K. L.; Shackleford, D. M.;

Ryan, E.; Gregg, A. D.; Charman, S. A.; von Geldern, T. W.; Scandale, I.; Chatelain, E. *Bioorg. Med. Chem.* **2013**, *21*, 1756.
(203) Keenan, M.; Chaplin, J. H.; Alexander, P. W.; Abbott, M. J.; Best, W. M.; Khong, A.; Botero, A.; Perez, C.; Cornwall, S.; Thompson, R. A.; White, K. L.; Shackleford, D. M.; Koltun, M.; Chiu, F. C.; Morizzi, J.; Ryan, E.; Campbell, M.; von Geldern, T. W.; Scandale, I.; Chatelain, E.; Charman, S. A. *J. Med. Chem.* **2013**, *56*, 10158.
(204) Lepesheva, G. I.; Waterman, M. R. *Curr. Top. Med. Chem.* **2011**, *11*, 2060.
(205) Ji, H.; Zhang, W.; Zhang, M.; Kudo, M.; Aoyama, Y.; Yoshida, Y.; Sheng, C.; Song, Y.; Yang, S.; Zhou, Y.; Lu, J.; Zhu, J. *J. Med. Chem.* **2003**, *46*, 474.
(206) Trzaskos, J. M.; Ko, S. S.; Magolda, R. L.; Favata, M. F.; Fischer, R. T.; Stam, S. H.; Johnson, P. R.; Gaylor, J. L. *Biochemistry* **1995**, *34*, 9670.
(207) Sanglard, D. *Curr. Opin. Microbiol.* **2002**, *5*, 379.
(208) ABalkis, M. M.; Leidich, S. D.; Mukherjee, P. K.; Ghannoum, M. A. *Drugs* **2002**, *62*, 1025.
(209) Morio, F.; Loge, C.; Besse, B.; Hennequin, C.; Le Pape, P. *Diagn. Microbiol. Infect. Dis.* **2010**, *66*, 373.
(210) Marichal, P.; Koymans, L.; Willemsens, S.; Bellens, D.; Verhasselt, P.; Luyten, W.; Borgers, M.; Ramaekers, F. C. S.; Odds, F. C.; Bossche, H. V. *Microbiology* **1999**, *145*, 2701.
(211) Perea, S.; Lopez-Ribot, J. L.; Kirkpatrick, W. R.; McAtee, R. K.; Santillan, R. A.; Martinez, M.; Calabrese, D.; Sanglard, D.; Patterson, T. F. *Antimicrob. Agents Chemother.* **2001**, *45*, 2676.
(212) Chau, A. S.; Mendrick, C. A.; Sabatelli, F. J.; Loebenberg, D.; McNicholas, P. M. *Antimicrob. Agents Chemother.* **2004**, *48*, 2124.
(213) Sanglard, D.; Ischer, F.; Koymans, L.; Bille, J. *Antimicrob. Agents Chemother.* **1998**, *42*, 241.
(214) Xiao, L.; Madison, V.; Chau, A. S.; Loebenberg, D.; Palermo, R. E.; McNicholas, P. M. *Antimicrob. Agents Chemother.* **2004**, *48*, 568.
(215) Dunkel, N.; Liu, T. T.; Barker, K. S.; Homayouni, R.; Morschhauser, J.; Rogers, P. D. *Eukaryotic Cell* **2008**, *7*, 1180.
(216) Coste, A.; Selmecki, A.; Forche, A.; Diogo, D.; Bougnoux, M. E.; d'Enfert, C.; Berman, J.; Sanglard, D. *Eukaryotic Cell* **2007**, *6*, 1889.
(217) Selmecki, A.; Gerami-Nejad, M.; Paulson, C.; Forche, A.; Berman, J. *Mol. Microbiol.* **2008**, *68*, 624.
(218) Timpel, C.; Strahl-Bolsinger, S.; Ziegelbauer, K.; Ernst, J. F. *J. Biol. Chem.* **1998**, *273*, 20837.
(219) Jensen-Pergakes, K. L.; Kennedy, M. A.; Lees, N. D.; Barbuch, R.; Koegel, C.; Bard, M. *Antimicrob. Agents Chemother.* **1998**, *42*, 1160.
(220) Kelly, S. L.; Lamb, D. C.; Kelly, D. E.; Manning, N. J.; Loeffler, J.; Hebart, H.; Schumacher, U.; Einsele, H. *FEBS Lett.* **1997**, *400*, 80.
(221) Venkateswarlu, K.; Taylor, M.; Manning, N. J.; Rinaldi, M. G.; Kelly, S. L. *Antimicrob. Agents Chemother.* **1997**, *41*, 748.
(222) Geber, A.; Hitchcock, C. A.; Swartz, J. E.; Pullen, F. S.; Marsden, K. E.; Kwon-Chung, K. J.; Bennett, J. E. *Antimicrob. Agents Chemother.* **1995**, *39*, 2708.
(223) Kelly, S. L.; Lamb, D. C.; Corran, A. J.; Baldwin, B. C.; Kelly, D. E. *Biochem. Biophys. Res. Commun.* **1995**, *207*, 910.
(224) Slaven, J. W.; Anderson, M. J.; Sanglard, D.; Dixon, G. K.; Bille, J.; Roberts, I. S.; Denning, D. W. *Fungal Genet. Biol.* **2002**, *36*, 199.
(225) Mellado, E.; Diaz-Guerra, T. M.; Cuenca-Estrella, M.; Rodriguez-Tudela, J. L. *J. Clin. Microbiol.* **2001**, *39*, 2431.
(226) Howard, S. J.; Webster, I.; Moore, C. B.; Gardiner, R. E.; Park, S.; Perlin, D. S.; Denning, D. W. *Int. J. Antimicrob. Agents* **2006**, *28*, 450.
(227) Diaz-Guerra, T. M.; Mellado, E.; Cuenca-Estrella, M.; Rodriguez-Tudela, J. L. *Antimicrob. Agents Chemother.* **2003**, *47*, 1120.
(228) Mann, P. A.; Parmegiani, R. M.; Wei, S. Q.; Mendrick, C. A.; Li, X.; Loebenberg, D.; DiDomenico, B.; Hare, R. S.; Walker, S. S.; McNicholas, P. M. *Antimicrob. Agents Chemother.* **2003**, *47*, 577.
(229) Howard, S. J.; Cerar, D.; Anderson, M. J.; Albarrag, A.; Fisher, M. C.; Pasqualotto, A. C.; Laverdiere, M.; Arendrup, M. C.; Perlin, D. S.; Denning, D. W. *Emerging Infect. Dis.* **2009**, *15*, 1068.
(230) Pfaller, M. A.; Diekema, D. J.; Ghannoum, M. A.; Rex, J. H.; Alexander, B. D.; Andes, D.; Brown, S. D.; Chaturvedi, V.; Espinel-Ingroff, A.; Fowler, C. L.; Johnson, E. M.; Knapp, C. C.; Motyl, M. R.; Ostrosky-Zeichner, L.; Sheehan, D. J.; Walsh, T. J. *J. Clin. Microbiol.* **2009**, *47*, 3142.
(231) Pinto e Silva, A. T.; Costa-de-Oliveira, S.; Silva-Dias, A.; Pina-Vaz, C.; Rodrigues, A. G. *FEMS Yeast Res.* **2009**, *9*, 626.
(232) Li, X.; Brown, N.; Chau, A. S.; Lopez-Ribot, J. L.; Ruesga, M. T.; Quindos, G.; Mendrick, C. A.; Hare, R. S.; Loebenberg, D.; DiDomenico, B.; McNicholas, P. M. *J. Antimicrob. Chemother.* **2004**, *53*, 74.
(233) Mellado, E.; Garcia-Effron, G.; Alcazar-Fuoli, L.; Cuenca-Estrella, M.; Rodriguez-Tudela, J. L. *Antimicrob. Agents Chemother.* **2004**, *48*, 2747.
(234) Rodriguez-Tudela, J. L.; Alcazar-Fuoli, L.; Mellado, E.; Alastruey-Izquierdo, A.; Monzon, A.; Cuenca-Estrella, M. *Antimicrob. Agents Chemother.* **2008**, *52*, 2468.
(235) Vermeulen, E.; Lagrou, K.; Verweij, P. E. *Curr. Opin. Infect. Dis.* **2013**, *26*, 493.
(236) Verweij, P. E.; Mellado, E.; Melchers, W. J. *N. Engl. J. Med.* **2007**, *356*, 1481.
(237) Mellado, E.; Garcia-Effron, G.; Alcazar-Fuoli, L.; Melchers, W. J.; Verweij, P. E.; Cuenca-Estrella, M.; Rodriguez-Tudela, J. L. *Antimicrob. Agents Chemother.* **2007**, *51*, 1897.
(238) van der Linden, J. W.; Camps, S. M.; Kampinga, G. A.; Arends, J. P.; Debets-Ossenkopp, Y. J.; Haas, P. J.; Rijnders, B. J.; Kuijper, E. J.; van Tiel, F. H.; Varga, J.; Karawajczyk, A.; Zoll, J.; Melchers, W. J.; Verweij, P. E. *Clin. Infect. Dis.* **2013**, *57*, 513.
(239) Snelders, E.; Camps, S. M.; Karawajczyk, A.; Schaftenaar, G.; Kema, G. H.; van der Lee, H. A.; Klaassen, C. H.; Melchers, W. J.; Verweij, P. E. *PLoS One* **2012**, *7*, e31801.
(240) Verweij, P. E.; Snelders, E.; Kema, G. H.; Mellado, E.; Melchers, W. J. *Lancet Infect. Dis.* **2009**, *9*, 789.
(241) Snelders, E.; Huis In 't Veld, R. A.; Rijs, A. J.; Kema, G. H.; Melchers, W. J.; Verweij, P. E. *Appl. Environ. Microbiol.* **2009**, *75*, 4053.
(242) Martin-Iguacel, R.; Kurtzhals, J.; Jouvion, G.; Nielsen, S. D.; Llibre, J. M. *Infection* **2014**, *42*, 611.
(243) Wheat, L. J.; Connolly, P.; Smedema, M.; Brizendine, E.; Hafner, R. *Clin. Infect. Dis.* **2001**, *33*, 1910.
(244) Wheat, L. J.; Connolly, P.; Smedema, M.; Durkin, M.; Brizendine, E.; Mann, P.; Patel, R.; McNicholas, P. M.; Goldman, M. *J. Antimicrob. Chemother.* **2006**, *57*, 1235.
(245) Friese, G.; Discher, T.; Fussle, R.; Schmalreck, A.; Lohmeyer, J. *AIDS* **2001**, *15*, 2344.
(246) Rodero, L.; Mellado, E.; Rodriguez, A. C.; Salve, A.; Guelfand, L.; Cahn, P.; Cuenca-Estrella, M.; Davel, G.; Rodriguez-Tudela, J. L. *Antimicrob. Agents Chemother.* **2003**, *47*, 3653.
(247) Sionov, E.; Chang, Y. C.; Garraffo, H. M.; Dolan, M. A.; Ghannoum, M. A.; Kwon-Chung, K. J. *Antimicrob. Agents Chemother.* **2012**, *56*, 1162.
(248) Sionov, E.; Lee, H.; Chang, Y. C.; Kwon-Chung, K. J. *PLoS Pathog.* **2010**, *6*, e1000848.
(249) Posteraro, B.; Sanguinetti, M.; Sanglard, D.; La Sorda, M.; Boccia, S.; Romano, L.; Morace, G.; Fadda, G. *Mol. Microbiol.* **2003**, *47*, 357.
(250) Buckner, F. S.; Wilson, A. J.; White, T. C.; Van Voorhis, W. C. *Antimicrob. Agents Chemother.* **1998**, *42*, 3245.
(251) Zingales, B.; Miles, M. A.; Campbell, D. A.; Tibayrenc, M.; Macedo, A. M.; Teixeira, M. M.; Schijman, A. G.; Llewellyn, M. S.; Lages-Silva, E.; Machado, C. R.; Andrade, S. G.; Sturm, N. R. *Infect., Genet. Evol.* **2012**, *12*, 240.
(252) Zingales, B.; Andrade, S. G.; Briones, M. R.; Campbell, D. A.; Chiari, E.; Fernandes, O.; Guhl, F.; Lages-Silva, E.; Macedo, A. M.; Machado, C. R.; Miles, M. A.; Romanha, A. J.; Sturm, N. R.; Tibayrenc, M.; Schijman, A. G. *Mem. Inst. Oswaldo Cruz* **2009**, *104*, 1051.
(253) Miles, M. A.; Llewellyn, M. S.; Lewis, M. D.; Yeo, M.; Baleela, R.; Fitzpatrick, S.; Gaunt, M. W.; Mauricio, I. L. *Parasitology* **2009**, *136*, 1509.
(254) Murta, S. M.; Gazzinelli, R. T.; Brener, Z.; Romanha, A. J. *Mol. Biochem. Parasitol.* **1998**, *93*, 203.

(255) Andrade, S. G.; Magalhaes, J. B.; Pontes, A. L. *Bull. W.H.O.* **1985**, *63*, 721.
(256) Molina, J.; Martins-Filho, O.; Brener, Z.; Romanha, A. J.; Loebenberg, D.; Urbina, J. A. *Antimicrob. Agents Chemother.* **2000**, *44*, 150.
(257) Villarreal, D.; Barnabe, C.; Sereno, D.; Tibayrenc, M. *Exp. Parasitol.* **2004**, *108*, 24.
(258) Toledo, M. J.; Bahia, M. T.; Carneiro, C. M.; Martins-Filho, O. A.; Tibayrenc, M.; Barnabe, C.; Tafuri, W. L.; de Lana, M. *Antimicrob. Agents Chemother.* **2003**, *47*, 223.
(259) Aquilino, C.; Gonzalez Rubio, M. L.; Seco, E. M.; Escudero, L.; Corvo, L.; Soto, M.; Fresno, M.; Malpartida, F.; Bonay, P. *PLoS One* **2012**, *7*, e40901.
(260) Moraes, C. B.; Giardini, M. A.; Kim, H.; Franco, C. H.; Araujo-Junior, A. M.; Schenkman, S.; Chatelain, E.; Freitas-Junior, L. H. *Sci. Rep.* **2014**, *4*, 4703.
(261) Girois, S. B.; Chapuis, F.; Decullier, E.; Revol, B. G. *Eur. J. Clin. Microbiol. Infect. Dis.* **2005**, *24*, 119.
(262) Sanderson, J. T. *Toxicol. Sci.* **2006**, *94*, 3.
(263) Taxvig, C.; Vinggaard, A. M.; Hass, U.; Axelstad, M.; Metzdorff, S.; Nellemann, C. *Int. J. Androl.* **2008**, *31*, 170.
(264) Pont, A.; Williams, P. L.; Azhar, S.; Reitz, R. E.; Bochra, C.; Smith, E. R.; Stevens, D. A. *Arch. Intern. Med.* **1982**, *142*, 2137.
(265) Pont, A.; Williams, P. L.; Loose, D. S.; Feldman, D.; Reitz, R. E.; Bochra, C.; Stevens, D. A. *Ann. Intern. Med.* **1982**, *97*, 370.
(266) Rafferty, S. W.; Eisner, J. R.; Moore, W. R.; Schotzinger, R. J.; Hoekstra, W. J. *Bioorg. Med. Chem. Lett.* **2014**, *24*, 2444.
(267) Hoekstra, W. J.; Garvey, E. P.; Moore, W. R.; Rafferty, S. W.; Yates, C. M.; Schotzinger, R. J. *Bioorg. Med. Chem. Lett.* **2014**, *24*, 3455.
(268) Trosken, E. R.; Adamska, M.; Arand, M.; Zarn, J. A.; Patten, C.; Volkel, W.; Lutz, W. K. *Toxicology* **2006**, *228*, 24.
(269) Warrilow, A. G.; Parker, J. E.; Kelly, D. E.; Kelly, S. L. *Antimicrob. Agents Chemother.* **2013**, *57*, 1352.